Zurich University of Applied Sciences

Department School of Engineering

Institute of Computer Science

MASTER THESIS

Tycho:

An Accuracy-First Architecture for Server-Wide Energy Measurement and Process-Level Attribution in Kubernetes

---

Author:
Caspar Wackerle

Supervisors:
Prof. Dr. Thomas Bohnert
Christof Marti

Submitted on
January 31, 2026

Study program:
Computer Science, M.Sc.

Imprint

Project: Master Thesis
Title: Tycho: An Accuracy-First Architecture for Server-Wide Energy Measurement and Process-Level Attribution in Kubernetes
Author: Caspar Wackerle
Date: January 31, 2026
Keywords: process-level energy consumption, cloud, kubernetes, kepler

Study program:
Computer Science, M.Sc.
Zurich University of Applied Sciences

Supervisor 1:
Prof. Dr. Thomas Bohnert
Zurich University of Applied Sciences
Email: thomas.michael.bohnert@zhaw.ch
Web: Link

Supervisor 2:
Christof Marti
Zurich University of Applied Sciences
Email: christof.marti@zhaw.ch
Web: Link

Abstract

Abstract

The accompanying source code for this thesis, including all deployment and automation scripts, is available in the **PowerStack**[1] repository on GitHub.

Contents

Abstract **iii**

1 Introduction **1**
1.1 Motivation . . . 1
1.2 Problem Context . . . 1
1.3 Position Within Previous Research . . . 2
1.4 Problem Statement . . . 2
1.5 Goals of This Thesis . . . 3
1.6 Research Questions . . . 3
1.7 Contributions . . . 3
1.8 Scope and Boundaries . . . 4
1.9 Origin of the Name "Tycho" . . . 4
1.10 Methodological Approach . . . 4
1.11 Thesis Structure . . . 4

2 Background and Related Research **5**
2.1 Energy Measurement in Modern Server Systems . . . 5
2.1.1 Energy Attribution in Multi-Tenant Environments . . . 5
2.1.2 Telemetry Layers in Contemporary Architectures . . . 6
2.1.3 Challenges for Container-Level Measurement . . . 6
2.2 Hardware and Software Telemetry Sources . . . 7
2.2.1 Direct Hardware Measurement . . . 7
2.2.2 Legacy Telemetry Interfaces (ACPI, IPMI) . . . 7
2.2.3 Redfish Power Telemetry . . . 8
2.2.4 RAPL Power Domains . . . 8
2.2.5 GPU Telemetry . . . 9
2.2.6 Software-Exposed Resource Metrics . . . 11
2.3 Temporal Behaviour of Telemetry Sources . . . 12
2.3.1 RAPL Update Intervals and Sampling Stability . . . 13
2.3.2 GPU Update Intervals and Sampling Freshness . . . 14
2.3.3 Redfish Sensor Refresh Intervals and Irregularity . . . 15
2.3.4 Timing of Software-Exposed Metrics . . . 16
2.4 Existing Tools and Related Work . . . 17
2.4.1 Kepler . . . 17
2.4.2 KubeWatt . . . 21
2.4.3 Other Tools (Brief Overview) . . . 22
2.4.4 Cross-Tool Limitations Informing Research Gaps . . . 22
2.5 Research Gaps . . . 23
2.6 Summary . . . 25

3 Conceptual Foundations of Container-Level Power Attribution **27**
3.1 Nature and Purpose of Power Attribution . . . 27
3.2 Workload Identity and Execution Boundaries . . . 28
3.3 Principles of Workload-Level Energy Attribution . . . 28
3.3.1 Aggregated Hardware Activity . . . 28
3.3.2 Domain Decomposition . . . 28
3.3.3 Conservation . . . 29

3.3.4 Static–Dynamic Separation . . . 29
3.3.5 Uncertainty and Non-Uniqueness . . . 29
3.3.6 Dependence on Metric Fidelity . . . 29
3.4 Temporal and Measurement Foundations . . . 29
3.4.1 Sampling vs Event-Time Perspectives . . . 30
3.4.2 Clock Models and Temporal Ordering . . . 30
3.4.3 Heterogeneous Metric Sources . . . 30
3.4.4 Delay, Jitter, and Temporal Uncertainty . . . 30
3.4.5 Temporal Alignment of Asynchronous Signals . . . 31
3.5 Conceptual Attribution Frameworks . . . 31
3.5.1 Proportional Attribution . . . 31
3.5.2 Shared-Cost Attribution . . . 31
3.5.3 Residual and Unattributed Energy . . . 31
3.5.4 Model-Based or Hybrid Attribution . . . 31
3.5.5 Causal or Explanatory Attribution . . . 32
3.6 Interactions and Complications . . . 32
3.7 Conceptual Challenges and System Requirements . . . 33
3.7.1 Requirement: Temporal Coherence . . . 33
3.7.2 Requirement: Domain-Level Consistency . . . 33
3.7.3 Requirement: Cross-Domain Reconciliation . . . 33
3.7.4 Requirement: Consistent Metric Interpretation . . . 33
3.7.5 Requirement: Transparent Modelling Assumptions . . . 34
3.7.6 Requirement: Lifecycle-Robust Attribution . . . 34
3.7.7 Requirement: Uncertainty-Aware Attribution . . . 34
3.8 Summary . . . 34

4 System Architecture **35**
4.1 Guiding Principles . . . 35
4.2 Traceability to Requirements . . . 35
4.3 High-Level Architecture . . . 36
4.3.1 Subsystem Overview . . . 36
4.3.2 Dataflow and Control Flow . . . 37
4.4 Temporal Model and Timing Engine . . . 38
4.4.1 Event-Time Model and Timestamp Semantics . . . 38
4.4.2 Independent Collector Schedules . . . 38
4.4.3 Window Construction and Analysis Triggering . . . 38
4.4.4 Comparison to Kepler Timing Model . . . 39
4.5 Metric Sources as Temporal Actors . . . 41
4.5.1 eBPF and Software Counters . . . 41
4.5.2 RAPL Domains . . . 42
4.5.3 Redfish/BMC Power Source . . . 42
4.5.4 GPU Collector Architecture . . . 43
4.6 Metadata Collection Subsystem . . . 46
4.7 Calibration . . . 48
4.8 Analysis and Attribution Architecture . . . 49
4.8.1 Pipeline Orchestration and Stage Execution . . . 49
4.8.2 Stage 1: Component Metric Construction . . . 51
4.8.3 Stage 2: System-Level Energy Model and Residual . . . 56
4.8.4 Stage 3: Idle and Dynamic Energy Semantics . . . 57
4.8.5 Stage 4: Workload Attribution and Aggregation . . . 60
4.8.6 Prometheus Exporter . . . 67
4.9 Architectural Trade-Offs and Alternatives Considered . . . 68
4.9.1 Timing and Data Collection Models . . . 68
4.9.2 Attribution Model Design Space . . . 68
4.9.3 Accuracy Versus Architectural Complexity . . . 69
4.10 Summary . . . 69

5 Implementation **71**

5.1 Purpose, Scope, and Execution-Time Structure . . . 71
5.1.1 Runtime Subsystems and Responsibilities . . . 71
5.1.2 Execution-Time Interaction Model . . . 72
5.2 Temporal Infrastructure and Window Realization . . . 72
5.2.1 Architectural Context and Implementation Problem . . . 72
5.2.2 Global Monotonic Time Realization . . . 72
5.2.3 Timing Engine and Hierarchical Cadence Alignment . . . 73
5.2.4 Analysis Window Realization and Trigger Semantics . . . 74
5.3 Historical Observation Retention . . . 74
5.4 Metric Collection Subsystems . . . 75
5.4.1 eBPF Collector Implementation . . . 75
5.4.2 RAPL Collector Implementation . . . 77
5.4.3 Redfish Collector Implementation . . . 79
5.4.4 GPU Collector Implementation . . . 81
5.5 Metadata and Identity Infrastructure . . . 85
5.5.1 Architectural Context . . . 85
5.5.2 Controller-Orchestrated Refresh and Lifetime Enforcement . . . 85
5.5.3 Metadata Store, Keys, and Temporal Alignment . . . 85
5.5.4 Proc Collector . . . 86
5.5.5 Kubelet Collector . . . 86
5.5.6 Metadata Contract and Join Surface . . . 87
5.5.7 Design Consequences and Exclusions . . . 89
5.6 Calibration . . . 89
5.6.1 Architectural Context . . . 89
5.6.2 Startup Strategy and Collector Gating . . . 89
5.6.3 Polling-Frequency Calibration Mechanism . . . 90
5.6.4 Delay Calibration Integration . . . 90
5.6.5 Implementation Consequences . . . 91
5.7 Analysis and Attribution Infrastructure . . . 91
5.7.1 Analysis Engine Responsibilities and Cycle Lifecycle . . . 91
5.7.2 Attribution Window Selection and Temporal Safety . . . 92
5.7.3 Staged Pipeline Execution and Dependency Discipline . . . 93
5.7.4 Metric Materialization and Intra-Cycle Visibility . . . 93
5.7.5 Cross-Window State and Explicit Memory . . . 94
5.7.6 Output Commit and Sink Boundary . . . 95
5.7.7 Implementation Consequences and Guarantees . . . 95
5.7.8 Stage 1: Component Metric Construction . . . 96
5.7.9 Stage 2: System-Level Energy Model and Residual . . . 102
5.7.10 Stage 3: Idle and Dynamic Energy Semantics . . . 103
5.7.11 Stage 4: Workload Attribution and Aggregation . . . 107
5.7.12 Prometheus Exporter Implementation . . . 113
5.8 Correctness, Robustness, and Degradation Behavior . . . 114
5.8.1 Architectural Invariant Enforcement . . . 114
5.8.2 Partial Observability and Missing Data . . . 114
5.8.3 Transient Pathologies . . . 114
5.8.4 Graceful Degradation Paths . . . 114
5.9 Implementation Trade-Offs and Design Decisions . . . 114
5.9.1 Accuracy vs Complexity . . . 114
5.9.2 Timing Precision vs System Overhead . . . 114
5.9.3 Alternatives Considered . . . 114
5.10 Summary . . . 114

Bibliography

List of Figures

2.1 Kepler's synchronous update loop 18

4.1 Subsystem Architecure, Dataflow and Control Flow 38
4.2 Analysis window W_i in relation to collectors 39
4.3 Comparison between Tycho and KeplerTiming Model 40
4.4 Comparison between Tycho and Kepler export behaviour 41
4.5 Phase-aware GPU polling timeline 45

List of Tables

5.1 Metrics collected by the kernel `eBPF` subsystem. 77
5.2 Metrics exported by the RAPL collector per `RaplTick`. 78
5.3 Metrics collected by the Redfish collector. 80
5.4 Device- and MIG-level metrics collected by the GPU subsystem. 84
5.5 Process-level metrics collected over a backend-defined time window. . 84
5.6 Process metadata collected by the process collector 87
5.7 Pod metadata collected by the kubelet collector 88
5.8 Container metadata collected by the kubelet collector 88
5.9 Exported utilization metrics derived from `eBPF` observations. 97
5.10 Exported RAPL component energy and power metrics. 98
5.11 Exported GPU metrics derived from the corrected reconstruction. . . . 100
5.12 Exported Redfish-derived system metrics. 102
5.13 Exported residual metrics. 103
5.14 Exported RAPL idle and dynamic metrics. 104
5.15 Exported residual idle and dynamic metrics. 106
5.16 Exported GPU idle and dynamic decomposition metrics. 107
5.17 Exported workload-attributed eBPF utilization counters. 108
5.18 Exported CPU dynamic workload energy metrics. 110
5.19 Exported CPU idle workload energy metrics. 111
5.20 Exported metrics for GPU dynamic workload attribution. 112
5.21 Exported metrics for GPU idle workload attribution. 113

The global climate crisis is one of humanity's greatest challenges in this century.
With this work, I hope to contribute a small part in the direction we urgently need to go.

Chapter 1

Introduction

XXXXXXXXXXXXXXXXXXXXXXXXXXXXXXXXXXXXXXXXXXXXXXXXXXXXXXXXXXXXXXXXXXXXXXX
REVISE ENTIRE CHAPTER LATER XXXXXXXXXXXXXXXXXXXXXXXXXXXXXXXXXXXXXXXXXXXXX

1.1 Motivation

Energy consumption in data centers continues to rise as demand for compute-intensive and latency-sensitive services increases. Modern cloud platforms host diverse workloads such as machine learning inference, analytics pipelines, and high-density microservices, all of which collectively contribute to a growing global electricity footprint. Container orchestration frameworks amplify these trends by enabling dense consolidation of workloads across shared servers. While this improves resource efficiency, it also introduces abstraction layers that obscure the relationship between workload behaviour and physical energy use.

As interest in sustainable cloud operations intensifies, there is increasing demand for precise, workload-level energy visibility. Fine-grained and reproducible energy measurements are essential for research domains such as performance engineering, scheduling, autoscaling, and the design of energy-aware systems. Existing tools provide valuable approximations but prioritise portability and low operational overhead, and therefore do not target the upper bounds of measurement fidelity. Research environments, by contrast, require methodologies that prioritise accuracy, control, and verifiability over deployability.

This thesis is motivated by the need for an accuracy-focused measurement approach that supports rigorous experimental work on containerised systems. Rather than proposing new optimisation mechanisms, this work concentrates on establishing a reliable methodological foundation for observing and analysing workload-induced energy consumption in controlled settings.

1.2 Problem Context

Modern multi-tenant servers host many short-lived and highly dynamic workloads that execute concurrently and compete for shared hardware resources. On such systems, the aggregate power draw represents the combined activity of numerous interacting subsystems, while the contributions of individual workloads remain deeply entangled. Containerisation further complicates this picture: processes belong to containers, containers belong to pods, and pods may change state rapidly under

orchestration. These abstractions improve system management but obscure how computational activity translates into power consumption.

At the same time, servers expose a heterogeneous collection of telemetry sources. Each source reflects different aspects of hardware behaviour, updates at its own cadence, and provides only a partial view of system activity. Because workload state changes and telemetry updates occur independently, they do not naturally align in time. The resulting temporal misalignment limits the reliability of workload-level energy attribution and leads to uncertainty in short-duration or phase-sensitive analyses.

Kubernetes introduces additional challenges. Workloads may start and terminate within milliseconds, metadata may appear with delays, and lifecycle events may interleave in complex ways. Existing tools often rely on coarse sampling windows or heuristic models that mask these inconsistencies. While sufficient for operational monitoring, such abstractions constrain the achievable accuracy in research settings. An accuracy-oriented approach requires explicit treatment of timing, metadata consistency, and correlation across heterogeneous measurement sources.

1.3 Position Within Previous Research

This thesis builds upon two earlier stages of work. The implementation-focused VT1 project developed an initial measurement pipeline and explored practical aspects of collecting hardware and system-level metrics in a Kubernetes environment. The subsequent VT2 project examined the state of the art in server-level energy measurement, validated the behaviour of commonly used telemetry sources, and identified methodological and technical limitations in existing tools such as Kepler. Both works are included in the appendix as supporting material.

The present thesis integrates these earlier insights but does not repeat them. Instead, it synthesises the essential findings from VT2 in a condensed form (Chapter 2), and introduces the conceptual foundations required to reason about accurate energy attribution (Chapter 3). These chapters provide the background necessary to understand the accuracy-focused architecture developed later in this thesis.

1.4 Problem Statement

Accurately determining how much energy individual workloads consume in a Kubernetes cluster remains a challenging open problem. Clusters host many short-lived and overlapping workloads whose behaviour evolves rapidly, while server-level power telemetry is exposed through heterogeneous interfaces that update asynchronously and lack consistent timestamps. These timing mismatches, combined with the abstraction layers introduced by container orchestration, obscure the relationship between workload activity and physical energy use. Existing approaches provide high-level estimates but cannot deliver the temporal alignment, attribution fidelity, or reproducibility required for rigorous experimental analysis. This thesis therefore addresses the problem of designing a measurement methodology and prototype system capable of producing time-aligned, workload-level energy attribution with sufficient accuracy for research environments.

1.5 Goals of This Thesis

The overarching goal of this thesis is to develop an accuracy-focused approach for measuring energy consumption in Kubernetes-based environments. To achieve this, the work pursues four concrete objectives:

- **Methodological objective:** Define a measurement methodology that aligns heterogeneous telemetry sources with dynamic workload behaviour under a unified temporal model suitable for controlled research settings.
- **Architectural objective:** Design an accuracy-first system architecture that explicitly handles timing, metadata consistency, and correlation across diverse metrics without relying on heuristic abstractions.
- **Prototype objective:** Implement a research prototype that realises this architecture on commodity server hardware and integrates workload metadata, timing information, and server-wide telemetry into a coherent measurement pipeline.
- **Foundational objective for future work:** Establish the methodological and architectural basis for subsequent validation studies that will evaluate measurement fidelity and explore trade-offs between accuracy, overhead, and operational constraints.

1.6 Research Questions

1. How reliably can an accuracy-focused measurement approach capture and represent workload-induced variations in energy consumption within dynamic, multi-tenant Kubernetes environments?
2. To what extent does a unified timing and attribution methodology improve the consistency and interpretability of workload-level energy measurements compared to existing estimation-oriented approaches?
3. In which contexts does high-fidelity energy measurement provide meaningful benefits for research and experimental analysis, and what trade-offs arise between accuracy, overhead, and operational constraints?

1.7 Contributions

This thesis makes several conceptual and methodological contributions to the study of energy measurement in container-orchestrated environments. First, it introduces an accuracy-focused measurement approach that prioritizes temporal consistency, reproducibility, and the faithful representation of workload behaviour. The work defines a methodology for unifying heterogeneous sources of server telemetry under a shared timing model, enabling coherent interpretation of workload activity and system-level energy use.

A second contribution is the development of a prototype system that operationalizes this methodology and provides a concrete platform for exploring the limits of

high-fidelity energy measurement in Kubernetes-based environments. The prototype integrates workload metadata, timing information, and server-wide telemetry into a coherent measurement pipeline designed for research and controlled experimentation.

Third, the thesis establishes a foundation for reliable workload-level attribution by describing a structured process for correlating dynamic workload behaviour with system energy consumption. This provides a basis for analysing short-lived workload phases, transient resource usage patterns, and other phenomena that require fine-grained temporal alignment.

Finally, the work prepares the methodological groundwork for subsequent validation studies by outlining experimental procedures, calibration strategies, and evaluation principles suited to accuracy-oriented measurement. Together, these contributions advance the methodological state of the art and offer a practical reference point for future research on energy transparency in modern cloud infrastructures.

1.8 Scope and Boundaries

This thesis focuses on high-level principles and methods for energy measurement in multi-tenant server environments. The primary scope includes conceptual design, prototype development, and preparation of the methodological foundation for subsequent evaluation work. The emphasis is on accuracy, reproducibility, and consistency rather than operational deployability or production-grade integration.

Several areas remain outside the scope of this work. The thesis does not propose scheduling policies, predictive models, or system-level optimisation mechanisms. It does not modify Kubernetes or introduce changes to cloud operators' workflows. The prototype developed in this thesis is intended for controlled research environments and does not aim to provide a turnkey solution for general-purpose use. The work assumes access to a server environment where low-level telemetry and measurement interfaces are accessible under suitable conditions.

1.9 Origin of the Name "Tycho"

The prototype developed in this thesis is named *Tycho*, a reference to the astronomer Tycho Brahe. Brahe is known for producing exceptionally precise astronomical measurements, which later enabled Johannes Kepler to formulate the laws of planetary motion. The naming reflects a similar relationship: while the upstream *Kepler* project focuses on modelling and estimation, this thesis explores the upper bounds of measurement accuracy. Tycho thus signals both continuity with prior work and a shift toward an accuracy-first design philosophy.

1.10 Methodological Approach

1.11 Thesis Structure

Chapter 2

Background and Related Research

This chapter summarises the current state of research and industrial knowledge on server-level energy measurement. Its focus is limited to what the literature reports about available telemetry sources, measurement techniques, and existing attribution tools. The discussion is descriptive rather than conceptual: it does not introduce attribution principles, methodological reasoning, or design considerations, which are addressed in Chapter 3. Extended background material is available in Appendix A and the present chapter integrates only those findings that are directly relevant for understanding the research landscape.

2.1 Energy Measurement in Modern Server Systems

The energy consumption of modern servers arises from a heterogeneous set of subsystems, including CPUs, GPUs, memory, storage devices, network interfaces, and platform management components. Prior research highlights that these subsystems expose highly unequal visibility into their power behaviour, since measurement capabilities, granularity, and accuracy differ significantly across hardware generations and vendors [2, 3]. Some domains provide direct telemetry, while others can only be approximated through software-derived activity metrics. As a result, no single interface offers complete or temporally consistent power information, and most studies rely on a single source or combine multiple sources to approximate system-level consumption. This fragmented measurement landscape forms the basis for much of the existing work on power modelling, validation, and multi-source energy estimation in server environments.

2.1.1 Energy Attribution in Multi-Tenant Environments

Several studies identify containerised and multi-tenant systems as challenging environments for energy attribution. Containers share the host kernel and rely on common processor, memory, storage, and network subsystems, which removes the isolation boundaries present in virtual machines and prevents direct measurement of per-container power. Research reports that workloads running concurrently on the same node create interference effects across hardware domains, leading to utilisation patterns that correlate only loosely with actual energy consumption [2]. Modern orchestration platforms further increase attribution difficulty through highly dynamic execution behaviour: containers are created, destroyed, and rescheduled at high frequency, often numbering in the thousands on large clusters. These rapid lifecycle changes produce volatile metadata and short-lived resource traces that are difficult

to align with node-level telemetry. Collectively, the literature treats container-level energy attribution as an estimation problem constrained by incomplete observability, heterogeneous measurement quality, and continuous runtime churn.

2.1.2 Telemetry Layers in Contemporary Architectures

Modern servers expose power and activity information through two largely independent telemetry layers. The first consists of in-band mechanisms that are visible to the operating system, including on-die energy counters, GPU management interfaces, and kernel-level resource statistics. These interfaces typically offer higher sampling rates and finer granularity, but their accuracy and coverage vary across hardware generations and vendors. Prior work notes that in-band telemetry often represents estimated rather than directly measured power and that several domains, such as network and storage devices, expose only partial or indirect information.

The second layer is out-of-band telemetry provided by baseboard management controllers through interfaces such as IPMI or Redfish. These systems aggregate sensor readings independently of the host and report stable, whole-system power values at coarse temporal resolution. Empirical studies show that out-of-band telemetry provides useful system-level accuracy, although update intervals and measurement precision differ substantially between vendors [4]. Compared with instrument-based measurements, which remain the benchmark for high-fidelity evaluation but are impractical at scale, both in-band and out-of-band methods represent trade-offs between granularity, availability, and measurement reliability.

Combined, these layers form a heterogeneous telemetry landscape in which sampling rates, accuracy, and domain coverage differ significantly, motivating the use of multi-source measurement approaches in research.

2.1.3 Challenges for Container-Level Measurement

Existing research identifies several factors that complicate accurate energy measurement for containerised workloads. Large-scale trace analyses show that cloud environments exhibit substantial churn, with many tasks being short-lived and resource demands changing rapidly over time [5]. Such dynamism limits the observability of fine-grained resource usage and makes it difficult to capture short execution intervals with sufficient temporal resolution.

Monitoring studies further report inconsistencies across the different layers that expose resource information for containers. In multi-cloud settings, observability often depends on heterogeneous monitoring stacks, leading to fragmented visibility and non-uniform coverage of system activity [6]. Even within a single host, performance counters obtained from container-level interfaces may diverge from system-level measurements. Empirical evaluations demonstrate that container-level CPU and I/O counters can underestimate actual activity by a non-negligible margin, and that co-located workloads introduce contention effects that distort these metrics [7].

These findings indicate that container-level measurement operates under conditions of rapid workload turnover, heterogeneous monitoring behaviour, and imperfect resource visibility. As a consequence, the literature treats container energy attribution as a problem constrained by incomplete and potentially biased measurement signals rather than as a directly measurable quantity.

2.2 Hardware and Software Telemetry Sources

This section outlines the primary telemetry sources used to observe power and resource behaviour in modern server systems. It summarises established research on external measurement devices, firmware-level interfaces, on-die energy counters, accelerator telemetry, and kernel-exposed resource metrics. The emphasis is on reporting the properties and empirical characteristics documented in prior work, without interpreting these signals conceptually or analysing their temporal behaviour, which are addressed in later sections. A comprehensive technical discussion is provided in Appendix A, Chapter **??**; the present section extracts only the findings relevant for understanding the measurement landscape.

2.2.1 Direct Hardware Measurement

Direct physical instrumentation remains the most accurate method for measuring server power consumption. External power meters or inline shunt-based devices can capture node-level energy usage with high fidelity, and research frequently uses such instrumentation as a ground truth for validating software-reported power values. Studies employing dedicated measurement setups, such as custom DIMM-level sensing boards, demonstrate that high-frequency sampling and component-level granularity are technically feasible but require bespoke hardware and non-trivial integration effort [8]. Lin et al. classify these approaches as offering very high data credibility but only coarse spatial granularity and limited scalability in operational environments [2].

Recent work on specialised sensors, such as the PowerSensor3 platform[9] for high-rate voltage and current monitoring of GPUs and other accelerators, illustrates ongoing interest in hardware-centric power measurement. However, these systems share the same fundamental drawback: deployment across production servers is complex, costly, and incompatible with large-scale or multi-tenant settings. As a consequence, direct instrumentation is predominantly used in controlled experiments or for validation of other telemetry sources, rather than as a primary measurement mechanism in real-world server infrastructures.

2.2.2 Legacy Telemetry Interfaces (ACPI, IPMI)

Early power-related telemetry on server platforms was primarily exposed through ACPI and IPMI. ACPI provides a standardised interface for configuring and controlling hardware power states, but it does not offer real-time energy or power readings. The interface exposes only abstract performance and idle states defined by the firmware [10], and these states do not include the instantaneous power information required for empirical energy measurement. Consequently, ACPI has seen little use in modern power estimation research.

IPMI, accessed through the baseboard management controller, represents an older class of out-of-band telemetry that predates Redfish. Although widely supported across server hardware, IPMI power values are known to be coarse, slowly refreshed, and often inaccurate when compared with external instrumentation. Empirical studies report multi-second averaging windows, substantial quantisation effects, and unreliable idle power readings [11, 12]. These limitations, together with the availability of more precise alternatives, have led IPMI to be largely superseded by Redfish on contemporary server platforms.

2.2.3 Redfish Power Telemetry

Redfish is the modern out-of-band management interface available on contemporary server platforms and is designed as the successor to IPMI. It exposes system-level telemetry through a RESTful API implemented on the baseboard management controller (BMC), providing access to whole-node power readings derived from on-board sensors. Prior work consistently shows that Redfish delivers higher precision than IPMI, with lower quantisation artefacts and more stable readings across power ranges [4]. In controlled experiments, Redfish achieved a mean absolute percentage error of roughly three percent when compared to a high-accuracy power analyser, outperforming IPMI in all evaluated power intervals.

A key limitation of Redfish is its temporal granularity. Empirical studies report that power values exhibit non-negligible staleness, with refresh delays of approximately 200 ms [4]. This latency restricts the ability of Redfish to capture short bursts of activity or rapid fluctuations in dynamic workloads. Accuracy and responsiveness also vary across vendors, reflecting differences in embedded sensors, BMC firmware, and management controller architectures.

The interface is widely deployed in real-world infrastructure. Modern enterprise servers from Dell, HPE, Lenovo, Cisco, and Supermicro routinely expose power telemetry via Redfish as part of their standard BMC firmware [13]. Out-of-band monitoring studies further highlight that Redfish avoids the overheads and failure modes associated with in-band agents [14]. In practice, Redfish implementations tend to provide stable low-frequency updates suitable for coarse-grained power reporting.

Preliminary measurements conducted for this thesis also observed irregular update intervals on the evaluated hardware, occasionally extending into the multi-second range. While this behaviour is specific to a single system and not generalisable, it reinforces the literature's position that Redfish telemetry exhibits meaningful vendor-dependent variability and remains unsuitable for fine-grained temporal correlation.

Overall, Redfish provides accessible, reliable whole-node power telemetry at coarse temporal resolutions, making it valuable for long-interval monitoring and for validating other measurement sources, but inappropriate for attributing energy consumption to short-lived or rapidly fluctuating containerised workloads.

2.2.4 RAPL Power Domains

Running Average Power Limit (RAPL) provides hardware-backed energy counters for several internal power domains of a processor package. Originally introduced by Intel and later adopted in a compatible form by AMD, RAPL exposes energy measurements via model-specific registers that can be accessed directly or through higher-level interfaces such as the Linux `powercap` framework or the `perf-events` subsystem [15, 16]. Raffin et al. provide a detailed comparison of these access mechanisms, noting that MSR, powercap, perf-events, and eBPF differ mainly in convenience, required privileges, and robustness; all can retrieve equivalent RAPL readings when implemented correctly [16]. They recommend accessing RAPL via the powercap interface, which is easiest to implement reliably and suffers from no overhead penalties when compared with more low-level methods.

Intel platforms typically expose several well-established RAPL domains, including the processor package, the core subsystem, and (on many server architectures) a DRAM domain [17]. These domains have been validated extensively against external measurement equipment. Studies report that the combination of package and DRAM energy tracks CPU-and-memory power with good accuracy from Haswell onwards, which has led to RAPL becoming the primary fine-grained energy source in server-oriented research [8, 18–20]. More recent work on hybrid architectures such as Alder Lake confirms that RAPL continues to correlate well with external measurements under load, while precision decreases somewhat in low-power regimes [21]. Across these studies, RAPL is generally regarded as sufficiently accurate for scientific analysis when its domain boundaries and update characteristics are considered [16].

AMD implements a RAPL-compatible interface with a similar programming model but a reduced set of domains. Zen 1 through Zen 4 processors expose package and core domains only, without a dedicated DRAM domain [16, 22]. Schöne et al. show that, as a consequence, memory-related energy may not be represented explicitly in AMD's RAPL output, leading to a smaller portion of total system energy being observable through the package domain alone [22]. This limitation primarily concerns domain completeness rather than measurement correctness: for compute-intensive workloads, package-domain values behave consistently, but workloads with significant memory activity exhibit a larger gap relative to whole-system measurements because DRAM energy is not separately reported. Raffin et al. further note that, on the evaluated Zen-based server, different kernel interfaces initially exposed inconsistent domain sets; this was later corrected upstream, illustrating that AMD support is evolving and still maturing within the Linux ecosystem [16].

Technical considerations also apply to both Intel and AMD platforms. RAPL counters have finite width and wrap after sufficiently large energy accumulation, requiring consumers to implement overflow correction [16, 23]. The counters do not include timestamps, and empirical work shows that actual update intervals may deviate from nominal values, complicating precise temporal correlation with other telemetry [18, 24]. On some Intel platforms, security hardening measures such as energy filtering reduce temporal granularity for certain domains to mitigate side-channel risks [21, 25, 26]. In virtualised environments, RAPL access may be trapped by the hypervisor, increasing latency and introducing small deviations from bare-metal behaviour [24].

In summary, RAPL provides a widely used and comparatively fine-grained source of processor-side energy telemetry. Intel platforms typically offer multiple validated domains, including DRAM, enabling a broader view of CPU-and-memory energy. AMD platforms expose fewer domains and therefore provide a more limited perspective on total system power, particularly for memory-intensive workloads. These differences in domain coverage, measurement scope, and software integration need to be taken into account when using RAPL as a basis for energy analysis.

2.2.5 GPU Telemetry

Unlike CPUs, where power and utilization telemetry is supported through standardised interfaces, GPU energy visibility relies primarily on vendor-specific mechanisms. For NVIDIA devices, two interfaces dominate this landscape: the *NVIDIA Management Library* (NVML), which has become the industry standard, and the *Data*

Center GPU Manager (DCGM), a less widely used management layer that also exposes telemetry.

2.2.5.1 NVML

NVML is NVIDIA's primary interface for device-level monitoring and underpins tools such as `nvidia-smi`. It provides access to power, energy (on selected data-center GPUs), GPU utilization, memory usage, clock frequencies, thermal state, and various health and throttle indicators. Among these, power and utilization are most relevant for energy analysis.

NVML power values represent board-level estimates derived from on-device sensing circuits and are shaped by internal averaging and architecture-dependent update behaviour. Recent empirical studies across modern devices show that NVML produces fresh samples only intermittently and applies smoothing that reduces the visibility of short-lived power changes, while steady-state power levels remain comparatively accurate [27]. On the Grace–Hopper GH200, these effects are pronounced: NVML reflects a coarse internal averaging interval and therefore underrepresents short kernels and transient peaks relative to higher-frequency system interfaces [28]. These findings indicate that NVML captures long-term power behaviour reliably but inherently limits fine-grained visibility. Despite these constraints, existing studies consistently find that NVML provides reasonably accurate steady-state power estimates on modern data-center GPUs and currently represents the most reliable and widely supported mechanism for obtaining GPU power telemetry in practical systems [28].

GPU utilization provides contextual information about device activity. It reports the proportion of time during which the GPU is executing any workload rather than the fraction of computational capacity in use, making it a coarse activity indicator rather than a detailed performance metric [29].

2.2.5.2 DCGM

DCGM is NVIDIA's management and observability framework designed for data-center deployments. It aggregates telemetry, performs health monitoring, exposes thermal and throttle state, and provides detailed visibility in environments that employ Multi-Instance GPU (MIG) partitioning. However, DCGM's power and utilization metrics are derived from the same underlying measurement sources as NVML. In practice, DCGM is far less commonly used for energy analysis because it does not provide higher-fidelity power telemetry; instead, it applies additional aggregation and is typically deployed with coarse sampling intervals, especially when used through exporters in cluster monitoring systems. DCGM therefore represents an alternative access path to the same measurements rather than a distinct source of energy-related information.

DCGM is considerably less common in both research and operational practice, with most GPU monitoring systems relying primarily on NVML while DCGM appears only occasionally in cluster-level deployments [29].

2.2.5.3 Summary

NVML and DCGM jointly define the available mechanisms for GPU telemetry in cloud environments. NVML is the dominant and broadly supported interface for power and utilization measurement, while DCGM extends it with operational metadata and management integration. Current studies consistently show that both interfaces expose averaged, device-level power estimates that capture long-term behaviour but are inherently limited in their ability to represent short-duration activity or fine-grained workload structure. These characteristics form the scientific foundation for later discussions of temporal behaviour and measurement methodology.

2.2.6 Software-Exposed Resource Metrics

In addition to hardware telemetry, Linux and Kubernetes expose a wide range of software-level resource metrics that describe system and workload activity. These metrics do not measure power directly but provide essential behavioural context that complements RAPL, Redfish, and GPU telemetry.

2.2.6.1 CPU and Memory Activity Metrics

Linux provides several complementary mechanisms for tracking CPU and memory usage. Global counters such as `/proc/stat` record cumulative CPU time since boot, while per-task statistics in `/proc/<pid>` expose user-mode and kernel-mode execution time with high granularity [30]. Control groups (cgroups) provide container-level CPU and memory accounting and form the primary basis for utilisation metrics inside Kubernetes [31, 32]. Higher-level tools such as cAdvisor and metrics-server aggregate this information via Kubelet, but at significantly lower update rates.

Event-driven approaches provide substantially finer resolution. eBPF allows dynamic attachment to kernel events such as context switches, scheduling decisions, and I/O operations, enabling near-real-time capture of per-task CPU activity with low overhead [33, 34]. Hardware performance counters accessed through `perf` offer insight into instruction counts, cycles, cache behaviour, and stalls [35]. These sources provide detailed behavioural information but still represent utilisation rather than energy.

2.2.6.2 Storage Activity Metrics

Storage subsystems do not expose real-time power telemetry, yet Linux provides a rich set of activity indicators. Per-process statistics in `/proc/<pid>/io` track bytes read and written, while cgroup I/O controllers report aggregated container-level metrics. Subsystem-specific tools such as `smartctl` and `nvme-cli` reveal additional device characteristics, queue behaviour, and state transitions [36, 37].

In the absence of hardware power sensors, multiple works propose workload-dependent energy models for storage devices [38–40]. These models can yield accurate estimates when calibrated for a specific device but do not generalise across heterogeneous hardware due to differences in flash controllers, firmware, and internal data paths.

2.2.6.3 Network and PCIe Device Metrics

Network interfaces provide byte and packet counters via `/proc/net/dev`, but expose no dedicated power telemetry. Research models for NIC energy consumption exist [41–43], yet all rely on device-specific idle and active power characteristics that are not available at runtime. Similarly, PCIe devices support abstract power states as defined by the PCIe specification [44], but these states do not reflect instantaneous power usage and thus offer only coarse activity signals.

2.2.6.4 Secondary System Components

Components such as fans, motherboard logic, and power delivery subsystems rarely expose fine-grained telemetry. Although some BMC implementations report coarse sensor values, these readings are inconsistent across platforms and generally unsuitable for high-resolution analysis. Consequently, research commonly treats these subsystems as part of the residual power that scales with the activity of primary components [42].

2.2.6.5 Model-Based Estimation Approaches

Because software-visible metrics capture detailed workload behaviour, many works propose inferring energy consumption from utilisation using regression or stochastic models [45–48]. While these models can be effective when fitted to a specific hardware platform, their accuracy depends heavily on device-specific parameters, making them unsuitable as a general mechanism for heterogeneous server environments. Machine-learning-based estimators share the same limitation: high accuracy when trained for a fixed configuration, poor portability without extensive retraining.

2.2.6.6 Summary

Software-exposed metrics provide high-resolution visibility into CPU, memory, I/O, and network activity. They are indispensable for correlating workload behaviour with hardware power signals, especially for components that lack native telemetry. Model-based estimation remains possible but inherently platform-specific, and therefore unsuitable as a universal foundation for fine-grained attribution in heterogeneous environments.

2.3 Temporal Behaviour of Telemetry Sources

A comprehensive treatment of temporal characteristics can be found in Appendix A, Chapter **??**, but the present section focuses on the empirical, source-specific behaviours that constrain fine-grained power and energy estimation on real systems. Modern server platforms expose a heterogeneous set of telemetry interfaces, and their timing properties vary substantially: some update at fixed intervals, others employ internal averaging or smoothing, several expose counters without timestamps, and many lack guarantees on refresh regularity. These behaviours shape the effective temporal resolution with which workload-induced power changes can be observed.

The purpose of this section is not to develop a conceptual theory of sampling or to explain why timing matters for attribution (both are deferred to Chapter 3), nor to

introduce Tycho's timing engine (Chapter 4). Rather, it establishes the empirical constraints imposed by the telemetry sources themselves. These include sensor refresh intervals, stability of consecutive updates, delays between physical behaviour and reported values, the presence or absence of timestamps, and the distinction between instantaneous versus internally averaged measurements.

The subsections that follow describe these temporal properties for each telemetry source individually and summarise the practical limits they impose on high-resolution energy analysis.

2.3.1 RAPL Update Intervals and Sampling Stability

RAPL exposes energy *counters* rather than instantaneous power values. These counters accumulate energy since boot and can be read at arbitrarily high frequency, but their usefulness is determined entirely by how often the internal measurement logic refreshes them, a timing behaviour that is undocumented and domain-dependent.

Domain-specific internal update rates Intel specifies the RAPL time unit as 0.976 ms for the slowest-updating domains, while others, notably the PP0 (core) domain, may refresh significantly faster [21]. In practice, however, these theoretical limits do not translate into usable temporal resolution because RAPL provides no timestamps: the moment of counter refresh is unknown to the reader. At sub-millisecond sampling rates, the lack of timestamps combined with irregular refresh behaviour introduces substantial relative error, since differences between consecutive reads may reflect counter staleness rather than actual power dynamics [23].

Noise introduced by security-driven filtering To mitigate power-side channels such as Platypus, Intel optionally introduces randomised noise through the `ENERGY_FILTERING_ENABLE` mechanism [26]. This filtering increases the effective minimum granularity from roughly 1 ms to approximately 8 ms for the PP0 domain [21]. While average energy over longer intervals remains accurate, instantaneous increments become less reliable at very short timescales.

Practical sampling limits Despite the nominal sub-millisecond timing, empirical work consistently shows that high-frequency polling offers no practical benefit. Multiple studies report that sampling faster than the internal update period only produces repeated counter values and amplifies read noise [23]. Jay et al. demonstrate that at polling rates slower than 50 Hz, the relative error falls below 0.5 % [24]. Consequently, typical measurement practice (and the limits adopted in this thesis) treats RAPL as reliable only at tens-of-milliseconds resolution, not at the theoretical millisecond scale suggested by its nominal time unit.

Summary Although RAPL counters can be read extremely quickly, the effective temporal resolution is constrained by undocumented refresh intervals, absence of timestamps, optional security filtering, and substantial measurement noise at high polling rates. For practical purposes, sampling at approximately 20–50 ms intervals yields the most stable and accurate results, while sub-millisecond polling is inadvisable due to high relative error and counter staleness.

2.3.2 GPU Update Intervals and Sampling Freshness

GPU power telemetry is exposed primarily through NVML, with DCGM providing an alternative access path that builds on the same underlying measurement source. Unlike CPU-side interfaces integrated into the processor package, GPU power monitoring is performed entirely by the device itself: internal sensing circuits and firmware determine how often new values are produced, how they are averaged, and when they are published to software. As a result, refresh behaviour varies substantially across architectures, and the temporal properties of the reported values depend on device-internal update cycles rather than the rate at which the host system issues queries, which limits the achievable resolution of any external sampling strategy.

Internal update cycles and sampling freshness Empirical studies consistently show that NVML publishes new power values only intermittently, even when queried at high frequency. Yang et al. report sampling availability as low as roughly twenty–twenty-five percent across more than seventy modern data-center GPUs, meaning that the majority of polls return previously published values rather than fresh measurements [27].

Typical internal update periods fall on the order of tens to several hundreds of milliseconds, with architectural variation between GPU generations. Hernandez et al. report that newer architectures apply more aggressive smoothing and exhibit longer gaps between updates, reflecting slower publication cadence at the firmware level [28]. Overall, empirical evaluations show that NVML's internal update interval may lie on the order of hundreds of milliseconds and that repeated queries do not guarantee the retrieval of a new sample at every call [27]. NVML power readings do not represent instantaneous electrical measurements; they reflect firmware-level integration and smoothing over a device-internal averaging window, the duration of which varies by GPU generation and is not publicly documented..

Reaction delay to workload-induced power changes A related characteristic is NVML's reaction delay: when GPU power changes due to workload activity, the corresponding update becomes visible only after a lag. Multiple studies document delays in the range of approximately one to three hundred milliseconds before a new NVML value reflects the underlying power transition [27]. This delay is distinct from averaging effects and arises from deferred publication of internally accumulated measurements. On some recent architectures, the delay can be longer due to device-level smoothing layers that defer updates until sufficient internal samples have been collected [28].

Update regularity and jitter NVML update cycles are not perfectly periodic. Even when a nominal internal cadence is observable, individual publish times exhibit modest jitter, and occasional missed or skipped updates can result in sequences of identical values. These effects are pronounced on certain consumer-class devices and in configurations that partition the GPU, such as MIG, although they are also present to a lesser degree on data-center accelerators [27]. Such irregularity introduces uncertainty regarding the true measurement time of any retrieved value, especially in the sub-second range.

DCGM sampling behaviour DCGM relies on the same underlying measurement path as NVML and therefore inherits NVML's internal update characteristics. In practice, DCGM is commonly accessed through its exporter, which introduces an additional periodic sampling stage (typically around one second) resulting in markedly coarser temporal behaviour than NVML's native cadence. As a result, DCGM-based power telemetry rarely offers sub-second resolution in operational environments [29].

GPU utilization update cycles NVML's GPU utilization metric follows its own internal update cadence, separate from power. It is typically refreshed more frequently (on the order of tens of milliseconds) although the exact timing remains undocumented. While this metric does not track computational efficiency, its shorter update interval provides a comparatively more responsive indicator of device activity [29].

2.3.3 Redfish Sensor Refresh Intervals and Irregularity

Redfish exposes power telemetry through the baseboard management controller (BMC) and therefore inherits the temporal behaviour of its embedded sensing hardware and firmware. In contrast to on-chip interfaces such as RAPL or NVML, Redfish is designed for management-plane observability rather than high-frequency monitoring. Prior studies consistently report that Redfish refreshes whole-node power values at coarse intervals, typically ranging from several hundred milliseconds to multiple seconds, with the exact cadence depending on vendor, BMC firmware, and underlying sensor design [4, 14]. The Redfish standard does not define a minimum update frequency, and available documentation provides little insight into internal sampling or averaging strategies.

Measurement semantics of Redfish power values Redfish does not expose instantaneous electrical measurements. Instead, the reported values originate from on-board monitoring chips connected to shunt-based sensors and are subsequently processed inside the BMC. Vendor documentation indicates that these sensors inherently integrate power over tens to hundreds of milliseconds, and that additional firmware-level smoothing may be applied before values are published through the Redfish API [14]. Empirical evaluations support this interpretation: Wang et al. show that Redfish exhibits reaction delays of roughly two hundred milliseconds and displays particularly stable behaviour under steady loads, consistent with block-averaged rather than instantaneous sampling [4]. Because neither the sensor integration window nor any BMC filtering policies are defined in the standard, the temporal semantics of published values remain implementation-dependent.

Redfish power readings include a timestamp field, but this value reflects the BMC's observation time rather than the sampling instant of the physical power sensor. In many implementations, timestamps are rounded to seconds, which limits their utility for reconstructing sub-second dynamics and prevents reliable inference of the underlying sampling moment.

Beyond published work, empirical observations from the system used in this thesis reveal that Redfish update intervals may exhibit substantial variability. While nominal refresh periods appear regular over longer windows, individual samples occasionally show multi-second gaps, repeated values, or irregular spacing. Such behaviour is consistent with a telemetry source operating on management-plane

scheduling and BMC workload constraints rather than real-time guarantees. These observations do not generalise across vendors but illustrate the degree of temporal uncertainty that can occur in practice.

Overall, Redfish provides a widely supported mechanism for obtaining whole-system power readings and is well suited for coarse-grained monitoring or validation of other telemetry sources. Its coarse refresh intervals, lack of sensor-level timestamps, and implementation-dependent irregularities, however, make it unsuitable for analysing short-duration phenomena or for use as a primary source in high-resolution energy attribution.

2.3.4 Timing of Software-Exposed Metrics

Software-exposed resource metrics differ fundamentally from hardware-integrated telemetry sources: rather than publishing sampled power or energy values at device-defined intervals, the Linux kernel exposes cumulative counters whose temporal behaviour is almost entirely determined by when they are read. These interfaces therefore provide quasi-continuous visibility into system activity, but without intrinsic update cycles or timestamps that would define the sampling moment of the underlying measurement.

Cumulative counters in `/proc` and cgroups Kernel interfaces such as `/proc/stat`, per-task entries under `/proc/<pid>`, and the CPU accounting files in cgroups expose resource usage as monotonically increasing counters. These values are updated by the kernel during scheduler events, timer interrupts, and context-switch accounting, rather than at fixed intervals. As a consequence, their effective temporal resolution is determined entirely by the user's polling cadence: reading them more frequently produces more detailed deltas, but the kernel does not provide any guarantee about when a counter was last updated. None of these counters include timestamps, and their update timing may vary across systems due to tickless operation, kernel configuration, and workload characteristics.

Disk and network I/O statistics I/O-related counters follow the same principle. Entries such as `/proc/<pid>/io`, cgroup I/O files, and interface statistics in `/proc/net/dev` are incremented as part of the corresponding driver paths when I/O operations occur. They do not refresh periodically and therefore exhibit update patterns that mirror workload activity rather than a regular cadence. Temporal interpretation again depends entirely on the polling rate of the monitoring system.

eBPF-based event timing In contrast to cumulative counters, eBPF enables event-driven monitoring with explicit timestamps. Kernel probes attached to scheduler events, I/O paths, or tracepoints can record event times with high precision using the kernel's monotonic clock. As a result, eBPF metrics provide effectively instantaneous temporal resolution and are limited only by the overhead of probe execution and user-space consumption of BPF maps. No internal refresh cycle exists; events are timestamped at the moment they occur.

Performance counters and `perf`-based monitoring Hardware performance monitoring counters (PMCs), accessed via `perf_event_open`, advance continuously

within the processor. They do not follow a publish interval, and their timing semantics are defined solely by the instant at which user space reads the counter. This provides fine-grained and low-latency access to execution metrics such as cycles and retired instructions, with overhead rising only when polling is performed at very high frequencies.

Overall, software-exposed metrics behave as cumulative or event-driven signals rather than sampled telemetry sources. Their temporal characteristics are dominated by polling strategy and kernel-level event timing, with eBPF representing the only interface that attaches precise timestamps directly to system events.

2.4 Existing Tools and Related Work

Energy observability in containerized environments has attracted increasing attention in recent years, leading to the development of several tools that combine hardware, software, and statistical telemetry to estimate per-workload energy consumption. Despite this diversity, only a small number of tools attempt to attribute energy at container or pod granularity with sufficient detail to inform system-level research. Among these, *Kepler* has emerged as the most widely adopted open-source solution within the cloud-native ecosystem, while *Kubewatt* represents the first focused research effort to critically evaluate and refine Kepler's attribution methodology. Other frameworks, such as Scaphandre, SmartWatts, or PowerAPI, offer relevant ideas but differ in scope, telemetry assumptions, or operational goals. For this reason, the remainder of this section concentrates primarily on Kepler and Kubewatt, using these two tools to illustrate the architectural and methodological challenges that motivate the research gaps identified at the end of this chapter.

2.4.1 Kepler

2.4.1.1 Architecture and Metric Sources

Kepler[49] is a node-local energy observability agent designed for Kubernetes environments. Its architecture follows a modular dataflow pattern: a set of collectors periodically ingests telemetry from hardware and kernel interfaces, an internal aggregator aligns and normalizes these inputs, and a Prometheus exporter exposes the resulting metrics at container, pod, and node granularity. This structure allows Kepler to integrate heterogeneous telemetry sources while presenting a unified metric interface to external monitoring systems.

Kepler's collectors obtain process, container, and node telemetry from standard Linux and Kubernetes subsystems. Resource usage statistics are taken from `/proc`, cgroup hierarchies, and Kubernetes metadata, while hardware-level energy data is read from RAPL domains via the `powercap` interface. Optional collectors provide GPU metrics through NVIDIA's NVML library and platform-level power measurements via Redfish or other BMC interfaces. All inputs are treated as cumulative counters or periodically refreshed state, and their effective resolution is therefore determined by Kepler's sampling configuration. All metrics are updated at same interval and at the same time (default: 60 seconds for redfish, 3 seconds for all other sources). A central responsibility of the aggregator is to map raw per-process telemetry to containers and pods, using cgroup paths and Kubernetes API metadata. The derived metrics

are finally exposed via a Prometheus endpoint, enabling integration into common cloud-native observability stacks.

In contrast to generic system monitoring agents, Kepler's architecture is tailored specifically to Kubernetes. Its emphasis on container metadata, cgroup-based accounting, and workload-oriented metric aggregation distinguishes it from tools that operate primarily at the host or VM level. At the same time, its reliance on standard Linux interfaces keeps deployment overhead low, requiring only node-local access to `/proc`, cgroups, and the `powercap` subsystem.

Overall, Kepler's architectural design reflects a trade-off between flexibility and granularity: while it can ingest diverse telemetry sources and attribute energy at container level, its accuracy is constrained by the timing and resolution of the underlying metrics, as well as the unified sampling cadence chosen for the collectors.

Kepler updates all metrics within a single synchronous loop that triggers every sampling interval. This design simplifies integration but enforces a uniform cadence across heterogeneous telemetry sources, which contributes to the timing and alignment issues discussed in § 2.4.1.3. The structure is shown in Figures 2.1.

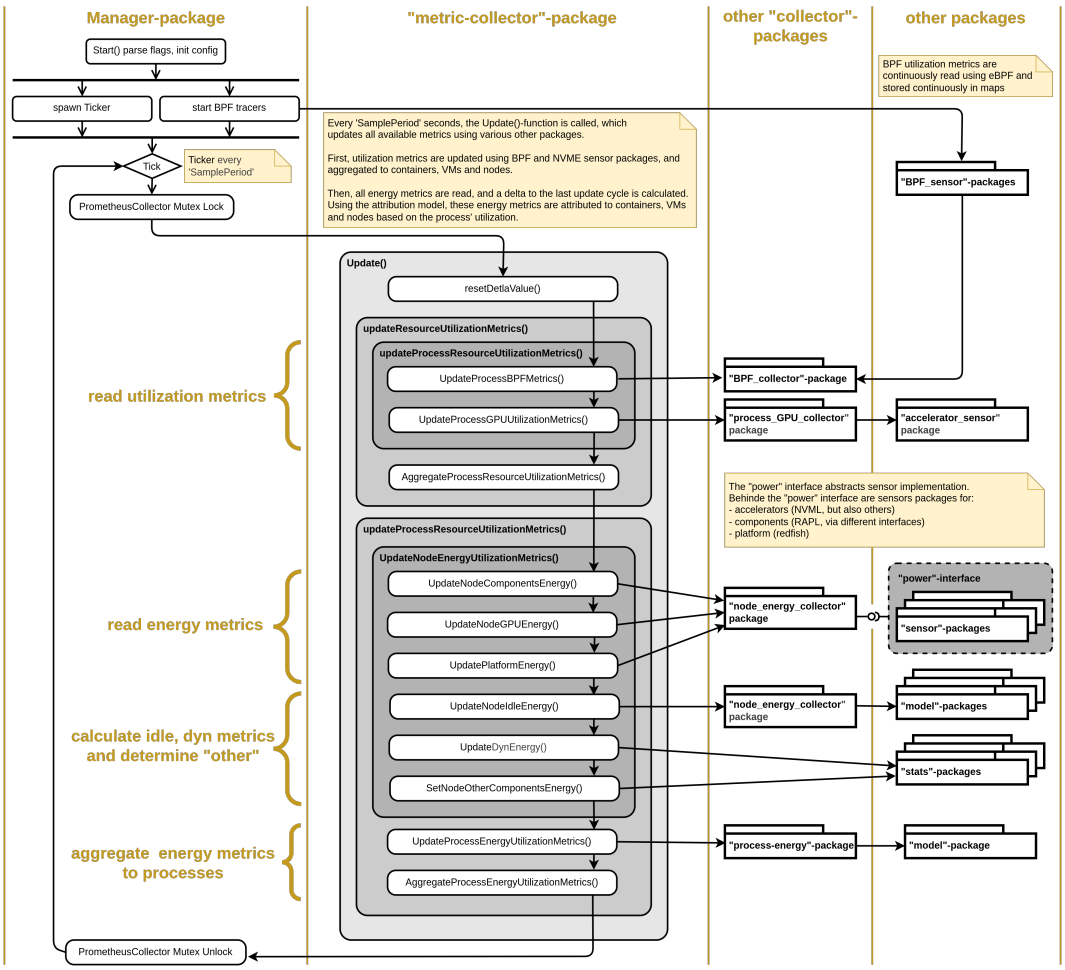

FIGURE 2.1: Kepler's synchronous update loop, where all collectors run at a unified sampling interval.

2.4.1.2 Attribution Model

Kepler's attribution logic follows a two-stage structure. First, node-level energy is decomposed into *idle* and *dynamic* components for each available power domain (package, core, uncore, DRAM, and optionally GPU or platform-level readings). Second, the dynamic portion is distributed across processes and containers according to their observed resource usage, while idle power is assigned using a domain-specific default policy.

Dynamic power is attributed proportionally using ratio-based models. For each domain, Kepler computes the energy delta over the sampling interval and distributes it according to a usage metric selected for that domain. Instructions, cache misses, and CPU time are used as primary signals, with fallbacks when a metric is unavailable. GPU dynamic power is attributed based on GPU compute utilization. Platform-level power, when available, is treated as a residual domain: after subtracting CPU and DRAM power, the remaining portion is shared across workloads using the designated default metric or, if none is configured (which is the case), an equal split.

Idle energy is handled separately. Kepler maintains a rolling estimate of minimum node-level power for each domain and treats these values as idle baselines. In the default configuration, idle energy is divided evenly across all active workloads during the attribution interval. While this behaviour differs from protocol recommendations that scale idle power by container size, Kepler applies a uniform policy across domains to ensure attribution completeness.

Attribution operates at process granularity, with container and pod values obtained by aggregating the processes mapped to each cgroup. This approach allows Kepler to attribute energy to short-lived or multi-process containers while retaining compatibility with Kubernetes metadata.

Kepler performs attribution at a fixed internal update interval (default: 3 s). All usage metrics and energy deltas within that interval are aggregated before attribution is computed. Because Prometheus scrapes occur independently of Kepler's internal loop, the exported time series may reflect misalignment when the scrape period is not a multiple of the update interval. This can lead to visible step patterns or oscillations, particularly for dynamic workloads. Despite these limitations, the model provides a coherent and workload-oriented view of node-level energy consumption suitable for cloud-native observability scenarios.

2.4.1.3 Observed Behavior and Limitations

Several studies and code-level inspections reveal that Kepler's attribution behaviour exhibits systematic limitations that affect accuracy and interpretability. The most comprehensive empirical evaluation to date, conducted by Pijnacker et al., demonstrates that attribution inaccuracies arise even when node-level power estimation is reliable[50]. Their experiments highlight that idle power is often distributed to containers that are no longer active, including Completed pods, and that dynamic power can be reassigned inconsistently when containers are added or removed. These effects stem from the coupling of process-level accounting with container lifecycle events, which may lag behind cgroup or Kubernetes metadata updates.

Timing mismatches further contribute to attribution artifacts. High-frequency CPU

and cgroup statistics are combined with slower telemetry sources such as Redfish, whose update intervals may span tens of seconds. When workload intensity changes during such periods, Kepler may assign disproportionately large or small dynamic energy shares to individual containers. Similar behavior occurs at the Prometheus interface when scrape intervals do not align with Kepler's internal update loop, producing visible oscillations in the exported time series.

Source-code inspection reinforces these observations. Numerous unimplemented or placeholder sections (e.g. TODO markers) affect key components of the ratio-based attribution model and default configuration paths. In particular, some domains lack explicit usage metrics, leading to fallback behaviour and equal-cost splitting regardless of container activity. GPU attribution relies on a single utilization metric and is therefore sensitive to the temporal behaviour of NVML's sampling. Together, these issues introduce variability across domains and reduce the transparency of the resulting per-container energy values.

Lifecycle handling also presents challenges. Because container metadata is aggregated from process-level information, short-lived or Completed pods may retain residual energy assignments. Conversely, system processes that cannot be mapped cleanly to Kubernetes abstractions may absorb unassigned power, obscuring the relationship between application behaviour and observed consumption.

Overall, these limitations underscore that Kepler provides a practical but imperfect approximation of container-level energy consumption. The observed behaviour motivates the research gaps identified at the end of this section, particularly the need for finer temporal resolution, explicit handling of idle and residual power, configurable attribution models, and more robust reconciliation across heterogeneous telemetry sources.

2.4.1.4 Kepler v0.10.0

In July 2025, Kepler underwent a substantial architectural redesign with the release of version 0.10.0[51]. The new implementation replaces many of the privileged operations used in earlier versions, removing the need for `CAP_BPF` or `CAP_SYSADMIN` and reducing reliance on kernel instrumentation. Instead, Kepler now obtains all workload statistics from read-only `/proc` and cgroup interfaces. This reduction in privilege requirements significantly improves deployability and security, particularly for managed Kubernetes environments where eBPF- or perf-based approaches are infeasible.

The redesign also introduces a markedly simplified attribution model. Whereas earlier versions combined multiple hardware and software counters (e.g. instructions, cache misses, GPU utilization) to estimate dynamic energy, Kepler v0.10.0 relies exclusively on CPU time as the usage metric. Node-level dynamic energy is computed by correlating RAPL deltas with aggregate CPU activity, and each workload receives a proportional share of this value based solely on its CPU time fraction. Idle energy is not distributed to containers and instead remains part of a node-level baseline. Containers, processes, and pods are treated as independent consumers drawing from the same active-energy pool, with no dependence on process-derived aggregation.

These changes increase robustness and predictability: the simplified model is easier to reason about, less sensitive to heterogeneous workloads or timing mismatches,

and compatible with environments where kernel-level measurement facilities are unavailable. However, the loss of metric flexibility substantially reduces modeling fidelity. Fine-grained distinctions between compute-bound and memory-bound tasks are no longer observable, and the attribution model presumes a strictly linear relationship between CPU time and power consumption. As a result, Kepler v0.10.0 no longer targets high-accuracy energy attribution but instead emphasises operational stability and minimal overhead.

For the purposes of this thesis, Kepler v0.10.0 is relevant primarily as an indication of the project's strategic shift toward simplicity and broad deployability. Its CPU-time-only model is not suitable as a basis for Tycho, whose objectives require higher temporal resolution, more diverse metric inputs, and explicit handling of domain-level energy contributions. Accordingly, the remainder of this chapter focuses on the behaviour of Kepler v0.9.x, which remains the most representative version for research-oriented attribution discussions.

2.4.2 KubeWatt

KubeWatt is a proof-of-concept exporter developed by Pijnacker as a direct response to the attribution issues uncovered in Kepler.[50, 52] Rather than extending Kepler's complex pipeline, KubeWatt implements a deliberately narrow but transparent model that focuses on correcting three specific problems: misattribution of idle power, leakage of energy into generic "system processes", and unstable behaviour under pod churn. It targets Kubernetes clusters running on dedicated servers and assumes that a single external power source per node is available (in the prototype, Redfish/iDRAC).

A central design decision is the strict separation between *static* and *dynamic* power. Static power is defined as the baseline cost of running the node and its control plane in an otherwise idle state. KubeWatt measures or estimates this baseline once and treats it as a constant; it is *not* attributed to containers. Dynamic power is then computed as the difference between total node power and this static baseline and is the only quantity distributed across workloads. Control-plane pods are explicitly excluded from the dynamic attribution set, so their idle consumption remains part of the static term and does not pollute application-level metrics.

To obtain the static baseline, KubeWatt provides two initialization modes. In *base initialization*, the cluster is reduced to an almost idle state (only control-plane components), and node power is sampled for a few minutes. The static power value is computed as a simple average, yielding a highly stable estimate under the test conditions. When workloads cannot be stopped, *bootstrap initialization* fits a regression model to time series of node power and CPU utilization collected during normal operation. The regression is evaluated at the average control-plane CPU usage to infer the static baseline. This mode is more sensitive to workload characteristics and SMT effects but provides a practical fallback when base initialization is not feasible.

During normal operation, KubeWatt runs in an *estimation mode* that attributes dynamic node power to containers proportionally to their CPU usage. CPU usage is obtained from the Kubernetes metrics API (`metrics.k8s.io`) at node and container level. The denominator explicitly sums only container CPU usage; system

processes, cgroup slices, and other non-container activity are excluded by construction. This corrects a key source of error in Kepler, where slice-level metrics and kernel processes could receive non-trivial fractions of node power. Under stable workloads and at the relatively coarse sampling interval used in the prototype, KubeWatt achieves container-level power curves that align well with both iDRAC readings and observed CPU utilisation, and it behaves robustly when large numbers of idle pods are created and deleted.

The scope of KubeWatt is intentionally narrow. It is CPU-only, uses a single external power source per node, assumes that Kubernetes is the only significant workload on the machine, and does not attempt to model GPU, memory, storage, or network energy. It also inherits the temporal limitations of the Kubernetes metrics pipeline and treats Redfish power readings as instantaneous, without explicit latency compensation. Nevertheless, KubeWatt demonstrates that a simple, well-documented ratio model with explicit static–dynamic separation and strict cgroup filtering can eliminate several of Kepler's most problematic attribution artefacts. These design principles are directly relevant for the attribution redesign pursued in this thesis and inform the requirements placed on Tycho's more general, multi-source architecture.

2.4.3 Other Tools (Brief Overview)

Beyond Kepler, several tools illustrate the methodological diversity in container- and process-level energy attribution, although they are not central to the Kubernetes-specific challenges addressed in this thesis. Scaphandre[53] provides a lightweight proportional attribution model based exclusively on CPU time and RAPL deltas. Its design emphasises simplicity and portability, offering basic container mapping through cgroups but limited control over sampling behaviour or attribution semantics. SmartWatts[54], by contrast, represents a more sophisticated approach: it builds performance-counter-based models that self-calibrate against RAPL measurements and adapt dynamically to the host system. While effective in controlled environments, SmartWatts requires access to perf events, provides only CPU and DRAM models, and is not deeply integrated with Kubernetes abstractions.

A broader ecosystem of lightweight tools (e.g. CodeCarbon[55] and related library-level estimators) demonstrates further variation in scope and assumptions, but these generally target high-level application profiling rather than system-wide workload attribution. Collectively, these tools highlight a spectrum of design choices (from simplicity and portability to model-driven estimation) but none address the combination of high-resolution telemetry, multi-tenant attribution, and Kubernetes metadata integration that motivates the development of Tycho.

2.4.4 Cross-Tool Limitations Informing Research Gaps

Across the surveyed tools, several structural limitations recur despite substantial differences in design philosophy and implementation. First, temporal granularity remains insufficient: although hardware interfaces such as RAPL support millisecond-level updates, most tools aggregate measurements over multi-second intervals. This obscures short-lived workload behaviour and reduces attribution fidelity, particularly in heterogeneous or bursty environments. Second, all tools depend on telemetry sources whose internal semantics are only partially documented. Ambiguities regarding RAPL domain coverage, NVML power reporting, or BMC-derived node

power constrain both the interpretability and the auditability of reported metrics, reinforcing the black-box character of current measurement pipelines.

Idle-power handling presents a further source of inconsistency. Tools differ widely in how idle power is defined, whether it is attributed, and to whom. These choices are often implicit, undocumented, or constrained by implementation artefacts, leading to attribution patterns that are difficult to interpret or reproduce. Multi-domain coverage is similarly limited: existing tools focus primarily on CPU and, to a lesser extent, DRAM or GPU consumption, leaving storage, networking, and other subsystems unmodelled despite their relevance to node-level energy use.

Metadata lifecycle management also emerges as a common limitation. Rapid container churn, transient pods, and the interaction between Kubernetes and cgroup identifiers can produce incomplete or stale workload associations, affecting attribution stability. Finally, attribution models themselves are typically rigid. Most tools hard-code a specific proportionality assumption (commonly CPU time or a single hardware counter) and provide limited support for calibration, uncertainty quantification, or alternative modelling philosophies.

Taken together, these limitations reveal structural gaps in current approaches to container-level energy attribution. They motivate the need for tools that combine high-resolution telemetry handling, transparent and configurable attribution logic, robust metadata management, and principled treatment of uncertainty. The next section distills these observations into concrete research gaps that inform the design objectives of Tycho.

2.5 Research Gaps

This section synthesises the findings from the preceding analyses of telemetry sources, temporal behaviour, and existing tools. Across these perspectives, a set of structural limitations emerges that fundamentally constrains accurate and explainable energy attribution in Kubernetes environments. These limitations arise at three intertwined layers: the measurement interfaces exposed by hardware and kernel subsystems, the attribution models built on top of these measurements, and the operational context in which Kubernetes workloads execute. Taken together, they demonstrate the absence of a framework that provides high temporal precision, transparent modelling assumptions, and robustness to container lifecycle dynamics. The gaps identified below define the technical requirements that motivate the design of Tycho.

(1) Measurement Gaps: Temporal Resolution and Telemetry Semantics

Existing tools do not exploit the full temporal capabilities of modern hardware telemetry. Interfaces such as RAPL offer fast, reliable update frequencies, yet tools operate on fixed multi-second loops, causing short-lived or bursty activity to be temporally averaged away. Moreover, latency mismatches between high-frequency utilization signals (e.g. cgroups, perf counters) and low-frequency power interfaces (e.g. Redfish/BMC) introduce structural attribution errors that are not explicitly modelled or corrected.

A related issue is the opacity of hardware telemetry. RAPL, NVML, and BMC power sensors provide indispensable data, but their domain boundaries, averaging windows, and internal update behaviour are insufficiently documented. This prevents rigorous interpretation of reported values and inhibits the development of calibration or uncertainty models. Finally, measurement coverage remains incomplete: while CPU and DRAM domains are widely supported, no standardised telemetry exists for storage, networking, or other subsystems. Current tools treat these components either implicitly (as part of "platform" power) or not at all.

(2) Attribution Model Gaps: Rigidity, Idle Power, and Domain Consistency

Current attribution models rely on rigid proportionality assumptions (typically CPU time, instructions, or a single hardware counter) without considering alternative modelling philosophies. Idle power remains a persistent source of inconsistency: tools variously divide it evenly, proportionally, or not at all, often without documenting the rationale. These choices have substantial effects on per-container energy values, particularly in lightly loaded or heterogeneous systems.

At the domain level, attribution methods are not unified. CPU, DRAM, uncore, GPU, and platform energy are treated through incompatible heuristics, and many domains fall back to equal distribution when no clear usage signal is defined. None of the surveyed tools quantify uncertainty, despite relying on noisy, coarse, or undocumented telemetry sources. As a result, attribution outputs appear deterministic even when they rest on incomplete or ambiguous measurement assumptions.

(3) Metadata and Lifecycle Gaps: Churn, Timing, and Virtualization

Container-level attribution requires consistent mapping between processes, cgroups, and Kubernetes metadata. Existing tools struggle in scenarios with rapid container churn, ephemeral or Completed pods, and multi-process containers. Mismatches between metadata refresh cycles and metric sampling lead to stale or missing associations, which propagate into attribution artefacts.

Energy attribution inside virtual machines remains essentially unsolved. No standard mechanism exists for exposing host-side telemetry to guest systems in a way that preserves temporal alignment and attribution consistency. The limited QEMU-based passthrough available in Scaphandre is not generalisable, and conceptual proposals (e.g. Kepler's hypercall mechanism) remain unimplemented. Given the prevalence of cloud-hosted Kubernetes clusters, this constitutes a major practical limitation.

(4) Usability, Transparency, and Operational Gaps

For most tools, implementation assumptions, fallback paths, and attribution decisions are implicit. Users cannot easily distinguish measured values from estimated ones, nor identify the assumptions underlying attribution outputs. This lack of transparency reduces trust and complicates debugging.

Operational constraints further restrict applicability. Tools that require privileged kernel instrumentation (eBPF, `perf_event_open`) are unsuitable for many production clusters, while tools designed around unprivileged access often sacrifice

modelling fidelity. At the same time, developers, operators, and researchers have fundamentally different observability needs, yet existing tools optimise for only one audience at a time. None provide configurable attribution modes or role-specific abstractions.

(5) Missing Support for Calibration and Validation

Beyond isolated exceptions, existing tools provide limited mechanisms for systematic calibration or validation of their attribution models. KubeWatt is one of the few systems that performs explicit baseline calibration, offering both an idle-power measurement mode and a statistical fallback for environments without idle windows. Kepler offers no structured calibration workflow, and its estimator models lack reproducible training procedures. SmartWatts introduces online model recalibration but focuses narrowly on performance-counter regression, leaving node-level baselines, multi-domain alignment, and external ground-truth integration unaddressed.

Across all tools, there is no standardized path to incorporate external measurements (for example from wall-power sensors or BMC-level telemetry) to validate or refine model behaviour. Idle power is seldom isolated as a first-class parameter, attribution error is rarely quantified, and no system provides uncertainty estimates that reflect measurement or modelling limitations. Without such calibration and validation capabilities, attribution accuracy cannot be assessed, corrected, or improved over time—an essential requirement for any system intended to provide trustworthy, high-resolution energy insights in Kubernetes environments.

2.6 Summary

The analyses in this chapter reveal that modern server platforms provide a heterogeneous and only partially documented set of telemetry interfaces whose temporal and semantic properties fundamentally constrain container-level energy attribution. Hardware-integrated sources such as RAPL and NVML expose valuable domain-level energy information but differ substantially in update behaviour, averaging semantics, and domain completeness. Out-of-band telemetry via Redfish provides stable whole-system measurements but at coarse and irregular temporal granularity. Software-exposed metrics offer fine-grained visibility into workload behaviour, yet they measure utilisation rather than power and depend entirely on polling strategies for temporal interpretation.

Temporal irregularities, internal averaging, and undocumented sensor behaviour reduce the effective precision of all telemetry sources, especially when attempting to capture short-lived workload dynamics. Existing tools aggregate these heterogeneous signals using fixed multi-second sampling loops and rigid proportionality assumptions, which leads to systematic attribution artefacts. Idle power is treated inconsistently across systems, residual power is frequently conflated with workload activity, and multi-domain attribution remains fragmented in both semantics and implementation. Metadata churn and asynchronous refresh cycles further complicate the mapping between processes, containers, and Kubernetes abstractions, reducing the stability and interpretability of attribution outputs.

The cross-tool evaluation confirms these structural limitations. Kepler provides broad telemetry integration but struggles with timing mismatches, incomplete domain semantics, and opaque idle handling. Kubewatt demonstrates the importance of explicit baseline separation and cgroup filtering, yet remains limited to single-domain CPU-based estimation. Other tools illustrate a spectrum of design choices but do not address the combined challenges of high-frequency telemetry, multi-domain attribution, container lifecycle dynamics, and Kubernetes integration.

Together, these findings motivate the need for a framework that provides high temporal fidelity, transparent modelling assumptions, unified domain treatment, explicit handling of idle and residual energy, and robust metadata reconciliation. These requirements form the conceptual and architectural foundations developed in Chapter 3, which introduces the methodological principles guiding the design of Tycho.

Chapter 3

Conceptual Foundations of Container-Level Power Attribution

Energy attribution explains how workloads contribute to the power consumed by a node. Hardware exposes only aggregate energy behaviour, so attribution constructs a model that distributes this aggregate across multiple sources of activity. The aim of this chapter is to establish the conceptual basis for such modelling. It introduces the abstractions needed to reason about workloads, execution units, temporal structure, and observation windows. It also presents the principles that constrain any defensible attribution model and identifies the interactions that make attribution non-trivial. The discussion is purely conceptual and does not rely on empirical detail from Chapter 2. These concepts form the foundation for the system requirements developed later in the chapter and for the architectural design presented in Chapter 4.

3.1 Nature and Purpose of Power Attribution

Power attribution is a modelling activity. Hardware reports only aggregate power or energy, and attribution constructs an explanation that distributes this aggregate across the workloads running on the node. The model is necessarily reactive because measurements become available only after the underlying activity has occurred. Attribution therefore explains past energy behaviour rather than providing realtime insight, although the resulting information can support optimisation and accountability.

Attribution is useful because it reveals how different workloads contribute to dynamic power consumption. This enables comparisons between workloads, supports evaluation of deployment or scheduling strategies, and provides interpretable information for higher level policy decisions.

For the purposes of this chapter, a workload is defined as a logical entity that groups one or more execution units into a stable attribution target. Execution units may include processes, threads, containers, virtual machines, or service components. Their membership can change over time, but the workload identity persists as the object to which energy is assigned.

3.2 Workload Identity and Execution Boundaries

Energy attribution operates on workload identities rather than on individual execution units. Execution units such as processes, threads, or container instances appear and terminate independently, often with lifetimes that do not align with observation windows. Their behaviour may overlap, interleave, or succeed one another in ways that complicate any direct mapping between activity and energy. A workload need not coincide with a single application; it may represent a subset of an application, a combination of cooperating services, or a logical grouping chosen purely for attribution.

Attribution therefore relies on a stable abstraction that groups such units into coherent entities. Orchestration frameworks, including systems such as Kubernetes, illustrate this principle by associating container instances with higher level constructs such as pods or services. The attribution target is the logical workload, not the transient units that realise it at any moment.

Short lived execution units raise specific challenges. Some may terminate between consecutive measurements, and their activity may be only partially observable. Others may overlap in time while belonging to the same workload identity. A consistent attribution model must track these changing memberships without losing energy when units disappear or double counting energy when multiple units contribute concurrently. Stable workload identities provide the conceptual basis for such tracking.

3.3 Principles of Workload-Level Energy Attribution

Several principles constrain how node-level energy can be attributed to workloads. These principles are intertwined and reflect structural properties of shared hardware, the limits of observability, and the semantics of available metrics. Some depend on how measurements are structured in time, while others remain independent of temporal detail. The temporal aspects are developed further in § 3.4, but the principles themselves abstract from any specific system and define the conditions that any defensible attribution model must satisfy.

3.3.1 Aggregated Hardware Activity

Hardware exposes only aggregate power or energy for the node or for coarse hardware domains. It does not reveal how much of this consumption originates from any specific workload. Attribution therefore begins with a single observable quantity that reflects the combined activity of all execution units. Any per workload assignment is an inferred decomposition of this aggregate and must remain consistent with the measured total.

3.3.2 Domain Decomposition

Total system power is composed of contributions from several hardware domains, such as compute, memory, accelerators, storage, and platform circuitry. These domains respond differently to workload behaviour, and their relative impact varies across systems. Attribution must therefore reason at the domain level before assigning energy to workloads. Without such decomposition, the resulting assignments

would combine unrelated forms of activity and obscure the link between workload characteristics and observed power.

3.3.3 Conservation

Node-level energy is a fixed quantity within any observation window. An attribution model must assign energy to workloads in a way that is consistent with this total. The sum of all assigned energy, including any explicitly modelled background components, must equal the measured dynamic energy. Violations of conservation indicate that the model is incomplete or internally inconsistent.

3.3.4 Static–Dynamic Separation

System power consists of a baseline component that persists regardless of workload activity and a dynamic component induced by the workloads. Attribution concerns only the dynamic portion, so the baseline must be treated explicitly rather than absorbed into workload assignments. Any remaining unexplained energy must appear as a residual component and must not be redistributed silently across workloads.

3.3.5 Uncertainty and Non-Uniqueness

Workload-level energy attribution has no unique ground truth. Limited observability, asynchronous measurements, and interactions between hardware domains allow multiple decompositions of the same aggregate energy to be consistent with the measurements. A defensible attribution model must acknowledge this non-uniqueness and avoid implying precision that the underlying information does not support.

3.3.6 Dependence on Metric Fidelity

Attribution quality depends on the fidelity of the metrics that describe workload activity. Each metric has specific semantics, precision, and temporal resolution, and these properties determine how reliably the metric reflects the underlying hardware behaviour. An attribution model must therefore interpret metrics consistently and acknowledge that limited or coarse measurements constrain the accuracy of any inferred energy assignments.

Hardware subsystems are shared and not fully partitionable. Execution units contend for caches, memory controllers, and shared frequency or power budgets, and these interactions alter the relation between observed activity and actual power consumption. Such interference reduces the ability of any metric to isolate per workload effects and increases attribution uncertainty. A defensible model must incorporate these limitations when relating activity signals to domain level energy.

3.4 Temporal and Measurement Foundations

Attribution depends not only on which quantities are measured but also on when they are measured. Telemetry sources observe system behaviour at different times, with different implicit meanings, and with no inherent coordination. A clear temporal framework is therefore required to interpret workload activity and relate it to the energy observed at the node.

Observation Windows

Attribution operates on observation windows. A window integrates power and activity over a chosen duration and provides the temporal unit within which energy is assigned to workloads. All attribution reasoning occurs within these windows, so their boundaries determine which activity contributes to the measured energy and how temporal ambiguity affects attribution accuracy.

3.4.1 Sampling vs Event-Time Perspectives

Sampling records system state at fixed intervals, independent of when the underlying activity changes. Event time reflects the moment when the activity occurs or when a telemetry source updates its value. These perspectives rarely coincide. If a workload is active between two samples, the sampled values do not reveal when within the interval the activity occurred. Misalignment between when work happens and when it is observed creates ambiguity about how activity should be mapped into the observation window.

3.4.2 Clock Models and Temporal Ordering

Attribution requires a consistent ordering of events and measurements. Realtime clocks track wall clock time but may jump when synchronised, which breaks temporal ordering. Monotonic clocks advance continuously and therefore provide a stable basis for placing events on a time axis. A coherent attribution model relies on such ordering to determine which activity belongs to which observation window and to avoid artefacts caused by clock adjustments.

3.4.3 Heterogeneous Metric Sources

Telemetry originates from sources with different update cycles and semantics. Hardware counters accumulate events continuously and reveal activity only when read. Operating system accounting updates periodically according to scheduler behaviour. Device telemetry and external power interfaces publish measurements based on internal schedules. These sources do not share cadence, precision, or timestamp meaning. Their values represent different kinds of temporal information, and none can be assumed to align with the others.

3.4.4 Delay, Jitter, and Temporal Uncertainty

Measurements do not appear at the moment the underlying behaviour occurs. Observation delay arises when a metric is read after the activity has taken place. Publication delay arises when a telemetry source exposes an updated value only after internal processing. Jitter denotes variations in these delays. Because different sources exhibit different forms of delay, the temporal relation between activity and observed energy is uncertain. This uncertainty limits the precision with which activity can be linked to energy within an observation window.

3.4.5 Temporal Alignment of Asynchronous Signals

Attribution requires heterogeneous signals to be interpreted within the same observation window even though they arrive at different times and represent different temporal semantics. Some values describe cumulative changes, others instantaneous states, and others discrete events. A temporal alignment model must reconcile these signals without assuming true synchronisation. The goal is not to remove temporal uncertainty but to structure it so that attribution remains coherent and consistent with the measured energy.

3.5 Conceptual Attribution Frameworks

Because hardware exposes only aggregate energy, several modelling philosophies can be used to distribute this energy across workloads. These frameworks differ in how they relate activity metrics to energy and in how they treat uncertainty. None yields a unique solution, since the same measurements can support multiple plausible decompositions. Instead, each framework reflects a particular set of priorities, such as stability, fairness, or explanatory power, and provides a structured interpretation of the same underlying observations.

3.5.1 Proportional Attribution

Proportional attribution assigns energy to workloads in proportion to an observed activity metric, such as CPU time or memory access volume. Its appeal lies in its simplicity and interpretability. However, different metrics emphasise different forms of behaviour, and proportionality with respect to one metric does not imply proportionality with respect to another. The choice of metric therefore has direct consequences for the resulting attribution.

3.5.2 Shared-Cost Attribution

Shared-cost attribution distributes some portion of the dynamic energy uniformly or proportionally across all active workloads, independent of their individual activity levels. This approach emphasises stability and fairness and is often used when activity metrics are incomplete or unreliable. Its limitation is that it may obscure relationships between workload behaviour and energy consumption, since unexplained costs are not tied to specific activity.

3.5.3 Residual and Unattributed Energy

Some energy cannot be explained by available metrics or by direct workload activity. Subsystems without meaningful utilisation signals, background services, and asynchronous events contribute to a residual component. Treating this component explicitly preserves conservation and avoids distorting the energy assigned to observable activity. Residual energy also delineates the boundary between explainable and unexplained behaviour within an attribution model.

3.5.4 Model-Based or Hybrid Attribution

Model-based or hybrid attribution combines several activity signals into an explicit model of energy consumption. Such a model may weight metrics from different domains, encode domain-specific relationships, or blend proportional and shared-cost

components. It does not attempt to establish strict causality, but it treats the mapping from activity to energy as a structured function rather than a single proportional rule. The quality of the resulting attribution depends on how well the model captures the relevant relationships and on how stable these relationships remain across workloads and system states.

3.5.5 Causal or Explanatory Attribution

Causal or explanatory attribution attempts to relate changes in workload activity to changes in power consumption. It seeks to model relationships between metrics and energy rather than applying proportionality directly. This approach can capture more nuanced behaviour, but its accuracy depends on metric fidelity and on the stability of the relationship between activity and power. Limited observability and shared subsystem interactions restrict the strength of causal inferences.

Link to System Requirements

These frameworks illustrate the range of assumptions an attribution model may adopt. They highlight the need for transparent modelling choices, consistent interpretation of metrics, explicit treatment of residual components, and temporal coherence when relating activity to energy. In practice, their behaviour is further constrained by shared hardware, domain interactions, and temporal misalignment, which shape how any chosen framework behaves under real workloads. These combined effects are examined in § 3.6 and motivate the system requirements developed in § 3.7.

3.6 Interactions and Complications

The principles and temporal concepts introduced above interact in ways that make workload-level attribution fundamentally approximate. These interactions arise from shared hardware, limited observability, asynchronous measurements, and the structure of workloads themselves.

Combined Effects of Shared Hardware and Temporal Misalignment

Shared subsystems create interference that couples the activity of different workloads. Contention for caches, memory controllers, or shared power and frequency budgets alters the relation between observed activity and actual energy consumption. Temporal misalignment compounds this effect. When activity and power are observed at different times and with different delays, the ambiguity introduced by interference cannot be resolved by sampling alone. The combined effect limits the extent to which per workload contributions can be isolated.

Cross-Domain Interactions

Hardware domains are not independent. Changes in compute activity can influence memory behaviour or power states, and accelerators may shift platform level consumption. These interactions mean that energy attributed to one domain may reflect behaviour originating in another. Attribution must therefore operate under the constraint that domain boundaries provide structure but not complete separation.

Attribution as an Inverse Problem

Because only aggregate energy is measured, attribution requires inferring per workload contributions from incomplete and asynchronous observations. This inference is an inverse problem with multiple admissible solutions. Limited metric fidelity, shared hardware behaviour, and temporal uncertainty restrict how precisely activity can be mapped to energy. A coherent attribution model acknowledges these limitations and structures them explicitly rather than treating them as noise.

3.7 Conceptual Challenges and System Requirements

The challenges identified above arise from shared hardware behaviour, asynchronous and heterogeneous measurements, limited metric fidelity, and volatile workload lifecycles. Any attribution system must address these challenges within a coherent conceptual framework. The requirements formulated in this section follow directly from the principles and temporal foundations established earlier and specify the conditions that an attribution model shall satisfy.

3.7.1 Requirement: Temporal Coherence

The system *must* maintain coherent temporal structure across all telemetry sources. Measurements that arrive with differing delays, cadences, or timestamp semantics *shall* be placed on a consistent time axis and related correctly to the boundaries of the observation window. The system *should* tolerate irregular update patterns without introducing artefacts, and it *may* employ temporal reconstruction provided that ordering and conservation are preserved.

3.7.2 Requirement: Domain-Level Consistency

The system *must* decompose node-level energy into meaningful hardware domains before workload-level assignment. Each domain *shall* be treated using internally consistent rules, and the system *must not* combine unrelated forms of activity into a single attribution pathway. When direct observability is incomplete, the system *should* incorporate explicit residual modelling, and it *may* use domain specific strategies when justified by domain characteristics.

3.7.3 Requirement: Cross-Domain Reconciliation

The system *must* reconcile energy information from different hardware domains in a coherent manner. When domain-level signals disagree, the reconciliation strategy *shall* be explicit and internally consistent rather than relying on implicit priority rules. The system *should* expose when domains provide conflicting indications about energy usage and clarify how such conflicts influence per workload assignments. Any reconciliation *must not* violate conservation across domains or undermine the stability of workload-level attribution.

3.7.4 Requirement: Consistent Metric Interpretation

The system *must* interpret activity metrics in a stable and coherent manner. Metrics that differ in semantics, resolution, or precision *shall* not be combined without clear conceptual justification. The system *must not* allow the meaning of a metric to

vary across time or domains. It *should* treat metric limitations explicitly, and it *may* disregard metrics whose quality does not support meaningful attribution.

3.7.5 Requirement: Transparent Modelling Assumptions

All assumptions used to relate activity to energy *must* be explicit. The basis on which energy is distributed *shall* be interpretable, including the choice of attribution framework, the handling of idle and residual energy, and any fallback behaviour in the presence of incomplete metrics. The system *should* separate measured quantities from inferred quantities to avoid ambiguity, and it *may* expose configurable modelling options provided they do not violate consistency or conservation.

3.7.6 Requirement: Lifecycle-Robust Attribution

The system *must* remain consistent under workload churn. Execution units that appear or terminate within an observation window *shall* be tracked in a way that avoids both loss of energy and double counting. Workload identities *must* remain stable even when their underlying execution units change. The system *should* support overlapping lifecycles and transient units without degrading attribution quality, and it *may* use buffering or reconciliation strategies when necessary.

3.7.7 Requirement: Uncertainty-Aware Attribution

The system *should* acknowledge uncertainty arising from limited observability, shared hardware behaviour, and temporal misalignment. It *shall* avoid implying precision that the measurements do not support. Where feasible, it *should* represent unexplained energy explicitly rather than absorbing it into unrelated workloads. Any handling of uncertainty *must not* violate conservation or temporal ordering.

Link to Architectural Considerations

These requirements imply that an attribution system must provide mechanisms for temporal alignment, domain level reasoning, stable metric interpretation, explicit residual handling, and robust tracking of workload identities. They form the basis for the architectural design presented in Chapter 4.

3.8 Summary

This chapter introduced the conceptual foundations of workload-level energy attribution. It defined workloads and execution units, presented the principles that govern how aggregate energy can be decomposed, and developed the temporal and measurement concepts required to interpret heterogeneous telemetry. It also showed how shared hardware behaviour, metric limitations, and asynchronous observations interact to make attribution inherently approximate. These considerations led to a set of system requirements that any attribution model must satisfy. The next chapter builds on these requirements and introduces an architecture designed to meet them.

Chapter 4

System Architecture

4.1 Guiding Principles

Tycho's architecture is shaped by a small set of foundational principles that govern how measurements are interpreted, combined and ultimately attributed. These principles are architectural in nature: they articulate *how* the system must reason about observations, not *how* it is implemented. They establish the conceptual baseline that the subsequent sections refine in detail.

- **Accuracy-first temporal coherence.** Architectural decisions prioritise the reconstruction of temporally coherent views of system behaviour. Observations are treated as samples of an underlying physical process, and the architecture is designed to preserve their temporal meaning rather than force periodic alignment.
- **Domain-aware interpretation.** Metric sources differ in semantics and cadence. The architecture respects these differences and avoids imposing artificial synchrony or uniform sampling behaviour across heterogeneous domains.
- **Transparency of assumptions.** All modelling assumptions must be explicit, inspectable and externally visible. The architecture prohibits implicit corrections or hidden inference steps that would obscure how measurements lead to attribution results.
- **Uncertainty as a first-class concept.** Missing, stale or delayed information is treated as uncertainty rather than error. Architectural components convey and preserve uncertainty so that later stages may interpret it correctly.
- **Separation of observation, timing and attribution.** Measurement collection, temporal interpretation and energy attribution form distinct architectural layers. This separation prevents cross-coupling, clarifies responsibilities and ensures that improvements in one layer do not implicitly alter the behaviour of others.

4.2 Traceability to Requirements

The architectural structure introduced in this chapter provides a direct response to the requirements established in § 3.7. Each requirement class corresponds to specific architectural mechanisms, ensuring that the system design follows from formal constraints rather than implementation convenience.

Requirement: Temporal Coherence. Satisfied through event-time reconstruction, independent collector timelines, and window-based temporal alignment.

Requirement: Domain-Level Consistency. Addressed by per-domain interpretation layers, domain-aware handling of metric semantics, and explicit decomposition of node-level signals.

Requirement: Cross-Domain Reconciliation. Supported by a unified temporal model, window-level aggregation boundaries, and explicit reconciliation logic across domains during analysis.

Requirement: Consistent Metric Interpretation. Ensured by separating observation from interpretation, enforcing stable metric semantics within each domain, and isolating heterogeneous metrics into dedicated processing paths.

Requirement: Transparent Modelling Assumptions. Realised through explicit modelling steps, external visibility of assumptions, and separation between measured and inferred quantities.

Requirement: Lifecycle-Robust Attribution. Enabled by metadata freshness guarantees, stable process–container mapping, and attribution rules that remain valid under workload churn.

Requirement: Uncertainty-Aware Attribution. Supported by explicit treatment of stale or missing data, uncertainty propagation in window evaluation, and preservation of unexplained residuals.

4.3 High-Level Architecture

4.3.1 Subsystem Overview

Tycho is organised into a small set of subsystems, each with a distinct responsibility. The following overview introduces these subsystems without yet describing their interactions.

Timing engine. Defines the temporal reference used throughout the system and provides the notion of analysis windows. It is responsible for deciding when a window is complete and ready to be evaluated.

Metric collectors. Acquire observations from hardware and software sources and attach timestamps in the global temporal reference. They expose their output as streams of samples without coordinating with each other.

Metadata subsystem. Maintains the mapping between operating-system level entities and workload identities. It tracks relationships between processes, cgroups, containers and pods over time.

Buffering and storage layer. Stores recent observations in bounded histories so that samples relevant to a given window can be retrieved efficiently. It treats metric streams and metadata as read-mostly records.

Analysis engine. Interprets temporally aligned observations and metadata to produce energy estimates for each analysis window. It forms the logical bridge between

measurement and attribution.

Calibration framework. Derives auxiliary information about typical delays, update patterns and idle behaviour. It produces constraints and characterisations that other subsystems rely on for interpretation.

Exporter. Exposes the results of the analysis engine to external monitoring systems as metrics ready for scraping and downstream processing.

4.3.2 Dataflow and Control Flow

Before Tycho enters normal operation, external calibration scripts determine approximate delay characteristics for all relevant metric sources. At startup, Tycho's internal calibration component derives suitable polling frequencies for metric collectors and metadata acquisition, providing the initial operating parameters for the system.

During runtime, control flow originates in the timing engine. It triggers each collector according to its calibrated polling frequency, but collectors operate independently: they sample their respective domains without synchronising with each other, and each observation is timestamped and appended to a buffering layer together with its associated quality indicators. This buffering layer retains a bounded history of raw observations per metric domain, with a default retention duration of approximately 90 s. The retained history deliberately exceeds the duration of a single analysis window, providing extended temporal context for downstream analysis and modeling rather than limiting interpretation to window-local samples.

In parallel, metadata acquisition proceeds on its own schedule, refreshing the mappings between processes, cgroups and workload identities in the metadata cache. Metadata is not synchronised with metric collection but is interpreted jointly with buffered observations during analysis.

The timing engine also governs when analysis occurs. At regular intervals, constituting fixed-length analysis windows, it initiates a new evaluation cycle irrespective of how many samples have been collected within the most recent window. Each cycle begins by estimating idle behaviour for the relevant hardware domains based on the buffered observation history. The analysis engine then interprets buffered metric samples, metadata and idle characterisations, taking calibrated delay characteristics into account when reconstructing the temporal structure of the window. Although attribution is performed only for the current window, historical observations within the retention horizon inform delay interpretation, baseline estimation and other modeling steps.

Once analysis completes, the exporter publishes the resulting metrics in a form suitable for ingestion by external monitoring systems. Calibration remains active in the background throughout the system's lifetime: it observes collector behaviour and derived quantities over longer time spans and refines its characterisations when needed, informing both the timing and analysis components without altering any collected data.

Figure 4.1 provides a consolidated view of Tycho's control flow and data flow, highlighting the buffering layer as the bounded temporal substrate that decouples collection, analysis and export.

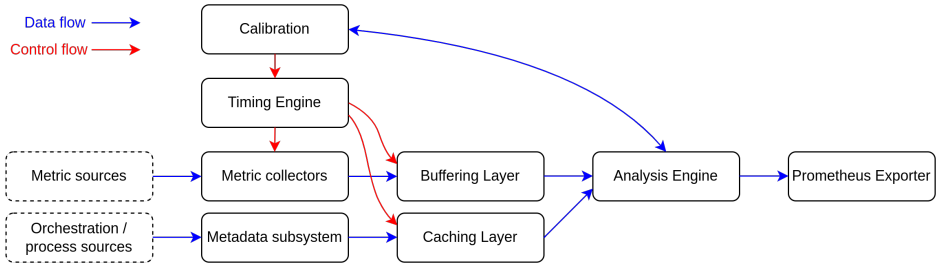

FIGURE 4.1: Subsystem Architecure, Dataflow and Control Flow

4.4 Temporal Model and Timing Engine

Tycho's temporal architecture provides a coherent framework for relating heterogeneous metric streams to fixed-duration analysis windows. It establishes a common time base, defines how collectors operate, and specifies how windows are formed and interpreted. The model is intentionally simple: collectors run independently, timestamps reflect poll time, and all temporal reasoning occurs during analysis.

4.4.1 Event-Time Model and Timestamp Semantics

Tycho adopts a single monotonic time base for all temporal coordination. Collectors timestamp each sample at the moment of observation; these timestamps reflect poll time, not the physical instant at which the underlying hardware event occurred. Event time is therefore a modelling construct used by the analysis engine when interpreting delay, freshness and update behaviour.

This separation keeps collectors lightweight and domain-agnostic. Each collector reports only what it directly observes; the analysis engine later interprets these timestamps in context, using calibration-derived delay characteristics to approximate underlying temporal structure.

4.4.2 Independent Collector Schedules

Tycho employs independent, domain-aware sampling schedules. During startup the timing engine configures one schedule per collector, after which each collector operates autonomously on its own periodic trigger. No global poll loop exists and collectors do not synchronise with one another. They push samples only when a new observation is available.

This decoupling avoids artificial temporal alignment and preserves each domain's intrinsic update behaviour. Collector timestamps are placed directly on the global monotonic time axis, allowing later reconstruction without imposing shared cadence or shared sampling semantics.

4.4.3 Window Construction and Analysis Triggering

Analysis proceeds in fixed-duration windows defined solely by periodic triggers from the timing engine. If the triggers occur at monotonic times $T_0, T_1, T_2, \ldots$, window W_i is the half-open interval $[T_i, T_{i+1})$. Window duration is nominally constant but may drift slightly, which is acceptable for attribution.

When a window closes, the analysis engine performs two conceptual phases:

(i) *idle characterisation*, using long-term buffered history across all relevant domains, and

(ii) *window reconstruction and attribution*, using all samples whose timestamps precede T_{i+1}.

Only energy for the current window is attributed and exported, but additional historical samples inform delay interpretation, idle estimation and interpolation.

Tycho treats domains asymmetrically: CPU and software metrics are always required; GPU and Redfish domains contribute when available. Samples too old to fall within the current window do not contribute directly but may still inform background characterisation. Windows remain valid when optional domains are absent.

A sample is considered stale relative to a window when its poll timestamp predates T_i by more than a domain-specific tolerance. Stale samples are ignored for direct reconstruction but do not invalidate the window.

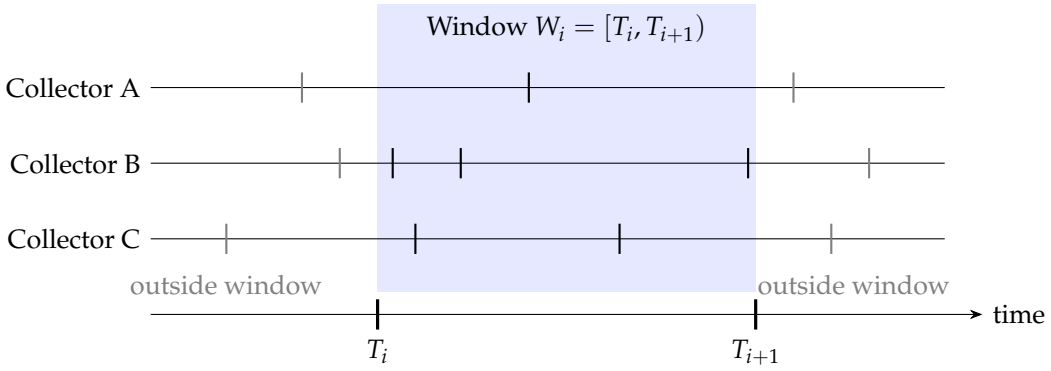

FIGURE 4.2: Analysis window W_i in relation to collectors

4.4.4 Comparison to Kepler Timing Model

Kepler employs a synchronous timing model in which all metric domains (except Redfish) are sampled within a single periodic poll cycle (default: 3 seconds). This fixed-length interval defines both the sampling cadence and the logical unit of attribution. Redfish updates occur at a much slower rate (default: 60 seconds), and the most recent Redfish value is reused across multiple attribution intervals. Export occurs on a separate cadence, which may not align with the attribution window.

Tycho diverges fundamentally: collectors run independently, analysis windows are defined by attribution triggers rather than poll cycles, heterogeneous update patterns are supported natively, and export occurs immediately after each attribution step. This structure enables finer temporal resolution, avoids dependence on synchronous polling behaviour, and eliminates inconsistencies between data collection and publishing intervals.

Figures 4.3a and 4.3b illustrate the respective timing behaviour of Tycho and Kepler, highlighting their polling patterns, sampling semantics and analysis-window alignment. Figures 4.4a and 4.4b provide a higher-level view to show the Prometheus

export behaviour more clearly.

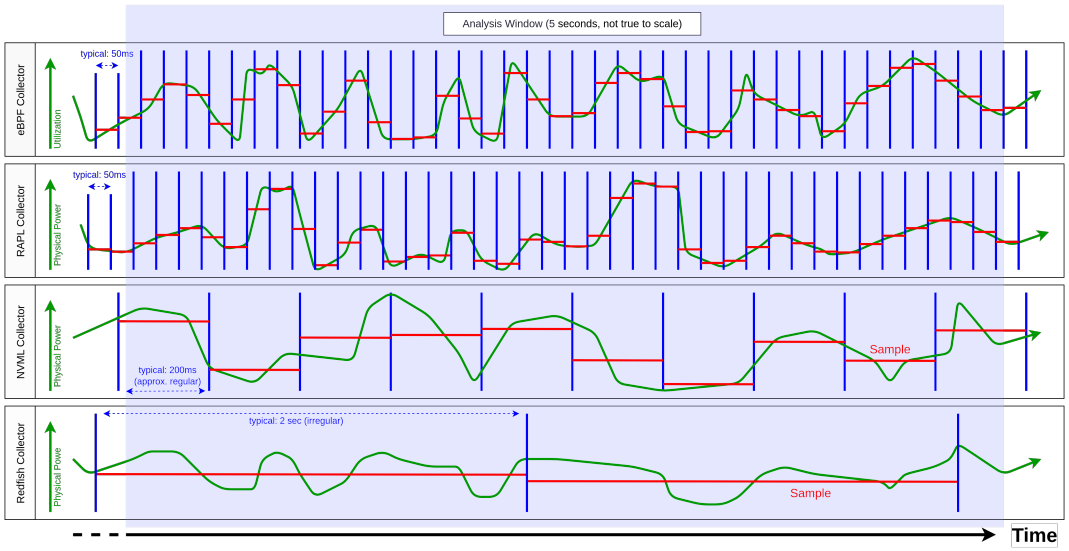

(A) Tycho Timing Model

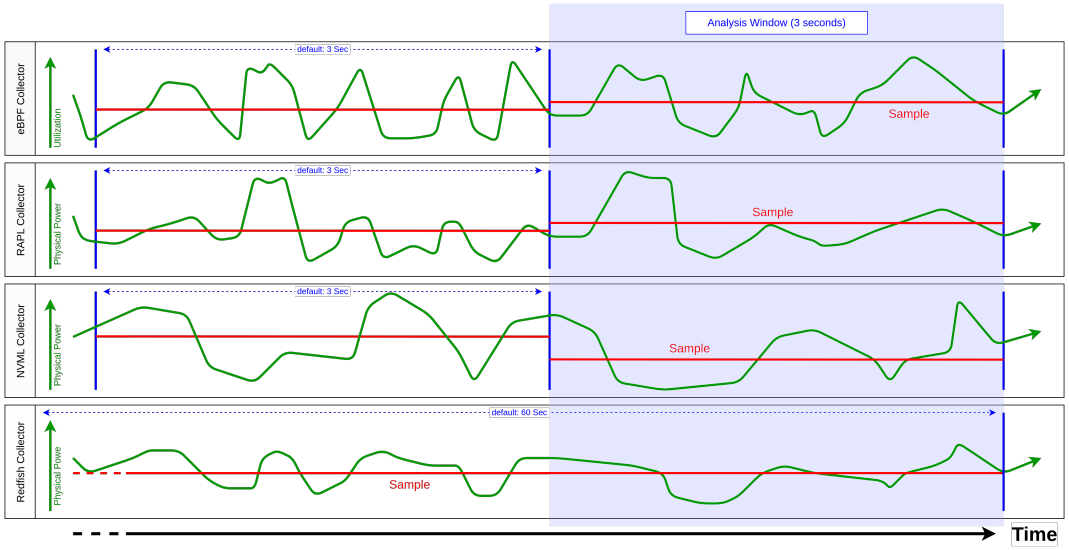

(B) Kepler Timing Model

FIGURE 4.3: Comparison: Tycho and Kepler Timing Model

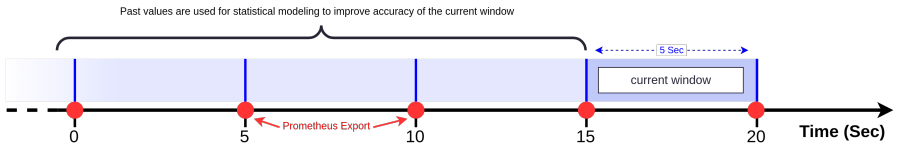

(A) Tycho Prometheus Export Timing Model

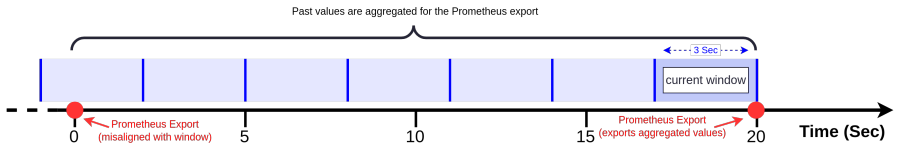

(B) Kepler Prometheus Export Timing Model

FIGURE 4.4: Comparison: Tycho and Kepler export behaviour

4.5 Metric Sources as Temporal Actors

This section characterizes all metric sources as temporal actors that emit observations under distinct timing, latency, and reliability constraints. Rather than treating collectors as passive data providers, it formalizes their role as asynchronous producers whose outputs define the raw temporal structure available to the analysis pipeline. The following subsections describe the observable properties, guarantees, and limitations of each source, establishing the bounds within which subsequent metric construction and attribution operate.

4.5.1 eBPF and Software Counters

The eBPF and software counter domain represents Tycho's event-driven view of CPU activity. Unlike hardware domains that report values at fixed sampling times, this domain emits utilisation information at the moment execution state changes occur. These events form a temporally dense and workload-dependent signal that describes how processor time is distributed across user tasks, kernel execution, interrupt handling, and idle periods. All higher-level aggregation is performed in userspace.

The domain contributes three classes of metrics with distinct temporal semantics.

- *Event-driven metrics* capture transitions in processor ownership and record the exact time at which execution begins or ends for a given context.
- *Cumulative counters* accumulate activity or duration over time and expose their values when queried.
- *Quasi-instantaneous counters* sample hardware performance state at activity boundaries, with semantics tied to the execution periods they describe.

Because event timestamps directly encode execution boundaries, no domain-level delay calibration is required, and collector polling cadence does not affect temporal alignment. Each event carries container context at the point of observation, enabling correct attribution under workload migration across control groups.

Within Tycho's temporal model, this domain provides fine-grained ownership information at execution boundaries and yields a complete temporal partition of CPU activity within each analysis window. These signals support proportional attribution and reduce uncertainty in downstream energy modelling, making eBPF-derived utilisation the most temporally precise workload activity signal available to the system.

4.5.2 RAPL Domains

RAPL exposes cumulative energy counters for a set of logical CPU-related domains, including package, cores, uncore, and memory. Each domain provides a monotonically increasing counter that reflects total energy consumed since a hardware-defined reference point and advances independently of the sampling schedule.

Within Tycho, RAPL counters are observed at fixed tick boundaries. At each tick the current counter values are recorded, and interval energy follows from the difference between consecutive readings. RAPL therefore contributes energy over time rather than instantaneous power, with temporal resolution defined by the tick interval. Because hardware updates occur at a much higher rate than sampling, the counters behave as effectively continuous at the chosen time scale.

RAPL sampling is aligned with Tycho's timing engine such that each analysis interval contains exactly one cumulative reading per domain. Internal update behaviour is already integrated into the counters and does not affect interval attribution. Architecturally, RAPL acts as a stable and low-noise source of CPU-adjacent energy.

The domain structure of RAPL aligns naturally with Tycho's requirement for domain-level consistency. Per-socket counters for package, core, uncore, and memory domains form a coherent decomposition of CPU energy that is preserved across intervals and provides a reliable baseline against which software-side utilisation signals can be related during attribution.

4.5.3 Redfish/BMC Power Source

Redfish provides an out-of-band view of total node power through the server's Baseboard Management Controller. It reports instantaneous power values at coarse and implementation-defined intervals and constitutes Tycho's only system-wide power observation.

Within Tycho's architecture, Redfish is treated as a *latently published external observation* rather than as a synchronisable metric source. Sampling is performed at fixed tick boundaries using the global monotonic timebase, but temporal authority remains with the BMC. Repeated values are common, and new measurements may appear only after several ticks; Redfish therefore constrains temporal interpretation rather than defining it.

To make this uncertainty explicit, each Redfish observation is annotated with a *freshness* value that expresses the temporal distance between the BMC's reported update time, when available, and Tycho's collection time. Freshness is an architectural quality indicator rather than a correction mechanism and allows downstream analysis to reason about temporal reliability without assuming regular publication or low latency.

When no new BMC update appears for an extended period, Tycho emits an explicit continuation of the last known power value. Continuation samples preserve a complete and chronologically consistent power timeline while making the absence of new information explicit; they do not indicate new measurements.

Despite its limited temporal resolution, Redfish serves as Tycho's authoritative source for total node power. It anchors the system's global energy view and provides a stable reference against which CPU- and accelerator-level energy estimates can be interpreted, with its coarse publication behaviour accommodated through explicit timestamping, freshness annotation, and controlled continuation.

4.5.4 GPU Collector Architecture

Accelerators form a significant share of the power consumption of modern compute nodes. Tycho therefore integrates GPU telemetry into the same unified temporal framework that governs RAPL, Redfish, and eBPF sources. NVIDIA devices expose energy-relevant information only at discrete publish moments inside the driver, so GPU sampling cannot rely on periodic polling alone. Instead, Tycho aligns sampling with the device's internal update behaviour and publishes at most one `GpuTick` for each confirmed hardware update. All GPU ticks share the global monotonic timebase that underpins Tycho's event-time model (§ 4.4). This section specifies the architectural guarantees, temporal contracts, and admissible interpretations of GPU telemetry; numerical reconstruction techniques, solver behavior, and backend-specific realization details are treated as implementation concerns and are not part of the architectural contract.

Architectural Role The GPU subsystem provides two forms of telemetry. Device-level metrics describe the instantaneous operating state of each accelerator, including power, utilisation, memory, thermals, and clock data. Process-level metrics describe backend-aggregated utilisation over a defined wall-clock window. Both streams are combined into a single `GpuTick` that represents the accelerator state at a specific moment in Tycho's global timeline. GPUs and MIG instances are treated as independent logical devices for the purpose of telemetry collection.

A central architectural design choice is the use of high-frequency *instantaneous* power fields exposed through NVIDIA's field interfaces, rather than relying exclusively on the conventional averaged power signal. Most existing GPU energy analyses depend on the one-second trailing average returned by `nvmlDeviceGetPowerUsage`, which obscures short-lived changes in power demand. By incorporating instantaneous power samples alongside averaged values, Tycho preserves substantially richer temporal structure at the telemetry source itself. This additional signal fidelity is a prerequisite for sub-second attribution and is later exploited by the analysis engine to improve temporal accuracy.

Backend Abstraction The GPU collector interfaces with NVIDIA hardware through `NVML`, which provides access to device-level and process-level telemetry. The architecture introduces a backend abstraction layer to decouple the collector from a specific vendor interface. This abstraction permits alternative backends, such as `DCGM`, to be integrated in the future without altering the surrounding timing and buffering logic. In the current system, `NVML` is the sole implemented backend.

The architecture does not assume uniform telemetry availability across devices. Cumulative energy counters, instantaneous power fields, and process-level utilisation may or may not be exposed depending on GPU generation and configuration. These capability differences are treated as properties of individual devices and handled through per-device feature masks within the implementation.

Conceptual Sampling Model GPU drivers update power and utilisation metrics at discrete, hardware-defined cadences that are not visible to callers. Polling at a fixed interval is fundamentally mismatched to this behaviour. If the polling frequency is lower than the internal publish cadence, updates are missed; if it is higher, the collector repeatedly observes identical values. Over time, this mismatch leads to aliasing, redundant samples, and temporal drift relative to other metric sources.

The sampling model distinguishes two conceptual modes. In base mode, the subsystem polls at a moderate frequency to track slow drift in the device's cadence. In *phase-aware sampling* mode, the subsystem temporarily increases its sampling frequency when Tycho's timebase approaches a predicted publish moment. This concentrates sampling effort where a fresh update is expected and reduces latency between the hardware update and Tycho's observation of it. As a result, a new sample can be detected earlier (and hence, with a more accurate timestamp), while avoiding additional overhead introduced by constant hyperpolling. The architecture guarantees that sampling remains event-driven rather than periodic, as formalised by the phase-aware timing model.

Formal Timing Model The GPU collector relies on a phase-aware timing model to align sampling with the implicit publish cadence of the device driver. Because this cadence is not exposed by the hardware or backend interface, it must be inferred from observed updates and expressed relative to Tycho's global monotonic timebase.

Let $t_{\text{obs},k}$ denote the monotonic timestamp of the k-th confirmed GPU publish event. Successive observations define inter-update intervals $\Delta t_k = t_{\text{obs},k} - t_{\text{obs},k-1}$, which serve as samples of the device's publish period. The model maintains a smoothed period estimate $\hat{T}$ and a phase offset $\hat{\phi}$ that jointly predict the timing of future publishes.

At any time t, the predicted next publish moment t_{next} is obtained by advancing the most recent observation by an integer multiple of $\hat{T}$, adjusted by $\hat{\phi}$, such that $t_{\text{next}} \geq t$. Sampling effort is concentrated in a narrow window around t_{next}, while lower-frequency polling maintains coarse alignment and tracks long-term drift.

This model establishes the following architectural guarantees:

- GPU sampling is aligned to inferred publish events rather than to a fixed polling interval.
- Each hardware publish produces at most one logical GPU event.
- No GPU event is emitted without a detectable device update.

The model is intentionally agnostic to backend-specific mechanisms used to detect freshness or to refine period and phase estimates. These concerns are delegated to

the implementation, which must realise the model under partial observability, jitter, and backend variability while preserving the guarantees above.

Figure 4.5 illustrates this behaviour at the architectural level, showing the relationship between the GPU's implicit publish events, Tycho's adaptive polling activity, and the resulting sequence of emitted `GpuTick`s.

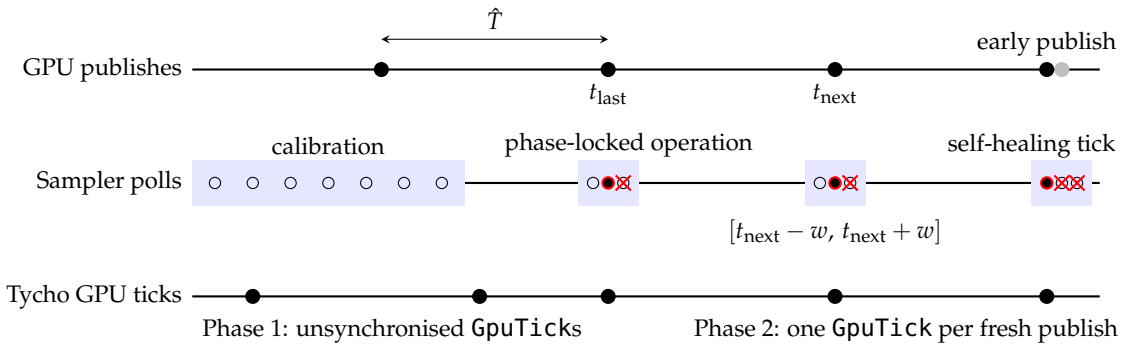

FIGURE 4.5: Phase-aware GPU polling timeline

Tick Semantics A `GpuTick` is emitted only when Tycho detects a genuinely new hardware update. Each tick contains a snapshot of device-level metrics and, when available, process-level utilisation aligned to the same monotonic timestamp. This design ensures that GPU measurements participate in Tycho's cross-domain correlation without interpolation, resampling, or ad hoc realignment. The one-to-one correspondence between hardware updates and GPU ticks is a core architectural guarantee and the primary distinction between Tycho's approach and traditional periodic sampling.

Process Telemetry Integration. Process-level metrics describe aggregated utilisation over a wall-clock window that is defined by the backend rather than Tycho's timing engine. The architecture treats these windows as retrospective measurements that must be aligned with the device timeline. Each process record is anchored to the timestamp of the device snapshot that triggered its acquisition. This preserves temporal coherence in spite of the retrospective semantics of process telemetry and supports multi-tenant attribution across GPU workloads.

Integration with the Global Timing Model All GPU ticks are timestamped using Tycho's global monotonic timebase and inserted into the multi-domain ring buffer. This ensures strict temporal ordering relative to RAPL, Redfish, and eBPF data. The architecture maintains the principle of domain autonomy: each subsystem generates updates according to its own temporal behaviour, while the analysis engine later fuses these streams into a consistent attribution result.

Architectural Limitations Although the architecture abstracts over backend differences, several structural constraints remain. Telemetry capabilities vary significantly across NVIDIA devices and driver configurations. Some accelerators expose high-quality instantaneous power fields and cumulative energy counters, while others provide only averaged power and coarse utilisation.

The implicit publish cadence may drift under DVFS or thermal transitions, which limits the predictability of update edges. Tycho mitigates these effects through robust sampling logic in the implementation, but the fidelity of the resulting GPU timeline remains bounded by the behaviour of the underlying hardware.

Overall, the GPU subsystem elevates accelerator telemetry to a first-class component of Tycho's energy model. By aligning sampling with the device's publish behaviour and unifying device and process metrics under a single timestamping model, the architecture enables precise, temporally consistent attribution in heterogeneous accelerator environments.

4.6 Metadata Collection Subsystem

Tycho treats workload identity as a first-class architectural concern that is strictly separated from numerical telemetry. While energy and utilisation collectors emit temporally ordered measurement streams, metadata captures the structural relationships required to interpret those streams during analysis. This includes the association of processes, containers, and pods as they evolve over the lifetime of a node.

Metadata is maintained as cached identity state rather than as a time series. It is neither aggregated nor iterated over analysis windows and does not participate directly in temporal correlation. Instead, metadata provides a bounded, continuously refreshed snapshot of recent workload structure that must remain sufficiently fresh and temporally consistent to support later attribution. Consequently, metadata collection prioritises controlled refresh and bounded lifetime over high-frequency or event-level precision.

Subsystem overview. The metadata subsystem forms a dedicated architectural layer that operates independently of metric collection and analysis. It consists of a small set of autonomous collectors coordinated through a single metadata controller, which constitutes the sole authority over metadata mutation and lifecycle management. Collectors observe the system independently, but all state updates are mediated by the controller, enforcing a clear separation between identity acquisition and subsequent analytical processing.

Dual-collector model. Workload identity is inherently multi-sourced. Tycho therefore integrates two complementary metadata collectors, each providing a partial and independently valid view of system state:

- **proc-collector:** observes process identity, execution context, and cgroup membership directly from the Linux kernel via the filesystem interface, providing authoritative runtime state independent of orchestration abstractions.
- **kubelet-collector:** acquires pod- and container-level identity from the Kubernetes node agent, exposing scheduling and lifecycle information unavailable at the operating-system level.

The metadata subsystem does not attempt to fuse or interpret these views at collection time. Instead, it records the most recent identity state observed by each source and defers reconciliation to analysis-time logic.

Controller-based coordination and scheduling. Metadata collection in Tycho is explicitly *analysis-driven*. The start of an analysis cycle constitutes the primary trigger for metadata refresh and is treated as the highest-priority collection opportunity. When an analysis window begins, the analysis engine requests a best-effort refresh of all registered metadata collectors in order to obtain the most recent possible identity state.

Autonomous metadata collectors exist as a secondary mechanism whose sole purpose is to bound metadata age when analysis intervals are long. These collectors execute under controller supervision and are explicitly subjugated to analysis-driven collection. If an analysis-triggered refresh is imminent, periodic collectors are suppressed and defer execution to the analysis engine, preventing redundant collection in short succession.

All collectors register with a central metadata controller, which arbitrates between analysis-triggered and background execution. The controller tracks the timestamp of the most recent successful observation for each collector and enforces source-specific freshness constraints. Collection is permitted only when required to satisfy source-specific freshness constraints. As a result, metadata may be refreshed multiple times within a single analysis window under long-running analysis, while redundant collection near analysis boundaries is suppressed to reduce overhead.

This prioritisation establishes a clear architectural guarantee. Metadata is maximally fresh at analysis start, redundant collection is avoided, and collection overhead remains bounded independently of both analysis frequency and global scheduling cadence.

Metadata state and lifetime model. Collected metadata is stored in a dedicated in-memory state that represents a bounded snapshot of recent workload identity. Unlike the ring-buffer–based design used for metric data, the metadata store retains only the most recent valid representation of each observed entity. Entries correspond to identity-bearing objects such as processes, containers, and pods and are keyed by stable identifiers. New observations update entries in place; historical versions and event sequences are not preserved.

Each metadata entry carries a monotonic timestamp anchored to Tycho's global timebase, allowing identity state to be interpreted consistently alongside energy and utilisation measurements. Metadata is considered valid from its most recent observation until it is removed by lifecycle management. Garbage collection is horizon-based and enforced exclusively by the controller, which removes entries once they fall outside the retained temporal window. Collectors never delete metadata directly, ensuring deterministic expiry and consistent memory bounds.

By coupling metadata lifetime to a bounded horizon rather than to explicit lifecycle events, the subsystem remains robust to incomplete or delayed observations. Terminated processes, containers, and pods persist only long enough to support overlapping analysis windows and are removed automatically thereafter.

4.7 Calibration

Calibration is an auxiliary architectural subsystem that bounds temporal uncertainty introduced by hardware-controlled metric publication. It exists to constrain polling behaviour and temporal alignment for metric sources whose update cadence or observable reaction latency is externally governed and not analytically predictable. Calibration is applied selectively and only where such uncertainty significantly affects the correctness of subsequent analysis.

Calibration produces static, conservative parameters that are consumed by the timing and analysis subsystems. It does not participate in runtime attribution, does not adapt dynamically, and does not operate on live metric streams. By resolving temporal uncertainty ahead of time, calibration allows the runtime system to remain deterministic, bounded, and non-intrusive.

Tycho distinguishes two independent calibration concerns: *polling-frequency calibration*, which bounds how often a metric source must be queried to avoid undersampling hardware updates, and *delay calibration*, which bounds the latency between a workload transition and the first observable reaction in a metric stream. These concerns are orthogonal and are applied only where their respective assumptions hold.

Polling-frequency calibration. Polling-frequency calibration applies to metric sources whose publish cadence is hardware-controlled and approximately regular. Its purpose is to derive a conservative polling interval that observes all published updates under nominal conditions without imposing unnecessary collection overhead.

Polling-frequency calibration is performed during Tycho startup. It relies exclusively on passive observation of device behaviour and does not require workload manipulation. This calibration is applied to GPU and Redfish power metrics, whose firmware- or BMC-controlled publication intervals are stable in expectation but not analytically documented. The resulting polling bounds are treated as configuration constraints by the timing subsystem and remain fixed during normal operation. For node-level execution, Tycho adopts the most conservative bound across all contributing devices to ensure uniform temporal coverage.

Polling-frequency calibration is not applied to RAPL or eBPF. RAPL energy counters update quasi-continuously at a granularity far below Tycho's sampling resolution, rendering undersampling architecturally irrelevant. eBPF metrics are event-driven and decoupled from device-side publish cadence, making polling-frequency discovery unnecessary.

Delay calibration. Delay calibration bounds the latency between a workload transition and the first observable change in a metric stream. This calibration applies only where such latency is stable, workload-independent, and sufficiently repeatable to be treated as a bounded constant.

Delay calibration is performed exclusively for GPU power metrics. GPU devices internally aggregate and buffer power readings prior to publication, introducing a measurable and consistent delay relative to workload onset. Accurate estimation of this delay requires the generation of controlled, high-intensity workload transitions to elicit clear device responses. As Tycho is architecturally constrained to non-intrusive observation, such stimulus-driven measurement is performed offline and

excluded from runtime operation. The resulting delay bounds are supplied as static configuration parameters and inform the analysis subsystem's temporal alignment logic without participating in runtime attribution.

No delay calibration is performed for RAPL or eBPF. At Tycho's temporal resolution, residual access latency in RAPL energy counters is negligible, and eBPF metrics reflect execution state transitions without device-side buffering. Both domains are therefore treated as temporally immediate at the architectural level.

Delay calibration is not applied to Redfish. Redfish power readings exhibit irregular publish intervals, variable network latency, and opaque BMC-internal behaviour, precluding stable delay estimation. Redfish metrics are consequently treated as coarse, low-resolution signals suitable for slow global trends, with temporal consistency enforced through separate freshness and scheduling mechanisms. Architecturally, calibration constrains admissible interpretation without introducing additional runtime state or adaptive behavior.

4.8 Analysis and Attribution Architecture

4.8.1 Pipeline Orchestration and Stage Execution

4.8.1.1 Problem Statement

Tycho's analysis layer must transform heterogeneous, asynchronous observations into window-scoped attribution results under three constraints. Inputs originate from independent sources with bounded but non-uniform delays and may be temporarily unavailable. Attribution further requires interdependent derived quantities, imposing strict ordering constraints. Finally, analysis must remain online, deterministic, and non-retrospective, excluding retrospective reinterpretation and any semantic coupling to exporter behavior. The orchestration problem is therefore to execute a deterministic, dependency-respecting transformation pipeline per attribution window while tolerating partial observability and enforcing the invariants defined in § 4.4.3.

4.8.1.2 Conceptual Model

Analysis proceeds as a sequence of discrete *cycles*. Each cycle selects a single attribution window, instantiates a self-contained execution context, executes a fixed set of transformations in a predefined order, and yields a logically atomic set of window-scoped derived quantities. The analysis engine acts solely as an orchestration authority. It determines the temporal scope of each cycle using the global monotonic timebase, enforces execution order, and commits results as a coherent unit. Collection, buffering, and metadata acquisition are upstream concerns and are assumed to have materialized raw observations into bounded-retention histories.

The pipeline is expressed as a set of *metrics*, each representing a typed transformation. Metrics consume raw observations or previously derived metrics and emit window-scoped results according to the semantic models defined in this chapter. Metrics may depend on earlier outputs within the same cycle but never on downstream publication state or future cycles.

4.8.1.3 Attribution Window Semantics

Let t_k denote the monotonic timestamp associated with the start of analysis cycle k. The attribution window for cycle k is defined as the half-open interval

$$W_k = (t_{k-1}, t_k].$$

Windows are defined on a global monotonic timebase, form a total order, and are non-overlapping.

Window selection incorporates a fixed intentional lag relative to real-time execution. The window end t_k is chosen such that it lags the most recent observations by at least the maximum admissible metric delay plus a safety margin, derived from configuration and optional calibration (§ 4.7). This bound is an architectural precondition for window validity and guarantees that all metrics participating in a cycle can interpret their contributions over W_k under their declared delay semantics. As a result, attribution correctness is decoupled from collector jitter, speculative window closure is avoided, and causality is preserved.

In steady state, attribution windows have a fixed duration. During startup, when insufficient history exists, the window start may be clamped to the beginning of the monotonic timeline. This is the only permitted deviation from the steady-state definition and preserves determinism.

4.8.1.4 Stage Model and Dependency Discipline

Analysis is structured as an ordered sequence of conceptual stages reflecting semantic dependencies between derived quantities. A stage delineates computations whose outputs serve as prerequisites for subsequent modeling or attribution steps. Within a cycle, stages execute strictly in order. Metrics may depend on raw observations and on outputs from earlier stages in the same cycle, but must not depend on later stages, future cycles, or sink side effects.

This discipline renders the pipeline compositional. Later attribution logic operates on materialized, window-scoped quantities rather than ad hoc joins over raw histories. Stages are semantic boundaries, not runtime entities, and exist to make dependency structure explicit when partial observability yields incomplete but internally consistent results.

4.8.1.5 Best-Effort Semantics Under Partial Observability

The analysis architecture is accuracy-first but not completeness-first. For a given window, Tycho produces the most complete set of derived quantities that can be computed without violating architectural invariants. If required inputs are unavailable or inadmissible under a metric's semantics, that metric is undefined for the window and does not materialize a result. Downstream metrics may still execute if their dependencies are satisfied, yielding partially populated but self-consistent outputs. As observability decreases, results degrade monotonically through omission or explicitly defined fallback semantics, and previously valid interpretations are never revised.

4.8.1.6 Output Commit and Sink Boundary

All results produced during a cycle belong to the same attribution window W_k and are committed as a logical batch. Sinks are strictly downstream observers and lie outside the correctness boundary of attribution. Exporter behavior may delay or drop publication but does not affect the meaning of computed window-scoped quantities. This separation prevents exporter mechanics from becoming an implicit part of attribution semantics and preserves reproducibility.

4.8.1.7 Architectural Consequences

The orchestration model establishes a stable execution contract. Stage-local computations may assume a well-defined attribution window, deterministic ordering, and read-only access to upstream histories. In return, analysis is constrained to be window-scoped and non-retrospective. Each cycle yields a single, maximal, internally consistent interpretation of the evidence available for its window, and later cycles do not revise earlier results. This contract supports the staged construction of increasingly sophisticated attribution models without altering orchestration semantics.

4.8.2 Stage 1: Component Metric Construction

This stage defines how raw observations emitted by the collectors are transformed into coherent per-component total energy and power metrics. Its purpose is to establish temporally aligned, conservation-preserving component signals from heterogeneous inputs, independent of any attribution or decomposition semantics. The resulting metrics form the authoritative total-energy basis for all subsequent stages and are exported as externally consumable component-level measurements.

4.8.2.1 Component-Level eBPF Utilization Metrics

Problem Statement eBPF exposes raw kernel execution signals and hardware event counts as per-tick deltas. These signals must be transformed into window-aligned utilization metrics with well-defined semantics and into cumulative counters suitable for direct export and downstream aggregation.

Conceptual Model Two classes of node-level metrics are constructed from eBPF observations. CPU execution time is expressed as normalized time-share ratios over a fixed analysis window. All other kernel and hardware signals are expressed as cumulative counters obtained by aggregating per-process deltas across the node.

Formalization Let a node expose C logical CPUs and let an analysis window of duration Δt define a total schedulable capacity

$$T_{\text{cap}} = C \cdot \Delta t. \tag{4.1}$$

Let T_{idle}, T_{irq}, and T_{softirq} denote the aggregated CPU time spent in idle, hardware interrupt, and software interrupt execution over the window. Normalized utilization ratios are defined as

$$r_x = \frac{T_x}{T_{\text{cap}}}, \quad x \in \{\text{idle}, \text{irq}, \text{softirq}\}. \tag{4.2}$$

Active execution is defined as the residual

$$r_{\text{active}} = 1 - (r_{\text{idle}} + r_{\text{irq}} + r_{\text{softirq}}). \tag{4.3}$$

By construction, all ratios are dimensionless, bounded in $[0, 1]$, and satisfy

$$r_{\text{idle}} + r_{\text{irq}} + r_{\text{softirq}} + r_{\text{active}} = 1. \tag{4.4}$$

For each kernel or hardware event type j, let ΔK_j denote the per-tick delta aggregated across all processes. The exported counter is defined as the cumulative sum

$$N_j(t) = \sum_{k \le t} \Delta K_j, \tag{4.5}$$

which is monotonically non-decreasing over the lifetime of the process.

Design Decisions CPU utilization is normalized to node capacity to make ratios invariant to window length and core count. Active CPU time is defined as a residual to enforce exact conservation of CPU capacity. All event-based metrics are exposed as cumulative counters to preserve monotonicity and allow rate derivation without reinterpreting window semantics.

Architectural Consequences The resulting metrics provide window-stable CPU utilization ratios and strictly monotonic kernel activity counters. These quantities can be consumed directly as observability metrics and reused unchanged by downstream attribution stages.

4.8.2.2 RAPL Component Metrics

Problem Statement RAPL exposes cumulative energy counters per hardware domain, but these counters are node-local, socket-scoped, and offset by an arbitrary hardware-defined origin. For Tycho, these signals must be transformed into a single, coherent component-level energy metric that is comparable across time and suitable as an authoritative input for later attribution stages. The core problem is therefore to define a metric that preserves the physical meaning of RAPL energy while eliminating hardware-specific offsets and remaining stable under windowed analysis.

Conceptual Model The RAPL component is modeled as a set of independent energy domains, treated as conceptually separate devices but belonging to the same component. For each domain, Tycho constructs a cumulative energy signal that represents the total physical energy consumed since Tycho start. This signal is defined independently of any windowing semantics and serves as the primary representation of RAPL energy within the system. A secondary, auxiliary power signal is derived from the same observations for user-facing inspection, but it is not authoritative.

Formalization Let $E_d^{\text{raw}}(t)$ denote the raw cumulative RAPL energy reading for domain d at time t, as provided by the underlying measurement subsystem. These raw counters are assumed to be strictly monotonic and already corrected for hardware wraparound.

For each domain d, Tycho defines an exported cumulative energy counter

$$E_d(t) = E_d^{\text{raw}}(t) - E_d^{\text{raw}}(t_0), \tag{4.6}$$

where t_0 is the time of the first observed sample for that domain. This construction yields a zero-based, monotonic energy counter with $E_d(t_0) = 0$.

An auxiliary average power signal is defined over an analysis window $[t_i, t_{i+1}]$ as

$$P_d^{(i)} = \frac{E_d(t_{i+1}) - E_d(t_i)}{t_{i+1} - t_i}. \tag{4.7}$$

This quantity is derived solely from the cumulative energy counter and has no independent physical authority.

Design Decisions The primary design choice is to treat cumulative energy as the first-class metric and to derive all other quantities from it. Using zero-based cumulative counters removes dependence on hardware-specific initial offsets and simplifies downstream reasoning. Power is intentionally modeled as a derived, window-local quantity rather than as a primary signal, reflecting its lower robustness and its lack of necessity for attribution. Domains are defined once and treated uniformly, avoiding domain-specific special cases in the metric definition.

Architectural Consequences The exported RAPL energy counters form the authoritative energy input for all later attribution and decomposition stages. Their monotonicity and zero-based semantics allow unambiguous differencing, aggregation, and conservation reasoning. By contrast, the power metrics are explicitly auxiliary, non-authoritative, and excluded from downstream attribution logic. This separation ensures that attribution correctness depends only on cumulative energy, while still permitting power-oriented inspection for diagnostic or user-facing purposes.

4.8.2.3 GPU-Corrected Energy Metric

Problem Statement GPU telemetry provides multiple power- and energy-related observations of the same physical process under incompatible temporal semantics. Instantaneous power samples, one-second averaged power values, and optional cumulative energy counters are reported concurrently but cannot be combined by direct integration or signal selection without introducing temporal bias or discarding information. Using any single signal in isolation either preserves absolute correctness at coarse granularity or improves temporal resolution at the cost of systematic error. The problem addressed here is therefore not measurement scarcity, but the absence of a principled method to reconcile redundant GPU observations into a single, temporally refined, internally consistent power and energy signal aligned to corrected time.

Conceptual Model GPU power is modeled as a latent, non-negative, continuous-time signal reconstructed on a uniform corrected-time grid and maintained over a retained history horizon that exceeds the current analysis window. This deliberate use of historical context is a central accuracy mechanism, allowing delayed, coarse, and partially redundant observations to be reconciled in a globally consistent manner that window-local estimation cannot achieve. All raw GPU observations are

interpreted as constraints on this latent signal, jointly shaping a single authoritative power timeline per device. Instantaneous and one-second averaged power samples impose soft consistency constraints, while cumulative energy counters, when available, act as dominant anchors that strongly influence the reconstruction without enforcing hard equality. Physical plausibility is enforced by penalizing implausible curvature while preserving total energy and long-term magnitude. Windowed GPU energy and power metrics are obtained by integrating sub-intervals of this maintained reconstructed signal, ensuring temporal coherence across windows and improved accuracy relative to any raw observation stream.

Formalization For each GPU device, power is represented by a reconstructed sequence $p = \{p_k\}_{k=0}^{N-1}$ on a uniform corrected-time grid with spacing Δt. Reconstruction is posed as a constrained optimization problem that minimizes weighted discrepancies to observed telemetry while enforcing physical plausibility. Let $\mathcal{R}$ denote the set of observation constraints derived from instantaneous power samples, one-second averaged power samples, and optional cumulative energy readings. Each constraint $r \in \mathcal{R}$ is expressed by a linear operator a_r acting on p with target value y_r and weight w_r.

The architectural objective is

$$\min_{p \geq 0} \sum_{r \in \mathcal{R}} w_r^2 \left(a_r^\top p - y_r \right)^2 + \lambda_D \sum_{k=1}^{N-2} \left(p_{k+1} - 2p_k + p_{k-1} \right)^2, \tag{4.8}$$

where the second-difference term penalizes curvature without imposing a prior on absolute magnitude. Non-negativity $p_k \geq 0$ enforces physical feasibility. Cumulative energy observations contribute constraints whose weights dominate when present, prioritizing energy consistency over time without enforcing exact equality. The solution p defines the authoritative GPU power signal; windowed GPU energy is obtained by integrating p over the corresponding corrected-time interval.

Design Decisions Constrained reconstruction is chosen over signal selection to avoid privileging any single telemetry source and to preserve all available information. Cumulative energy counters are treated as dominant but soft constraints to exploit their reliability while tolerating gaps, resets, and delayed reporting. Instantaneous and averaged power samples are retained as complementary observations that improve temporal resolution and stabilize reconstruction when energy counters are absent. Smoothness is imposed via second differences to suppress implausible oscillations without biasing total energy or sustained power level. No magnitude prior is introduced, as any bias toward lower power would conflict with the accuracy-first objective. Numerical conditioning and solver-specific stabilization are intentionally excluded from the architectural model.

Architectural Consequences The architecture yields a single corrected GPU power signal per device that is temporally finer than any raw input and internally consistent across power and energy representations. All downstream GPU metrics are derived exclusively from this reconstructed signal, eliminating ambiguity from heterogeneous telemetry. Historical retention becomes a first-class correctness mechanism, enabling stable, coherent windowed estimates under delayed and coarse observation regimes. The design explicitly acknowledges the modeled nature of the result while guaranteeing physical plausibility and maximal energy consistency given

available observations, establishing a stable foundation for subsequent attribution and aggregation stages.

4.8.2.4 Redfish-Corrected System Energy Metric

Problem Statement Raw Redfish power telemetry is sparse, irregular, and subject to delay that can vary over time. Direct window integration of held power values yields a valid low-rate estimate, but it cannot provide temporally granular system power that is consistent across windows when sample timing drifts. A second construction is therefore required that treats Redfish as the authoritative system-level anchor while reconstructing a higher-rate system power trajectory from contemporaneous component-proxy signals.

Conceptual Model The metric family exports a canonical system power series and its cumulative energy counter, parameterized by a 'source' label. During warmup or when insufficient Redfish anchoring is available, `source="redfish_raw"` is formed by integrating the held Redfish power trajectory. Once sufficient Redfish observations exist over a reconstruction horizon, `source="redfish_corrected"` replaces the raw series and represents a reconstructed system power trajectory on a fine time grid. Reconstruction is posed as fitting a non-negative linear combination of proxy signals that are expected to co-vary with system power, while strongly anchoring the fit to the observed Redfish samples.

Formalization Let $p_{\mathrm{RF}}(t)$ denote Redfish-reported system power (in mW), observed at irregular raw times t_j^{raw}. Redfish observations are subject to an unknown, time-varying reporting delay. The construction therefore introduces an explicit delay parameter $\delta_{\mathrm{RF}} \geq 0$, mapping raw timestamps into a corrected domain

$$t_j = t_j^{\mathrm{raw}} - \delta_{\mathrm{RF}}. \tag{4.9}$$

For the raw series, $p_{\mathrm{raw}}(t)$ is defined as a zero-order-hold trajectory of $p_{\mathrm{RF}}(t)$ in corrected time. For an analysis window $W = [t_s, t_e]$ of duration Δ_W seconds, the window energy and average power are

$$E_{\mathrm{raw}}(W) = \int_{t_s}^{t_e} p_{\mathrm{raw}}(t)\, dt, \qquad P_{\mathrm{raw}}(W) = \frac{E_{\mathrm{raw}}(W)}{\Delta_W}. \tag{4.10}$$

For the corrected construction, system power is reconstructed on a uniform grid of bins k with width Δ seconds over a finite horizon. Let $p_{\mathrm{hat}}[k]$ denote reconstructed system power in bin k. For each bin, proxy features are derived from contemporaneous component metrics: average package, DRAM, and GPU powers $p_{\mathrm{pkg}}[k]$, $p_{\mathrm{dram}}[k]$, $p_{\mathrm{gpu}}[k]$, and the CPU instruction rate $r_{\mathrm{instr}}[k]$.

Redfish observations are projected into the corrected domain at times t_j and interpreted as constraints on the reconstruction (optionally corresponding to a trailing-average kernel over a fixed interval). Let y_j denote the Redfish power value associated with observation j. Reconstruction fits parameters $\theta = (\alpha, \beta, \gamma, \delta, b)$ such that

$$p_{\mathrm{hat}}[k] = \max\big(0,\, \alpha\, p_{\mathrm{pkg}}[k] + \beta\, p_{\mathrm{dram}}[k] + \gamma\, p_{\mathrm{gpu}}[k] + \delta\, r_{\mathrm{instr}}[k] + b\big)\,, \tag{4.11}$$

where $\alpha, \beta, \gamma, b \geq 0$ enforce physical non-negativity.

Crucially, δ_{RF} is not fixed. For each analysis cycle, a finite candidate set of delays is evaluated, and the delay is selected that minimises the unexplained system power relative to the proxy sum over recent bins, subject to stability constraints. This adaptive delay selection aligns Redfish observations to the proxy domain in a best-effort sense and is recomputed as system behaviour changes.

Window energy and power for the corrected series are obtained by integrating p_{hat} over the overlap of W with the reconstruction grid:

$$E_{\mathrm{corr}}(W) = \int_{t_s}^{t_e} p_{\mathrm{hat}}(t)\, dt, \qquad P_{\mathrm{corr}}(W) = \frac{E_{\mathrm{corr}}(W)}{\Delta_W}. \tag{4.12}$$

Design Decisions Redfish is treated as the system-level anchor rather than as a weak label, so the fit objective is defined in observation space and evaluated only where Redfish provides constraints. Delay is treated as an explicit degree of freedom in the construction because raw Redfish timestamps are not sufficient to guarantee stable alignment. Proxy features are restricted to quantities that are already available at fine granularity, enabling reconstruction without introducing additional sensors. Non-negativity constraints on physically interpretable coefficients prevent the model from compensating Redfish irregularities by introducing negative component contributions or a negative baseline.

Architectural Consequences The construction yields a single canonical system series that remains available during warmup via `source="redfish_raw"` and transitions to a higher-rate anchored estimate via `source="redfish_corrected"` without changing metric IDs. Downstream stages can treat the corrected series as the system-level power baseline for further decomposition, while retaining the provenance of the construction through the 'source' label. The reconstruction is intentionally conservative: when anchoring observations are insufficient or alignment is unreliable, corrected output is withheld and raw integration remains authoritative.

4.8.3 Stage 2: System-Level Energy Model and Residual

Problem Statement After Stage 1, Tycho provides multiple component-level energy signals that are individually conservative but incomplete. No combination of RAPL and GPU measurements can fully account for total node energy consumption, and a system-level reference is required to constrain attribution. However, the only available system-wide signal, Redfish-reported power, exhibits limited and variable temporal fidelity. This creates a fundamental tension between physical conservation and temporal alignment that cannot be resolved by algebraic refinement alone.

Conceptual Model Stage 2 introduces a system-level energy balance scoped to a single node and a single analysis window. Total system energy is taken from the Redfish-integrated signal, while accounted component energy is defined as the sum of all modeled contributors. Any remaining energy is captured explicitly as a residual term, which represents unmodeled components and temporal mismatch rather than error. Residual energy is therefore treated as a first-class quantity within the attribution pipeline.

Formalization Let E_{sys} denote total system energy for a window, obtained from the system-level source. Let E_{parts} denote the sum of all accounted component energies for the same window. The residual energy E_{res} is defined as:

$$E_{\text{res}} = E_{\text{sys}} - E_{\text{parts}}. \tag{4.13}$$

This definition is local to a node and window and does not imply workload attribution. The architectural invariant enforced by Stage 2 is strict energy conservation at the window level.

Design Decisions Residual energy is modeled explicitly rather than absorbed into noise or redistributed across components. This avoids introducing hidden assumptions about unmodeled hardware behavior and preserves auditability. Temporal misalignment between system and component signals is tolerated at the power level but never allowed to violate energy conservation. No attempt is made at this stage to reinterpret or smooth the residual term.

Architectural Consequences Stage 2 establishes a closed system-level energy budget that constrains all downstream attribution. Later stages may further decompose or attribute residual energy, but they cannot eliminate it without introducing additional assumptions. The explicit residual also enables the system to signal when residual-based interpretation is unreliable, without compromising conservation.

4.8.4 Stage 3: Idle and Dynamic Energy Semantics

This stage defines how total component energy is partitioned into idle and dynamic contributions prior to attribution. Because CPU packages, residual system energy, and GPUs differ in observability, baseline stability, and utilization coupling, the decomposition semantics are specified per component rather than uniformly. The following subsubsections formalize these component-specific rules while preserving energy conservation and temporal consistency, and while establishing dynamic signals suitable for downstream attribution. Each decomposition defined below follows the same architectural pattern: a conservative baseline definition, a non-negative dynamic remainder obtained by conservation, and explicit admissibility conditions that bound when the resulting quantities may be interpreted.

4.8.4.1 RAPL Idle and Dynamic Decomposition

Problem Statement RAPL exposes per-domain total energy that merges baseline platform consumption with workload-induced variation. For attribution and downstream fairness policies, Tycho requires a conservative split into an approximately stable idle component and a residual dynamic component while preserving per-window energy conservation.

Conceptual Model For each RAPL domain $d \in \{\texttt{pkg}, \texttt{core}, \texttt{uncore}, \texttt{dram}\}$, Tycho treats the exported total power $P_d^{\text{tot}}(t)$ as the sum of an idle baseline $P_d^{\text{idle}}(t)$ and a dynamic remainder $P_d^{\text{dyn}}(t)$. Idle is estimated from low-activity operating points using an external utilization proxy $u_d(t)$ and a model that targets the theoretical $u_d = 0$ intercept, avoiding reliance on observing a true zero-load system. This preference follows the empirical finding that linear models yield robust idle estimates while higher-order fits tend to be unreliable in practice [52].

Formalization Let W_k denote an analysis window of duration Δt_k and let $\Delta E_{d,k}^{\text{tot}}$ be the total domain energy increment over W_k. Tycho defines the decomposition by a baseline power estimate $\beta_{d,k}$ and constructs window energies as:

$$\Delta E_{d,k}^{\text{idle}} = \min\left(\Delta E_{d,k}^{\text{tot}},\ \max(0, \beta_{d,k}) \cdot \Delta t_k\right), \tag{4.14}$$

$$\Delta E_{d,k}^{\text{dyn}} = \Delta E_{d,k}^{\text{tot}} - \Delta E_{d,k}^{\text{idle}}. \tag{4.15}$$

The baseline $\beta_{d,k}$ is obtained by fitting a linear model $P_d^{\text{tot}} \approx \alpha_d u_d + \beta_d$ using only samples drawn from stable, low-utilization regimes and evaluating the intercept β_d as the idle estimate.

Design Decisions Tycho adopts utilization-conditioned estimation rather than pure lower-bound tracking to remain meaningful on continuously active Kubernetes nodes where true idle is rarely observed. Model fitting is restricted to low-utilization operating points to prioritise identifiability of the intercept and avoid distortion by high-load regimes. The decomposition is defined per RAPL domain, permitting distinct baselines for domains whose activity sensitivity differs. Conservative clamping enforces non-negativity and prevents idle from exceeding total within a window, ensuring that the decomposition cannot create energy.

Architectural Consequences The resulting per-domain $(\Delta E_{d,k}^{\text{idle}}, \Delta E_{d,k}^{\text{dyn}})$ split provides a stable baseline for policy-driven idle allocation while reserving fine-grained attribution capacity for the dynamic remainder. Energy conservation holds per window by construction, enabling downstream stages to distribute dynamic energy without ambiguity and to route any non-attributable portions explicitly to the system bucket.

4.8.4.2 Residual Idle and Dynamic Decomposition

Problem Statement Residual energy is defined as the portion of system-level energy not explained by explicitly modeled components. While this residual budget is energy-consistent by construction, its instantaneous power signal is affected by temporal misalignment and measurement latency. As a result, residual power cannot be interpreted uniformly across analysis windows. A decomposition is required that preserves conservation of the residual budget while preventing transient artifacts from corrupting persistent state or downstream learning.

Conceptual Model The residual budget is decomposed into two modeled components: a residual idle component and a residual dynamic component. Residual idle represents a persistent, low-variance baseline within the residual budget, while residual dynamic captures the remaining window-local variation. The decomposition is explicitly conditional. Its semantic validity depends on a window usability predicate that identifies windows dominated by temporal misalignment. When this predicate is false, the decomposition remains defined but must not be interpreted or used for learning.

Formalization Let P_w^{res} denote the non-negative residual total power for window w. For every window satisfying the usability predicate, the residual decomposition is defined as:

$$P_w^{\text{res}} = P_w^{\text{res,idle}} + P_w^{\text{res,dyn}} \tag{4.16}$$

with the invariants:

$$P_w^{\text{res,idle}} \geq 0, \qquad P_w^{\text{res,dyn}} \geq 0, \qquad P_w^{\text{res,idle}} \leq P_w^{\text{res}} \tag{4.17}$$

Residual idle power is defined using a persistent modeled baseline B^{res}:

$$P_w^{\text{res,idle}} = \min\left(B^{\text{res}}, P_w^{\text{res}}\right) \tag{4.18}$$

Residual dynamic power is defined by conservation:

$$P_w^{\text{res,dyn}} = P_w^{\text{res}} - P_w^{\text{res,idle}} \tag{4.19}$$

The interpretive contract of this decomposition holds only when the window usability predicate is true. No fallback semantics are defined when this condition is violated.

Design Decisions Residual idle is modeled as a persistent baseline rather than a per-window estimate. This choice prevents transient measurement artifacts from collapsing the baseline and destabilizing downstream stages. The model deliberately avoids any physical interpretation of residual idle or dynamic components. By enforcing exact conservation and non-negativity, the decomposition remains bounded and conservative under all conditions.

Architectural Consequences This decomposition provides a stable internal structure over unmodeled energy while explicitly limiting its semantic scope. Downstream stages may rely on residual idle and dynamic quantities only when window usability is asserted. At the same time, the model constrains interpretation by requiring consumers to treat usability as a hard semantic gate rather than a soft quality indicator.

4.8.4.3 GPU Idle and Dynamic Decomposition

Problem Statement The corrected GPU power signal contains both an idle baseline and workload-induced dynamic consumption. For attribution and energy accounting, Tycho must separate these components such that idle reflects the lowest sustainably attainable device power under low utilization, while dynamic captures the residual induced by activity. This separation must be defined per device, since baseline power differs across GPUs and operating conditions.

Conceptual Model For each GPU device identified by *uuid*, Tycho maintains an idle power estimate β_{uuid} derived from the corrected total power signal under low and stable utilization. The dynamic power is defined as the non-negative residual between total and idle. Idle and dynamic energy increments are obtained by applying the same window duration used for the corresponding total power observation, ensuring that the decomposition is temporally consistent within each window.

Formalization Let $P_{uuid}(w)$ denote the corrected total GPU power associated with analysis window w, and let $\beta_{uuid}(w)$ denote the idle power estimate available for

that window. Tycho defines the power decomposition as

$$P^{\text{idle}}_{uuid}(w) = \text{clip}(\beta_{uuid}(w),\, 0,\, P_{uuid}(w))\,, \tag{4.20}$$

$$P^{\text{dyn}}_{uuid}(w) = \max\Big(0,\, P_{uuid}(w) - P^{\text{idle}}_{uuid}(w)\Big)\,. \tag{4.21}$$

With window duration $\Delta t(w)$, the corresponding per-window energy increments are

$$\Delta E^{\text{idle}}_{uuid}(w) = P^{\text{idle}}_{uuid}(w)\,\Delta t(w), \tag{4.22}$$

$$\Delta E^{\text{dyn}}_{uuid}(w) = P^{\text{dyn}}_{uuid}(w)\,\Delta t(w). \tag{4.23}$$

The decomposition is conservative by construction:

$$\Delta E^{\text{idle}}_{uuid}(w) + \Delta E^{\text{dyn}}_{uuid}(w) = P_{uuid}(w)\,\Delta t(w), \tag{4.24}$$

up to discretization and clipping effects, and with all terms constrained to be non-negative.

Design Decisions Tycho derives β_{uuid} from the corrected power signal rather than raw device telemetry to preserve temporal consistency with the exported total power and to avoid bias from known sampling and delay artifacts. Idle estimation is gated by stability of recent utilization observations and restricted to low-utilization regimes to prevent transient load onsets from being absorbed into the baseline. The model is defined per device to avoid cross-GPU coupling and to allow heterogeneous baselines within the same node.

Architectural Consequences Downstream stages may treat $(P^{\text{idle}}_{uuid}, P^{\text{dyn}}_{uuid})$ and their cumulative energies as a stable, non-negative decomposition of corrected total power per device. The stability gate implies that β_{uuid} evolves only under sufficiently stationary conditions, so dynamic power absorbs short-lived transients by default. This design intentionally prioritizes robustness of the idle baseline over rapid adaptation to changing operating points.

4.8.5 Stage 4: Workload Attribution and Aggregation

Stage 4 realises workload-level attribution by mapping system- and component-level signals to concrete execution contexts. It defines the admissible scope of attribution, resolves workload identity under partial observability, and materialises utilization metrics and CPU and GPU energy at the workload level, while explicitly bounding what is not attributed.

4.8.5.1 Workload Resolution and the `__system__` Class

Problem Statement Energy signals observed by Tycho are not intrinsically associated with Kubernetes workloads. Attribution therefore requires an explicit resolution step that maps low-level execution identities to container, pod, and namespace labels. This mapping is inherently partial, asynchronous, and failure-prone due to process churn, PID reuse, delayed metadata visibility, and non-Kubernetes activity. An architectural treatment is required to ensure that attribution remains total, conservative, and interpretable under these conditions.

Conceptual Model Stage 4 operates on energy quantities that are already temporally aligned and semantically classified (total, idle, dynamic). Workload attribution is defined as a conditional labeling step that associates each attributable energy portion with a Kubernetes workload identity when such an identity can be resolved with sufficient confidence. Resolution is based on a best-effort join between execution-level observations and a metadata view that reflects the current Kubernetes state. Energy portions for which no workload identity can be resolved are assigned to a distinguished workload class, denoted `__system__`, which represents non-attributable, infrastructural, or unresolved activity.

Formalization and Invariants. Let E denote an energy quantity produced by earlier stages and let $\mathcal{W}$ be the set of resolvable Kubernetes workload identities. Workload attribution defines a partial mapping $f : E \to \mathcal{W}$. To preserve totality, this mapping is extended to a total function $\hat{f} : E \to \mathcal{W} \cup \{\texttt{__system__}\}$ by assigning all unresolved energy to `__system__`. The following invariants hold for all Stage 4 outputs: (i) conservation: the sum of workload-attributed energy equals the input energy, (ii) non-negativity: no workload receives negative energy, (iii) monotone degradation: loss of metadata resolution increases the share attributed to `__system__` but never reallocates energy between resolved workloads.

Design Decisions The `__system__` label is treated as a first-class workload class rather than an absence of labeling. This avoids silent energy loss, preserves comparability across runs with different metadata quality, and makes unresolved attribution explicit. Workload resolution is deliberately decoupled from the attribution mathematics itself: the attribution model consumes resolved identities as inputs but does not embed resolution logic into its equations. This separation ensures that attribution correctness degrades conservatively under partial observability.

Architectural Consequences All workload-attributed metrics in Stage 4 share a common resolution boundary and a uniform interpretation of unattributable energy. Metric-specific attribution logic may differ in how energy is distributed among resolved workloads, but unresolved energy is always surfaced explicitly via `__system__`. This abstraction enables consistent downstream analysis while preventing speculative attribution beyond what the available metadata supports.

4.8.5.2 Attribution Goals, Admissible Degrees of Freedom, and Temporal Granularity

Problem Statement Even when workload identities are available, distributing energy among workloads is fundamentally underdetermined. Energy signals originate from shared components, while explanatory signals (utilization, activity, requests) are incomplete, indirect, and metric-specific. An architectural framing is required that defines what attribution must guarantee, what it may choose freely, and where Tycho deliberately refrains from speculative precision.

Attribution Goals and Invariants Stage 4 attribution is governed by a small set of global goals that apply uniformly across metrics. Attribution must conserve energy, remain non-negative, and be complete over the workload domain extended by `__system__`. Attribution must not retroactively reinterpret past decisions and must degrade monotonically under loss of explanatory signals. Beyond these invariants,

attribution is explicitly not required to recover a unique or physically exact decomposition.

Admissible Degrees of Freedom Within these constraints, Tycho allows metric-specific definitions of *fairness*. A metric may distribute energy proportionally to observed activity, declared resource requests, or other admissible proxies, provided that the global invariants are preserved. Fallback rules are permitted when proxies are missing or ill-defined, but such fallbacks must be explicit and must not introduce hidden redistribution between resolved workloads. This separation allows each metric to encode its own fairness assumptions without contaminating the shared attribution framework.

Fine-Grained Temporal Attribution as a Core Principle. A defining architectural choice of Tycho is that attribution is performed at the finest temporal granularity supported by the underlying signal, prior to any window-level aggregation. Energy portions are first attributed to workloads at this fine granularity and only then aggregated over the analysis window. This design enables Tycho to distinguish workloads with different energy characteristics even when their aggregate utilization within a window is similar. In contrast to window-pooled attribution schemes, this approach preserves temporal structure as an explanatory signal and avoids conflating heterogeneous workload behavior.

Architectural Consequences. Stage 4 defines attribution as a constrained optimization problem with explicit degrees of freedom rather than a fixed formula. Metric-specific attribution sections instantiate these freedoms while inheriting the same invariants and temporal discipline. As a result, Tycho can express nuanced workload energy differentiation when supported by data, while remaining conservative and interpretable when it is not.

4.8.5.3 Explicit Non-Attribution of Redfish Metrics

Redfish provides system-level power measurements that lack reliable workload-level explanatory signals. Attributing these measurements to Kubernetes workloads would therefore require speculative assumptions about the contribution of individual activities to shared components such as memory subsystems, interconnects, storage, or firmware-controlled behavior. Such assumptions are incompatible with Tycho's accuracy-first design philosophy.

Consequently, Redfish metrics are excluded from Stage 4 workload attribution. They are neither distributed across workloads nor labeled with `__system__` identities. Instead, Redfish metrics remain system-scoped signals that may be used for validation, bounding, or cross-checking of attributed energy, but not as sources of workload-resolved energy data.

This exclusion is a deliberate architectural decision rather than a limitation of the implementation. It preserves semantic clarity of workload-attributed metrics and prevents the introduction of unverifiable attribution artifacts.

4.8.5.4 Workload Attribution of eBPF Utilization Counters

Problem Statement Fine-grained execution activity signals collected via eBPF are emitted at process scope and are not intrinsically associated with Kubernetes workloads. To support workload-level analysis, these signals must be attributed to workload identities without modeling assumptions, while preserving conservation, non-negativity, and monotone degradation under partial observability. Unlike energy signals, eBPF counters represent directly observed activity and therefore admit attribution by aggregation rather than distribution, but only if unresolved activity is handled explicitly and conservatively.

Conceptual Model Each eBPF utilization signal is treated as a stream of per-process activity deltas observed at high temporal resolution. Stage 4 attribution maps each process delta to a workload identity when resolution succeeds, and otherwise assigns it to a distinguished `__system__` workload class. Workload-level utilization is obtained by summing all resolved process deltas per workload, while `__system__` captures the residual activity not attributable to any resolved workload. No reweighting, normalization, or inference across workloads is performed.

Formalization Let $\Delta u_p(t)$ denote the utilization delta of process p over an attribution interval at time t, and let $R(p,t)$ be the workload resolution function, which yields either a workload w or $\varnothing$.

The workload-attributed utilization $U_w(t)$ is defined as

$$U_w(t) = \sum_{p|R(p,t)=w} \Delta u_p(t), \tag{4.25}$$

and the system residual is defined by construction as

$$U_{\texttt{\_\_system\_\_}}(t) = \sum_p \Delta u_p(t) - \sum_{w \neq \texttt{\_\_system\_\_}} U_w(t). \tag{4.26}$$

This definition guarantees conservation, completeness, and non-negativity, independent of resolution success.

Design Decisions Utilization attribution is realized as aggregation rather than proportional distribution, reflecting that eBPF counters already encode directly attributable activity. The `__system__` workload is defined as a residual class by construction rather than as a fallback resolution outcome, ensuring that all unresolvable activity is captured without bias toward resolved workloads. Alternative schemes that discard unresolved activity or redistribute it among workloads were rejected due to violation of conservation and monotone degradation requirements.

Architectural Consequences The resulting workload-level utilization counters form a complete and conservative attribution surface for execution activity. They are directly comparable across workloads and over time, and remain interpretable under partial observability. These metrics provide the explanatory substrate required for energy attribution analysis and validation, without introducing additional modeling assumptions or temporal coupling.

4.8.5.5 CPU Dynamic Energy Attribution

Problem Statement CPU dynamic energy is exposed only as an aggregate per-domain signal for each RAPL CPU domain (`pkg`, `core`, `uncore`, `dram`) and is not intrinsically associated with individual workloads. At the same time, workload activity is observable only indirectly through execution-level proxies with finite resolution and partial coverage. The core problem is therefore to distribute a domain-level dynamic energy budget across workloads in a way that is conservative, temporally faithful, and robust to incomplete observability, while ensuring that attribution degrades monotonically toward the `__system__` class rather than redistributing energy among resolved workloads.

Conceptual Model For a given analysis window W and RAPL domain B, the authoritative input is the window-level dynamic energy budget $\Delta E_{B,\mathrm{dyn}}(W)$. Attribution proceeds at native eBPF bin resolution and follows a two-stage model. First, the window-level energy budget is distributed across fine-grained temporal bins proportionally to observed CPU activity in each bin. Second, each bin's energy share is distributed across workloads proportionally to their activity within that bin. This preserves temporal structure as an explanatory signal while ensuring that attribution decisions are local to each bin and degrade conservatively when activity proxies are absent.

Formalization Let $b \in W$ index the 50 ms bins contained in window W. For a given domain B, let $T_B(b)$ denote the total activity mass observed in bin b, and let $W_B(\ell, b)$ denote the activity mass attributed to workload ℓ in bin b. The per-bin energy share is defined as

$$\Delta E_B(b) = \begin{cases} \Delta E_{B,\mathrm{dyn}}(W) \cdot \dfrac{T_B(b)}{\sum_{b' \in W} T_B(b')} & \text{if } \sum_{b' \in W} T_B(b') > 0, \\ 0 & \text{otherwise.} \end{cases} \tag{4.27}$$

Within each bin, workload attribution is defined as

$$\Delta E_B(\ell, b) = \begin{cases} \Delta E_B(b) \cdot \dfrac{W_B(\ell, b)}{T_B(b)} & \text{if } T_B(b) > 0, \\ 0 & \text{otherwise.} \end{cases} \tag{4.28}$$

If either $\sum_b T_B(b) = 0$ or $T_B(b) = 0$ for a given bin, the corresponding energy mass is assigned to the `__system__` workload, preserving completeness and conservation.

Design Decisions Observed CPU activity is used as the sole fairness basis. For the `pkg`, `core`, and `uncore` domains, activity is measured via per-process retired instruction counts. For the `dram` domain, activity is measured via cache-miss counts, with a window-scoped fallback to CPU cycle counts when cache-miss mass is zero but cycle mass is non-zero. This choice reflects the closest available causal relationship between workload behavior and domain-specific dynamic energy, while remaining explicit and conservative under missing signals.

Architectural Consequences The resulting attribution is causal, temporally fine-grained, and strictly conservative. All dynamic CPU energy is assigned either to resolved workloads or to `__system__`, with no redistribution between workloads

under metadata loss. The bin-level structure remains an explicit part of the architectural contract, enabling later extensions such as non-linear attribution rules or idle–dynamic decomposition without revisiting the core attribution model.

4.8.5.6 CPU Idle Energy Attribution

Problem Statement CPU idle energy represents background consumption that cannot be causally attributed to instantaneous workload execution. Unlike dynamic CPU energy, idle energy persists in the absence of activity and reflects platform state, reservation, and scheduling slack. Attribution must therefore define a fairness policy that preserves strict conservation and monotone degradation under partial observability, without asserting unsupported causal relationships.

Conceptual Model Idle energy attribution is modeled as a policy-driven distribution of a per-window idle energy budget across workloads. The model separates declarative reservation from observed activity by partitioning the idle budget into two conceptual pools. Reservation captures long-lived entitlement to capacity, while activity captures short-term presence and participation. The distinguished `__system__` workload is a first-class participant that absorbs unavoidable background and remainder energy.

Formalization For each analysis window W and RAPL domain d, a conservative idle energy budget $E^{d}_{\text{idle}}(W)$ is given. A reservation fraction $\beta \in [0, 1]$ partitions this budget:

$$E^{d,\text{req}}_{\text{idle}}(W) = \beta \cdot E^{d}_{\text{idle}}(W), \qquad E^{d,\text{opp}}_{\text{idle}}(W) = E^{d}_{\text{idle}}(W) - E^{d,\text{req}}_{\text{idle}}(W). \tag{4.29}$$

For CPU domains (`pkg`, `core`, `uncore`), β is derived from the ratio of declared CPU requests to node CPU capacity. For `dram`, β is derived analogously from declared memory requests and node memory capacity.

The reserved pool $E^{d,\text{req}}_{\text{idle}}$ is distributed proportionally among workloads with strictly positive requests. The opportunistic pool $E^{d,\text{opp}}_{\text{idle}}$ is distributed proportionally according to window-aggregated dynamic activity weights. Workloads without requests participate only in the opportunistic pool. The `__system__` workload always participates in the opportunistic pool and receives any residual energy required for exact conservation.

Design Decisions A two-pool policy is chosen over pure activity-based allocation to preserve the semantic distinction between reserved capacity and opportunistic use. Using conservative per-window idle budgets preserves strict decomposition of total CPU energy into idle and dynamic components. Applying the same attribution structure across all CPU-related RAPL domains ensures interpretability and comparability, while allowing domain-specific reservation signals.

Architectural Consequences Idle energy attribution is explicitly defined as a fairness policy rather than a causal reconstruction. The model guarantees conservation, non-negativity, and completeness per window, and degrades monotonically toward `__system__` under reduced observability. The resulting workload-level idle energy

counters are directly comparable to dynamic CPU attribution outputs and provide a stable basis for downstream analysis without retroactive reinterpretation.

4.8.5.7 GPU Dynamic Energy Attribution

Problem Statement GPU dynamic energy must be attributed to Kubernetes workloads without directly observable per-workload energy counters. Attribution must remain conservative under incomplete proxy coverage and must not force energy onto workloads when the proxy signal cannot support it.

Conceptual Model For each GPU device, dynamic energy is treated as a window budget derived from the corrected GPU energy signal. Workloads receive shares of this budget proportional to per-process GPU compute utilization, aggregated over the window and mapped to workloads via the established resolver. Any fraction of dynamic energy that cannot be supported by resolvable process activity is assigned to `__system__`.

Formalization Let W be an analysis window and let $\Delta E_{\text{gpu}}(W, \text{uuid})$ denote the corrected total GPU energy over W for device uuid. Let $\Delta E_{\text{gpu,dyn}}(W, \text{uuid})$ denote the dynamic GPU energy budget for the same window and device. Tycho allocates dynamic energy at the granularity of process-sample intervals. For an interval $I \subseteq W$, let $\Delta E_{\text{gpu}}(I, \text{uuid})$ be the corrected interval energy, and let

$$f(W, \text{uuid}) = \text{clip}_{[0,1]}\left(\frac{\Delta E_{\text{gpu,dyn}}(W, \text{uuid})}{\Delta E_{\text{gpu}}(W, \text{uuid})}\right). \tag{4.30}$$

The interval dynamic budget is

$$\Delta E_{\text{gpu,dyn}}(I, \text{uuid}) = f(W, \text{uuid}) \cdot \Delta E_{\text{gpu}}(I, \text{uuid}). \tag{4.31}$$

Let $\mathcal{P}_I$ be the set of observed GPU PIDs in I, and let $u_p(I) \in [0, 100]$ be the held utilization proxy for PID p over I. Define proxy mass

$$U(I) = \sum_{p \in \mathcal{P}_I} \max(0, u_p(I)). \tag{4.32}$$

If $U(I) = 0$, then $\Delta E_{\text{gpu,dyn}}(I, \text{uuid})$ is assigned to `__system__`. Otherwise, each PID receives a process-level share

$$\Delta E_{\text{gpu,dyn}}(p, I, \text{uuid}) = \Delta E_{\text{gpu,dyn}}(I, \text{uuid}) \cdot \frac{u_p(I)}{U(I)}. \tag{4.33}$$

Each process share is mapped to a workload key via the resolver; unresolved shares are assigned to `__system__`. Workload energy is the sum of mapped process shares across all intervals in W and all contributing PIDs.

Design Decisions Dynamic GPU energy is distributed exclusively using per-process `ComputeUtil` as the proxy basis. This choice preserves conservative semantics: any dynamic energy not supported by positive proxy mass, or not attributable through the resolver, is routed to `__system__`. A per-window dynamic fraction $f(W, \text{uuid})$ scales interval energy to reconcile sub-window corrected energy structure with a

separately constructed dynamic budget, without introducing an independent dynamic model at sub-window granularity.

Architectural Consequences Dynamic GPU workload attribution is proxy-limited. Even under purely Kubernetes-driven GPU load, a non-zero `__system__` dynamic share is admissible and expected when driver overhead, sampling noise, or incomplete per-process accounting prevents full proxy coverage. Attribution remains conservative because unresolved or weakly supported energy increases `__system__` share rather than being forced onto resolved workloads.

4.8.5.8 GPU Idle Energy Attribution

Problem Statement GPU idle energy lacks a defensible workload-level proxy and must not be speculatively distributed across workloads.

Conceptual Model GPU idle energy is treated as non-attributable and is assigned in full to the canonical `__system__` workload class, per GPU device.

Formalization For each window W and device uuid, let $\Delta E_{\text{gpu,idle}}(W, \text{uuid})$ be the corrected idle GPU energy. Tycho defines workload-attributed idle energy as

$$\Delta E_{\text{gpu,idle}}(\texttt{\_\_system\_\_}, W, \text{uuid}) = \Delta E_{\text{gpu,idle}}(W, \text{uuid}), \tag{4.34}$$

and emits no non-`__system__` idle workload series.

Design Decisions Idle attribution is intentionally degenerate. The only emitted idle workload series is `__system__`, enabling a complete workload accounting view over GPU energy without introducing speculative distribution.

Architectural Consequences GPU idle energy is explicitly interpreted as infrastructural or non-attributable device cost. Completeness is achieved by construction, while preserving the accuracy-first constraint that idle energy is not redistributed to workloads.

4.8.6 Prometheus Exporter

Problem Statement Tycho produces window-committed analysis points that must be exposed to external systems without introducing additional semantics, temporal reinterpretation, or ownership over metric meaning.

Conceptual Model The exporter is defined as a passive sink that materializes the latest committed analysis points into a pull-based observation interface. It does not interpret, aggregate, or transform metrics beyond name normalization and schema stabilization. Exposition semantics, scraping cadence, retention, and downstream labeling are explicitly outside Tycho's architectural scope.

Formalization For each analysis point emitted at the end of an analysis cycle, the exporter exposes exactly one observable value per metric key corresponding to the most recently committed window. No historical state, interpolation, or backfilling is performed.

Design Decisions Metric exposition is deliberately decoupled from analysis execution. Tycho does not define scrape timing, persistence, or query semantics, and does not distinguish between metric consumers. All exported metric names are prefixed with `tycho_` to ensure namespace isolation and unambiguous attribution.

Architectural Consequences Metric meaning and correctness are fully determined upstream of the exporter. Downstream systems may freely attach additional labels such as node identity or perform aggregation without affecting Tycho's attribution guarantees.

4.9 Architectural Trade-Offs and Alternatives Considered

Tycho adopts an explicitly *accuracy-first* architectural stance. This choice prioritises preservation of temporal structure and interpretability of uncertainty over simplicity of implementation. As a result, the system deliberately rejects several simpler architectural alternatives that would reduce complexity by discarding information or by enforcing assumptions that are incompatible with heterogeneous, asynchronous metric sources. This section briefly situates Tycho's design within the broader architectural design space and clarifies why these alternatives were not adopted.

4.9.1 Timing and Data Collection Models

A common design choice in monitoring systems is to impose a single global polling loop or a strictly synchronised sampling schedule across all metric sources. Such designs are attractive because they simplify implementation and produce visually aligned time series. However, this alignment is artificial: it reflects the sampling strategy rather than the behaviour of the underlying systems.

Tycho rejects globally synchronised sampling because the metric domains it observes do not share a natural clock. CPU energy counters, accelerator telemetry, kernel execution events, and out-of-band system power measurements each exhibit distinct update semantics and latency characteristics. Forcing these domains into a single synchronous schedule necessarily introduces aliasing, under-sampling, or false simultaneity, thereby destroying temporal meaning rather than revealing it.

In an accuracy-first architecture, temporal structure is part of the signal. Tycho therefore treats domain-specific timing behaviour as a first-class property and preserves it through independent, domain-aware collection. The resulting increase in architectural complexity is a direct consequence of respecting how information is produced, rather than a by-product of implementation choices.

4.9.2 Attribution Model Design Space

Workload-level energy attribution is fundamentally underdetermined. Multiple attribution paradigms exist that reduce this ambiguity by imposing strong simplifying assumptions, such as static proportionality, fixed analytical models, or globally normalised distributions. While these approaches yield concise formulations, they also collapse uncertainty and obscure the limits of what can be inferred from the available data.

Tycho deliberately avoids committing to such simplifications at the architectural level. An accuracy-first system must remain explicit about what is supported by observation and what is not. This requires attribution mechanisms that degrade conservatively under partial observability, preserve conservation and non-negativity, and avoid redistributing energy based on unverifiable assumptions.

Accordingly, Tycho's architecture constrains attribution through invariants and admissible degrees of freedom rather than prescribing a single closed-form solution. This preserves interpretability and makes uncertainty visible, at the cost of increased conceptual and structural complexity.

4.9.3 Accuracy Versus Architectural Complexity

The architectural complexity of Tycho is not incidental. It arises from the decision to preserve information across heterogeneous domains, to maintain temporal coherence under asynchronous observation, and to expose uncertainty rather than masking it. Simpler architectures achieve tractability primarily by discarding these properties.

From an accuracy-first perspective, complexity is acceptable where it prevents semantic loss and bounded where it does not. Tycho confines complexity through explicit abstraction boundaries between collection, timing, analysis, and attribution, ensuring that individual components remain understandable even as the system as a whole addresses a challenging problem space.

Reducing architectural complexity in this context would primarily eliminate information and weaken interpretability rather than improve correctness. The resulting system might appear simpler, but it would do so by obscuring the very phenomena that Tycho is designed to measure.

4.10 Summary

This chapter defined the architectural foundation of Tycho as an accuracy-first energy attribution system for Kubernetes environments. The design is derived directly from the requirements established in Chapter 3, in particular temporal coherence across heterogeneous metric sources, domain-level consistency, transparent modelling assumptions, lifecycle-robust workload identity handling, and explicit treatment of uncertainty.

The architecture is organised around a small number of clearly separated concerns. Independent, domain-aware metric collectors acquire observations without imposing artificial synchrony. A global event-time-based timing engine defines attribution windows and provides a coherent temporal reference for all analysis. Calibration serves as an auxiliary subsystem that constrains polling and delay uncertainty where hardware-controlled publication behaviour would otherwise undermine temporal interpretation.

Analysis is structured as a deterministic, staged pipeline that transforms buffered observations into window-scoped quantities under explicit dependency and conservation rules. Component-level metric construction establishes authoritative energy and power signals, which are subsequently decomposed into idle and dynamic

contributions before being mapped to workload identities. Workload attribution is explicitly bounded: energy is attributed conservatively where explanatory signals permit, and unresolved or infrastructural consumption is surfaced explicitly via the `__system__` class rather than being redistributed speculatively.

Metadata collection and lifecycle management are treated as architectural prerequisites for attribution correctness rather than as auxiliary implementation details. By enforcing freshness bounds and separating identity resolution from attribution mathematics, the architecture ensures monotone degradation under partial observability. Finally, metric export is defined as a passive sink, preserving the semantic boundary between attribution logic and downstream monitoring systems.

Together, these architectural elements specify *what* Tycho must do and *why* it must do so to meet its accuracy and transparency goals, without committing to specific implementation mechanisms. The following chapter describes the concrete implementation of these architectural components, including the collectors, timing engine, metadata subsystem, calibration routines, and the realisation of the analysis and attribution pipeline.

Chapter 5

Implementation

5.1 Purpose, Scope, and Execution-Time Structure

This chapter explains how Tycho's architectural abstractions are realised at runtime under the constraints of discretization, partial observability, and asynchronous execution. Its role is to describe how responsibility boundaries defined in the architecture are enforced concretely, and how correct attribution is achieved despite imperfect and delayed inputs. Architectural concepts, models, and invariants are assumed from earlier chapters and are not reintroduced here.

At execution time, Tycho is structured as a set of long-lived subsystems with strictly separated responsibilities and unidirectional interaction. Each subsystem exercises authority over a narrow concern, and no subsystem compensates implicitly for the behaviour of others. This execution-time separation forms the foundation for correctness, auditability, and robustness throughout the implementation.

Additional implementation detail that is not required for understanding the runtime structure or correctness arguments is intentionally deferred to Appendix C. The appendix collects auxiliary material such as extended configuration descriptions, supporting scripts, and low-level operational notes that aid reproducibility and inspection without obscuring the main implementation narrative.

5.1.1 Runtime Subsystems and Responsibilities

Tycho's runtime consists of the following subsystems, each of which is examined in detail later in this chapter:

- The **timing engine** provides execution-time coordination by triggering collection and analysis actions according to a global schedule, without participating in interpretation or attribution (§ 5.2).
- **Metric collectors** act as independent observers that acquire raw measurements from individual hardware and software domains and emit timestamped samples without coordination or semantic interpretation (§ 5.4).
- The **metadata subsystem** maintains a refreshed view of workload identity and hierarchy, supplying identity context during attribution without joining metric streams or performing analysis (§ 5.5).

- **Calibration mechanisms** derive auxiliary parameters that characterise source behaviour and contextualise interpretation, executing outside steady-state attribution and without modifying observations (§ 5.6).
- The **analysis engine** is the sole authority responsible for interpreting observations, fusing domains, applying attribution models, and enforcing architectural invariants on a per-window basis.
- **Export** observes the results of analysis and exposes them to external systems without influencing upstream execution or attribution semantics

5.1.2 Execution-Time Interaction Model

Interaction between these subsystems follows a strictly unidirectional pattern. Temporal authority originates in the timing engine, observation authority in collectors and metadata acquisition, and semantic authority exclusively in the analysis engine. Data flows forward through explicit handoff only: raw observations and identity context are materialised upstream and consumed read-only during analysis, while attribution results flow downstream to export.

This interaction model deliberately excludes feedback paths, implicit coordination, and retroactive modification of observations. Once emitted, samples are immutable; once a window is analysed, its results are final. These constraints ensure that attribution semantics remain explicit, reproducible, and independent of scheduling or export behaviour.

The remainder of this chapter elaborates on how each subsystem realises its assigned responsibility in practice, addressing temporal realisation, collection mechanics, identity handling, calibration, attribution, and robustness in turn (§ 5.2–§ 5.9).

5.2 Temporal Infrastructure and Window Realization

5.2.1 Architectural Context and Implementation Problem

§ 4.4 defines Tycho's temporal model in abstract terms: a single monotonic time base, independently operating collectors, and fixed-duration analysis windows triggered by a timing engine. The implementation task is to realize this model under real execution constraints while preserving its guarantees, rather than restating its semantics.

Collectors are scheduled by a general-purpose operating system and are subject to jitter, preemption and variable execution latency. Polling callbacks may execute late, at uneven intervals, or out of phase with one another. Analysis must therefore not depend on execution order, callback timing, or implicit synchronization effects. Temporal correctness must derive exclusively from explicit timestamps attached to observations, not from when code happens to execute. The temporal infrastructure enforces this separation rigorously.

5.2.2 Global Monotonic Time Realization

The architectural event-time model relies on a single system-wide monotonic time base. Its implementation elevates monotonic time to a first-class dependency rather

than treating it as an incidental property of the runtime environment. All collectors, the timing engine and the analysis engine obtain temporal information exclusively through a dedicated clock abstraction.

Wall-clock time is excluded from analysis-critical paths and appears only where external representation is unavoidable. The clock abstraction provides monotonic timestamps for observations and analysis boundaries, mediates conversion between real-time and monotonic representations where required, and is injected into downstream components to ensure consistent and testable temporal behavior across subsystems.

As a result, scheduling jitter becomes an explicit input to analysis rather than a hidden source of error. A collector that executes late produces a correspondingly late timestamp. No corrective action is taken at collection time; timestamps are interpreted during analysis according to the delay and freshness assumptions defined in § 4.4. Monotonic timestamps thus constitute the sole temporal authority within the system.

5.2.3 Timing Engine and Hierarchical Cadence Alignment

Independent collector schedules are a central architectural principle. Realizing this independence without sacrificing determinism requires a controlled mechanism for initiating periodic actions. Tycho employs a centralized timing engine to which all periodic activities register during system initialization.

Each registration specifies a period expressed as an integer multiple of a global base quantum (default: 1 ms). All registrations are aligned to a shared epoch defined by this quantum, establishing deterministic phasing across the system. Collector and analysis triggers are hierarchically derived from this common cadence rather than started opportunistically, ensuring that identical configurations produce identical temporal behavior across runs. Alignment does not impose a shared frequency: collectors with different periods remain independent, but their triggers occur at deterministic offsets on the global monotonic axis.

The timing engine is deliberately non-semantic. It does not inspect collected data, adapt schedules, or coordinate collectors. Its sole responsibility is to emit triggers at predetermined monotonic times. Work performed in response to a trigger is constrained to be minimal and non-blocking, typically limited to recording an observation and placing it into a buffer, preventing local execution delays from propagating into global timing behavior.

Analysis triggering is implemented using the same registration mechanism. The analysis engine registers a periodic trigger alongside collectors, making analysis execution subject to the same alignment and determinism guarantees. This design enforces single-cycle exclusivity by construction: a new analysis cycle cannot begin before the previous trigger boundary has been established, without requiring additional synchronization logic.

5.2.4 Analysis Window Realization and Trigger Semantics

Analysis windows are realized when an analysis trigger fires. At that instant, the timing engine provides a single monotonic timestamp t_{now}, which defines the upper boundary of the current window. This timestamp is captured exactly once and propagated unchanged throughout the entire analysis cycle. All metrics are evaluated against windows derived from this shared boundary, and no component recomputes or refines the window definition during analysis. Consequently, all attribution decisions within a cycle refer to an identical temporal interval, independent of execution order or internal processing latency.

Window boundaries are defined by trigger times rather than sample arrival. Samples collected before t_{now} may be included or excluded according to domain-specific delay and freshness rules as defined in § 4.4. Samples arriving after the trigger are attributed to subsequent windows. This separation prevents double-counting and omission even under heterogeneous collector rates.

Temporal complexity is intentionally confined to timestamping and delay interpretation. Window construction itself remains simple and predictable, providing a stable temporal substrate on which later analysis stages can reason about delay, partial observation and attribution correctness without embedding scheduling assumptions or compensating for execution artifacts.

5.3 Historical Observation Retention

Tycho retains a bounded history of raw observations in order to support downstream analysis that requires temporal context beyond a single attribution window. This retention is an explicit implementation responsibility derived from the temporal model in § 4.4. Rather than operating exclusively on window-local samples, Tycho preserves historical signal to mitigate discretization effects, tolerate heterogeneous collector cadences, and enable mathematically stable downstream interpretation.

5.3.0.1 Metric Observation Retention

Historical retention is realized through per-collector observation buffers with time-based semantics. Each collector appends observations to its own buffer, which retains a fixed-duration history with a default horizon of approximately 90 s. This horizon deliberately exceeds the nominal analysis window length and is chosen to provide substantial temporal context for downstream analysis. Buffer capacity is computed at startup from the collector's polling interval and the configured analysis window, ensuring that retained history covers at least twice the longer of these durations, augmented by a small safety margin. Under Tycho's default configuration for high-frequency analysis, this corresponds to retention spanning approximately 18 full analysis windows, providing substantial historical context for downstream analysis models. Retention is bounded and fixed for the lifetime of the process.

Buffered samples are append-only and immutable once written. Downstream components access buffered data strictly in a read-only manner. No guarantee is made

that all collectors contribute samples to every window or that samples are temporally aligned across collectors. Partial observability and heterogeneous update patterns are therefore preserved explicitly and interpreted by the analysis engine rather than hidden by synchronization.

5.3.0.2 Metadata Retention

In addition to metric observations, Tycho maintains a bounded cache of metadata describing process, cgroup and workload identities. This cache employs a time-based retention policy aligned with the metric retention horizon to ensure that buffered observations can be joined with valid identity information during analysis. Metadata history is not used for long-term modeling and is removed once it exceeds the retention window.

5.4 Metric Collection Subsystems

5.4.1 eBPF Collector Implementation

This section describes how Tycho realises the event-driven CPU ownership and activity model introduced in § 4.5.1. The eBPF collector implements a kernel-level acquisition path that captures execution boundaries precisely and exposes the resulting activity as bounded, per-window deltas for downstream analysis.

5.4.1.1 Implementation Strategy

The implementation follows a split-surface strategy that separates *attributable* activity from *non-attributable* CPU time. Attributable activity is accumulated per process at scheduler boundaries, together with stable identity and classification metadata. Non-attributable activity, including idle time and interrupt handling, is accumulated per CPU and exported independently. This separation reflects Tycho's attribution requirements: process-level ownership must be preserved without ambiguity, while certain CPU time categories cannot be meaningfully assigned to workloads. All kernel programs operate strictly locally, without cross-CPU or cross-process aggregation; consolidation and interpretation are deferred to userspace and later analysis stages.

5.4.1.2 Core Mechanisms

Process-level accounting is driven by scheduler transitions. At each context switch, the outgoing execution interval is closed and its duration is accumulated into the corresponding process aggregate, together with hardware performance counters sampled at the same boundary. Process identity, control-group association, and kernel-thread classification are captured at these execution boundaries and stored alongside the counters. By aligning accumulation with actual ownership changes, the implementation preserves the architectural guarantee that execution intervals form precise attribution boundaries.

CPU-local accounting handles activity that is not attributable to individual processes. Each CPU maintains a local state machine that tracks the currently active context and the timestamp of the last transition. Idle time is detected explicitly via the scheduler's idle task and accumulated when the CPU executes in this state. Hard interrupt and soft interrupt handling are measured as outermost intervals using entry

and exit hooks, with durations accumulated into per-CPU bins. This design avoids double counting under nested interrupts while preserving a complete partition of CPU time at the node level.

Userspace collection materialises kernel-side accumulation into analysis-ready deltas. At a fixed polling cadence, the collector snapshots all process aggregates and resets only their counter fields while preserving identity metadata. This stable-key snapshot design avoids missing-entry artefacts that can occur if keys are deleted while scheduler updates are in flight. CPU-level bins are read and reset in the same cycle, defining a clear collection boundary for idle and interrupt time. The result of each collection cycle is a single tick record that represents all observed activity since the previous boundary, without overlap or double counting.

5.4.1.3 Robustness and Edge Cases

Several implementation choices ensure robustness under concurrent kernel activity. Process aggregates persist across collection cycles, and only delta-relevant fields are reset, preventing transient key loss under concurrent scheduler updates. All kernel-side state is bounded through per-CPU arrays, bounded per-process maps, and fixed-size histograms for interrupt vector enrichment. Reset failures or map evictions are treated as non-fatal; correctness is restored automatically in subsequent cycles. A fundamental observability limit remains: processes that execute entirely between two collection boundaries may not be observed. This limitation is inherent to discrete materialisation and is not compensated by inference.

5.4.1.4 Implementation Consequences

In practice, the eBPF collector produces a fixed-resolution utilisation and activity surface that preserves execution-boundary accuracy and stable process identity. Per-window deltas are exported without imposing additional timing constraints on the analysis engine, enabling proportional attribution and energy modelling in later stages.

5.4.1.5 Collected Metrics

The process-level and CPU-level metrics exported by the eBPF collector are listed in table Table 5.1.

Metric	Source hook	Description
Time-based metrics		
Process runtime	`tp_btf/sched_switch`	Per process. Elapsed on-CPU time accumulated at context switches.
Idle time	Derived from `sched_switch`	Per node. Aggregated idle time across CPUs.
IRQ time	`irq_handler_{entry,exit}`	Per node. Aggregated duration spent in hardware interrupt handlers.
SoftIRQ time	`softirq_{entry,exit}`	Per node. Aggregated duration spent in deferred kernel work.
Hardware-based metrics		
CPU cycles	PMU (`perf_event_array`)	Per process. Retired CPU cycle count during task execution.
Instructions	PMU (`perf_event_array`)	Per process. Retired instruction count.
Cache misses	PMU (`perf_event_array`)	Per process. Last-level cache misses; indicator of memory intensity.
Classification and enrichment metrics		
Cgroup ID	`sched_switch`	Per process. Control group identifier for container attribution.
Kernel thread flag	`sched_switch`	Per process. Marks kernel threads executing in system context.
Page cache hits	`mark_page_accessed`	Per process. Read or write access to cached pages; proxy for I/O activity.
IRQ vectors	`softirq_entry`	Per process. Frequency of specific soft interrupt vectors.

TABLE 5.1: Metrics collected by the kernel `eBPF` subsystem.

5.4.2 RAPL Collector Implementation

This section realizes the architectural model of cumulative CPU-domain energy sampling described in § 4.5.2. The collector's responsibility is strictly limited to observing hardware-provided cumulative energy counters at tick boundaries and preserving their semantics.

5.4.2.1 Implementation Strategy

To preserve domain-consistent CPU energy measurement across vendors, the collector employs a dual-backend strategy selected at runtime via CPUID. On Intel systems, energy is obtained through the RAPL interface exposed via the `powercap` subsystem. On AMD systems, the collector preferentially uses `amd_energy` via the `hwmon` interface, which provides accurate CPU energy telemetry on these platforms. The powercap path is used on AMD only if no CPU-labeled hwmon energy source is present. This strategy ensures that the architectural RAPL domain abstraction is realized consistently, independent of vendor-specific exposure mechanisms.

5.4.2.2 Core Mechanisms

At each tick, the collector obtains a single snapshot of cumulative energy counters for all available CPU domains and sockets and records them unchanged. All values

are stored as cumulative microjoule counters, matching the native units of the underlying sources. Supported domains include package and core on all platforms, with uncore (PP1) and DRAM recorded when exposed by the hardware. On AMD systems, `amd_energy` publishes per-logical-core energy values; these are aggregated by summation into a single cumulative core-domain counter to preserve domain semantics. Domains not provided by the platform are recorded as zero to maintain a stable domain set across ticks.

5.4.2.3 Robustness and Edge Cases

Powercap-backed RAPL counters may wrap and are corrected at collection time to maintain monotonicity. The hwmon-backed `amd_energy` counters do not wrap and require no correction. Each sample is tagged exclusively with a monotonic timestamp provided by Tycho's timing engine. Partial reads are permitted and result in partial ticks; no backend instability was observed in practice.

5.4.2.4 Implementation Consequences

In practice, the collector guarantees exactly one cumulative energy sample per supported domain and socket at each tick, with vendor-independent domain semantics and bounded noise. The resulting time series form a stable input for downstream differencing and attribution. The only remaining limitation is platform-dependent domain availability, which is intentionally exposed rather than approximated.

5.4.2.5 Collected Metrics

The RAPL collector exports raw cumulative energy counters once per tick. Table 5.2 summarizes the metrics recorded per `RaplTick`.

Metric	Unit	Description
Per-socket energy counters		
`Pkg`	mJ	Cumulative package energy per socket (RAPL `PKG` domain).
`Core`	mJ	Cumulative core energy per socket (RAPL `PP0` domain), when available.
`Uncore`	mJ	Cumulative uncore energy per socket (RAPL `PP1` or uncore domain), when available.
`DRAM`	mJ	Cumulative DRAM energy per socket (RAPL `DRAM` domain), if the platform exposes it.
Metadata		
`Source`	–	Identifier of the active RAPL backend (for example `powercap`)
`Sockets`	–	Map from socket identifier to the corresponding set of domain counters.
`SampleMeta.Mono`	–	Monotonic timestamp assigned by Tycho's timing engine at the moment of collection.

TABLE 5.2: Metrics exported by the RAPL collector per `RaplTick`.

5.4.3 Redfish Collector Implementation

This section describes how Tycho realizes the Redfish power source defined in § 4.5.3. Redfish is treated as an externally clocked, latently published observation whose update cadence and timing semantics are controlled by the Baseboard Management Controller. The implementation must therefore tolerate missing observations, expose temporal uncertainty explicitly, and avoid manufacturing samples while still enabling a coherent downstream power timeline.

5.4.3.1 Implementation Strategy

The Redfish collector issues at most one query per engine tick and emits a record only when a power value can be obtained reliably or when an explicit continuity fallback is required. The collector is permitted to emit no record for a tick. This choice reflects the architectural intent to avoid speculative continuity and to preserve the distinction between absence of information and persistence of state. Temporal alignment to Tycho's monotonic timebase is achieved by timestamping at collection time, without attempting synchronization or correction of BMC time.

5.4.3.2 Freshness Realization and Semantics

Freshness is realized as a best-effort quality annotation computed as the difference between the local monotonic collection time and the timestamp provided by the BMC, when available. Given the limited and vendor-specific semantics of BMC timestamps, the collector applies no correction, filtering, or normalization. Freshness therefore represents observed latency and staleness rather than a validity constraint.

When continuation records are emitted, the collector reuses the most recent BMC timestamp and recomputes freshness accordingly. As a consequence, freshness increases during prolonged publication gaps, making temporal uncertainty explicit. The collector never suppresses, alters, or reclassifies samples based on freshness. All values are forwarded unchanged as downstream quality indicators.

5.4.3.3 Heartbeat-Based Continuity as Fallback

Irregular Redfish publication implies that fixed-cadence sampling may observe extended periods without new measurements. The collector therefore supports an optional heartbeat mechanism whose role is explicitly fallback-oriented. Heartbeat does not operate on every missed tick. Instead, it re-emits a specially marked continuation record only when no fresh observation has been obtained for a comparatively long interval relative to the engine cadence.

By default, this interval substantially exceeds the collection period, ensuring that short-lived access failures or transient gaps result in silence rather than artificial continuity. If enabled, the heartbeat threshold may be configured statically or derived adaptively from observed inter-arrival times of fresh Redfish updates, with conservative bounds to avoid pathological behavior under highly irregular BMC implementations. Heartbeat emission never invents new measurements. It explicitly signals persistence of the last known value when prolonged absence would otherwise break temporal continuity.

5.4.3.4 Robustness Under Partial Observation

Redfish access failures and missing timestamps are treated as normal operating conditions. If a Redfish query fails, the collector emits no record for that tick. No retries, backoff strategies, or suppression mechanisms influence the semantic output. Only when the heartbeat threshold is exceeded does the collector emit a continuation record, clearly distinguishing prolonged absence from transient failure.

Multiple chassis are handled independently. Freshness computation, heartbeat state, and continuation decisions are maintained per chassis and never synchronized across nodes. This preserves architectural assumptions about the independence of Redfish power sources in multi-node deployments.

5.4.3.5 Implementation Consequences

In practice, the collector emits at most one record per chassis per engine tick, with zero records as a valid and expected outcome. Continuity is preserved only when absence becomes prolonged, and even then without obscuring staleness. The resulting stream provides a stable, monotonic reference for total node power while exposing uncertainty rather than masking it.

This implementation anchors Tycho's global energy view and supports later reconciliation with in-band estimates without conflating observation authority or temporal semantics. Its limitations are deliberate. Temporal resolution and accuracy are bounded by the BMC, and no component-level attribution is attempted at this stage.

5.4.3.6 Collected Metrics

The Redfish collector emits instantaneous chassis power together with identity and temporal metadata. Only raw observations are produced. Derived quantities such as energy are computed by downstream analysis stages. The exported fields are summarized in Table 5.3.

Metric	Unit	Description
Primary power metric		
`PowerWatts`	W	Instantaneous chassis power reported by the BMC.
Temporal and identity metadata		
`ChassisID`	-	Identifier of the chassis or enclosure.
`Seq`	-	Server-provided sequence number indicating new measurements.
`SourceTime`	s	Timestamp provided by the BMC, if available.
`CollectorTime`	s	Local collection time of the measurement.
`FreshnessMs`	ms	Difference between `SourceTime` and `CollectorTime`.

TABLE 5.3: Metrics collected by the Redfish collector.

5.4.4 GPU Collector Implementation

The GPU collector realises the architecture described in § 4.5.4 and integrates accelerator telemetry into Tycho's unified temporal framework. In contrast to other energy domains, GPU telemetry is published at discrete, driver-controlled moments that are neither continuous nor externally observable. The implementation is therefore responsible for enforcing phase-aligned, event-driven sampling under partial observability, backend variability, and timing jitter, while preserving strict monotonic ordering across all domains.

The central implementation invariant is that at most one `GpuTick` is emitted per confirmed hardware publish, and that no tick is emitted without a detectable device update. All mechanisms described in this section exist to uphold this invariant in practice, including the integration of retrospective process-level telemetry under wall-clock semantics.

5.4.4.1 Implementation Strategy

The implementation treats GPU sampling as an inference problem rather than a periodic measurement task. Because the driver's publish cadence is implicit, polling is used only as a means to detect new hardware updates, not as a proxy for time. Sampling effort is modulated according to the phase-aware timing model defined in § 4.5.4, concentrating observation near predicted publish moments while suppressing redundant reads elsewhere.

Freshness detection and event emission are deliberately decoupled. Polling may occur at high frequency, but a `GpuTick` is emitted only when a previously unseen device update is detected and can be placed monotonically into Tycho's multi-domain buffer. This separation ensures that increased polling density improves detection latency without inflating the event stream or distorting temporal structure.

Device-level and process-level telemetry are integrated asymmetrically. Device snapshots define the temporal anchor of each `GpuTick`, while process-level records are attached retrospectively to confirmed device updates to accommodate backend-imposed wall-clock windows. This strategy preserves the architectural timing guarantees while enabling multi-tenant attribution under heterogeneous backend constraints.

5.4.4.2 Phase-Aware Sampling Realisation

The phase-aware timing model defined in § 4.5.4 is realised through a conservative observation pipeline that separates sampling attempts from update confirmation. Polling is driven by predicted publish moments, but observations are accepted only when they provide evidence of a previously unseen hardware update. This prevents both aliasing and redundant emission under irregular driver cadence.

Freshness detection prioritises the strongest available backend signal. When reliable cumulative energy counters are present, monotonic advancement of these counters serves as the authoritative indicator of a new publish. On devices lacking such counters, freshness is inferred from instantaneous power changes exceeding a noise-tolerant threshold. In both cases, snapshots that do not satisfy freshness criteria are discarded without affecting estimator state or downstream timelines.

Duplicate suppression is enforced by conditioning all state updates on confirmed freshness. Period and phase estimators are advanced only when a new publish is detected, ensuring that redundant polls neither bias cadence inference nor generate spurious alignment corrections. This guarantees that increased polling density reduces detection latency without inflating the logical event stream.

5.4.4.3 Event Construction and Emission

When a fresh device update is confirmed, the collector constructs a `GpuTick` that represents the accelerator state at a single monotonic timestamp. The device snapshot defines the temporal anchor of the event. If process-level telemetry is available, the corresponding utilisation records, aggregated over a backend-defined wall-clock window, are attached retrospectively to the same tick.

Tick emission is strictly conditional on update confirmation. No `GpuTick` is produced for redundant or ambiguous observations, and no tick is emitted retroactively. Each emitted tick is inserted into Tycho's multi-domain buffer in monotonic order, preserving causal alignment with RAPL, Redfish, and eBPF data without interpolation or reordering.

This construction enforces a one-to-one correspondence between hardware publishes and GPU events. As a result, the GPU timeline reflects device behaviour rather than sampling artefacts and provides a temporally consistent input to subsequent attribution stages.

5.4.4.4 Process Telemetry Integration

Process-level GPU telemetry is exposed by the backend only as utilisation aggregated over an explicit wall-clock interval. This constraint is external to Tycho's timing model and cannot be eliminated at the architectural level. The implementation therefore treats process telemetry as a retrospective signal that must be aligned to, but not conflated with, the device-level event timeline.

To preserve temporal consistency, process queries are issued in conjunction with device polling, but their results are attached only to confirmed device updates. Each process record is associated with the monotonic timestamp of the corresponding device snapshot, establishing a clear temporal anchor without implying instantaneous semantics. Wall-clock durations are tracked independently per device or MIG instance to ensure that backend windows advance correctly regardless of monotonic tick spacing.

Failure handling is deliberately non-blocking. If a process query fails or returns incomplete data, the collector advances the wall-clock origin to avoid repeated zero-length windows, while device-level sampling proceeds unaffected. This ensures that transient backend failures degrade attribution fidelity locally without destabilising cadence inference or event emission.

5.4.4.5 Robustness and Failure Modes

GPU telemetry exhibits substantial variability across hardware generations, driver versions, and backend capabilities. The implementation is therefore designed to

preserve architectural guarantees under incomplete or degraded signals rather than to assume uniform availability.

Missing cumulative energy counters are handled through per-device capability tracking. When authoritative counters are unavailable or non-monotonic, freshness detection falls back to power-based inference with conservative thresholds, preventing noise-induced duplicate events at the cost of increased uncertainty. Backend-specific differences between NVML and DCGM are treated as input variability, not as control flow, ensuring that sampling and emission semantics remain consistent.

Publish cadence jitter is absorbed by the phase-aware inference mechanism. Because estimators are updated only on confirmed publishes, short-term timing irregularities do not propagate into spurious alignment corrections or event duplication. At worst, detection latency increases temporarily, while the one-tick-per-publish invariant remains intact.

MIG instances are handled uniformly as independent telemetry sources during collection. No additional analytical assumptions are introduced at this stage, and MIG metadata is propagated without special treatment. This conservative stance avoids overstating attribution guarantees in configurations where downstream analysis does not explicitly model MIG topologies.

5.4.4.6 Implementation Consequences

The GPU collector implementation enforces the architectural timing guarantees in the presence of implicit publish cadences, heterogeneous backend capabilities, and partial observability. In practice, this ensures that the GPU event stream is free of redundant samples, causally ordered with respect to all other measurement domains, and aligned to genuine hardware updates rather than to polling artefacts. The one-to-one correspondence between confirmed device publishes and emitted `GpuTick` events is preserved even under jitter, missing counters, or transient backend failures.

At the same time, the implementation inherits unavoidable limitations from the telemetry ecosystem. Publish cadence inference is necessarily approximate, and process-level utilisation remains aggregated over backend-defined wall-clock windows. These constraints bound the temporal precision of attribution but do not violate the correctness or ordering guarantees of the GPU timeline.

By producing a temporally consistent, event-driven GPU measurement stream, the collector enables downstream analysis stages to correlate accelerator activity with CPU, memory, and platform power without resampling or heuristic alignment. This integration is a prerequisite for accurate cross-domain attribution and allows later stages to reason about GPU energy consumption under the same invariants that govern all other Tycho subsystems.

5.4.4.7 Collected Metrics

The GPU collector reports both device-level and process-level telemetry for each emitted `GpuTick`. Device metrics capture the instantaneous operational state of the accelerator at the time of a confirmed publish, while process metrics describe aggregated utilisation over the corresponding backend window. Tables 5.4 and 5.5 summarise the metrics collected at each level.

Metric	Unit	Description
Utilisation metrics		
`SMUtilPct`	%	Streaming multiprocessor (SM) utilisation.
`MemUtilPct`	%	Memory controller utilisation.
`EncUtilPct`	%	Hardware video encoder utilisation.
`DecUtilPct`	%	Hardware video decoder utilisation.
Energy and thermal metrics		
`PowerMilliW`	mW	Instantaneous power via NVML/DCGM (1s average).
`InstantPowerMilliW`	mW	High-frequency instantaneous power from NVIDIA field APIs.
`CumEnergyMilliJ`	mJ	Cumulative energy counter (preferred freshness signal).
`TempC`	°C	GPU temperature.
Memory and frequency metrics		
`MemUsedBytes`	bytes	Allocated framebuffer memory.
`MemTotalBytes`	bytes	Total framebuffer memory.
`SMClockMHz`	MHz	SM clock frequency.
`MemClockMHz`	MHz	Memory clock frequency.
Topology and metadata		
`DeviceIndex`	–	Numeric device identifier.
`UUID`	–	Stable device UUID.
`PCIBusID`	–	PCI bus identifier.
`IsMIG`	–	Indicates a MIG instance.
`MIGParentID`	–	Parent device index for MIG instances.
`Backend`	–	Backend type (`NVML` or `DCGM`).

TABLE 5.4: Device- and MIG-level metrics collected by the GPU subsystem.

Metric	Unit	Description
Per-process utilisation metrics		
`Pid`	–	Process identifier.
`ComputeUtil`	%	Per-process SM utilisation aggregated over the query window.
`MemUtil`	%	Per-process memory controller utilisation.
`EncUtil`	%	Per-process encoder utilisation.
`DecUtil`	%	Per-process decoder utilisation.
Device and timing metadata		
`GpuIndex`	–	Device or MIG instance to which the sample belongs.
`GpuUUID`	–	Corresponding device UUID.
`TimeStampUS`	µs	Backend timestamp associated with the utilisation record.
MIG metadata (when applicable)		
`GpuInstanceID`	–	MIG GPU instance identifier.
`ComputeInstanceID`	–	MIG compute-instance identifier.

TABLE 5.5: Process-level metrics collected over a backend-defined time window.

5.5 Metadata and Identity Infrastructure

5.5.1 Architectural Context

This section realises the metadata subsystem defined in § 4.6 as a refresh-driven, bounded cache that supplies joinable workload identity to the analysis engine. Metadata does not form a time series and is not evaluated over analysis windows. Its function is to provide sufficiently fresh identity state at analysis boundaries while remaining robust under partial observability, workload churn, and asynchronous sources.

5.5.2 Controller-Orchestrated Refresh and Lifetime Enforcement

All metadata mutation is centralized in a metadata controller, which constitutes the sole authority over state updates and lifecycle management. Collectors never modify analysis-visible state directly and never delete entries. They submit observations to the controller, which serializes updates and enforces freshness and retention rules. This separation is required to ensure that identity state is maximally fresh at analysis boundaries while remaining bounded and deterministic under missing or partial updates.

At the start of every analysis cycle, the analysis engine triggers exactly one metadata refresh. This refresh dominates all other scheduling and ensures that identity state reflects the most recent observable system structure at the moment the analysis window is evaluated. Additional refreshes within the same cycle are unnecessary, as the window is closed at the cycle boundary and later identity changes cannot affect its evaluation.

To bound metadata age when analysis cycles are long or sparse, the controller may execute collectors periodically. Each collector has an independent freshness target, with defaults of 1 s for the proc collector and 3 s for the kubelet collector. Background execution is suppressed when an analysis-triggered refresh is imminent, specifically when it lies within 250 ms, ensuring that the cycle-start refresh dominates and that redundant collection near analysis boundaries is avoided.

Metadata collection is explicitly best-effort. Collectors do not define a notion of success and may submit partial updates. The controller accepts all updates without requiring a complete snapshot, and cache convergence is achieved through repeated refreshes. Missing observations are handled exclusively through horizon-based expiry rather than through collection-time interpretation, preserving a strict separation between identity acquisition and attribution logic.

5.5.3 Metadata Store, Keys, and Temporal Alignment

Metadata is stored in an in-memory cache partitioned by entity type. Entries represent the most recent known identity state and are overwritten in place on update; historical versions are not retained. Pod entries are keyed by pod UID, container entries by normalized runtime container ID, and process entries by PID with the process start token (`StartJiffies`) retained for disambiguation.

PID reuse is handled by treating the pair (PID, `StartJiffies`) as the effective process identity. When a PID is reused, a new entry is created rather than overwriting

the prior instance, preventing stale process metadata from being joined with unrelated activity during overlapping analysis windows.

All metadata updates within a refresh are timestamped once using Tycho's global monotonic timebase. The same timestamp is applied uniformly to all entries updated in that refresh, ensuring consistent temporal alignment with metric observations without introducing enumeration-induced skew. An auxiliary wall-clock timestamp is recorded for diagnostics but is not used in attribution logic.

Garbage collection is executed periodically by the controller and independently of refresh scheduling. Entries whose last-seen timestamp falls outside the same retention horizon used for metric buffers are removed. This alignment guarantees that any retained metric observation remains joinable with identity metadata while providing deterministic memory bounds and natural cache drainage under missing updates.

5.5.4 Proc Collector

The proc collector provides the operating-system view required to associate process-level activity with container identity. It enumerates processes via the proc filesystem and records a deliberately minimal attribute set consisting of process identifiers, command name, and cgroup membership. This minimalism avoids unstable or expensive enrichment at collection time while retaining all information required for later joins.

Process-to-container association is derived from cgroup membership and normalized into a runtime container identifier. Both cgroup version 1 and version 2 layouts are supported, and normalization targets containerd and CRI-O runtimes. Processes that cannot be mapped to a Kubernetes container are labeled with a sentinel container identifier stored directly in the process entry, avoiding synthetic container objects and keeping system activity explicit at analysis time.

Process enumeration is inherently racy. Processes may disappear during traversal and individual reads may fail due to lifecycle races. Such failures are treated as normal; only successfully read entries are updated, and stale state is removed by horizon-based expiry.

5.5.5 Kubelet Collector

The kubelet collector supplies the authoritative Kubernetes node-local view required for correct pod and container attribution. It periodically retrieves the kubelet `/pods` endpoint and persists only identity information that cannot be reliably reconstructed after termination.

Container identifiers are normalized at collection time, and only the normalized form is stored. Init containers and ephemeral containers are represented uniformly as container entries with lifecycle-dependent status categories. Termination state and exit codes are recorded when available, allowing analysis to avoid attributing energy to completed workloads without relying on event histories.

The kubelet view is the sole stable source of resource specifications once workloads terminate. Tycho therefore stores CPU and memory requests and limits for both containers and aggregated pods. If the kubelet is temporarily unreachable, no updates are applied for that refresh. There is no explicit freshness gating in analysis; degradation manifests through missing or stale joins bounded by the retention horizon.

5.5.6 Metadata Contract and Join Surface

The metadata subsystem exposes a fixed set of identity fields that define the complete join surface available to the analysis engine. Tables 5.6, 5.7, and 5.8 summarize the fields collected by the proc and kubelet collectors. This inventory constitutes an implementation contract: attribution feasibility and correctness depend directly on the presence and semantics of these fields, and no additional identity information is assumed downstream.

Field	Source	Description
Process identity		
PID	`/proc`	Numeric process identifier; unique at any moment but reused over time.
StartJiffies	`/proc/<pid>/stat`	Kernel start time of the process in clock ticks (jiffies), used to detect PID reuse.
Container and system classification		
Container ID	Kepler cgroup resolver	Normalized container identifier for pod processes; `system_processes` for host and kernel processes.
Command	`/proc/<pid>/comm`	Short command name for debugging and manual inspection.
Timestamps		
LastSeenMono	Monotonic timebase	Timestamp aligned with metric collectors.
LastSeenWall	Controller timestamp	Wall-clock timestamp for GC.

TABLE 5.6: Process metadata collected by the process collector

Field	Source	Description
Pod identity		
PodUID	Kubelet PodList	Stable pod identifier for correlation and container grouping.
PodName, Namespace	Kubelet PodList	Human-readable pod identity and namespace.
Lifecycle and scheduling context		
Phase	PodStatus	Coarse pod state (Pending, Running, Succeeded, Failed).
QoSClass	PodStatus	Kubernetes QoS classification (Guaranteed, Burstable, BestEffort).
OwnerKind / OwnerName	Pod metadata	Controller reference (e.g. ReplicaSet, DaemonSet).
Resource specifications		
Requests (CPU, Memory)	`pod.spec.containers`	Aggregate pod-level requests following Kubernetes scheduling semantics.
Limits (CPU, Memory)	`pod.spec.containers`	Aggregate pod-level limits following Kubernetes scheduling semantics.
Timestamps		
LastSeenMono	Monotonic timebase	Timestamp aligned with metric collectors.
LastSeenWall	Controller timestamp	Wall-clock timestamp for GC.

TABLE 5.7: Pod metadata collected by the kubelet collector

Field	Source	Description
Container identity		
ContainerID	PodStatus	Normalized container identifier.
ContainerName	PodStatus	Declared container name within pod.
Lifecycle state		
State	ContainerStatus	Fine-grained state (Running, Waiting, Terminated).
ExitCode	ContainerStatus	Termination exit code when available.
Resource specifications		
Requests (CPU, Memory)	`pod.spec.containers`	Container-level resource requests; preserved for terminated containers.
Limits (CPU, Memory)	`pod.spec.containers`	Container-level resource limits.
Timestamps		
LastSeenMono	Monotonic timebase	Timestamp aligned with metric collectors.
LastSeenWall	Controller timestamp	Wall-clock timestamp for GC.

TABLE 5.8: Container metadata collected by the kubelet collector

5.5.7 Design Consequences and Exclusions

By centralizing lifecycle enforcement and treating sources as independently valid, the subsystem provides maximally fresh identity at analysis boundaries while remaining robust to partial observability and transient failures. Correctness relies on bounded freshness and explicit joins rather than on point-in-time snapshots or event histories.

5.6 Calibration

This section describes how the calibration architecture introduced in § 4.7 is realized in Tycho's implementation. Calibration is implemented as a bounded, startup-time procedure whose sole role is to reduce temporal uncertainty in hardware-controlled metric publication before steady-state collection begins. It exists to improve the correctness of downstream timing and attribution under partial observability, without introducing runtime adaptation or feedback.

Calibration is optional and can be disabled via configuration. When enabled, it is executed at most once per Tycho process lifetime and is not re-entered or repeated. All calibration results are node-local and apply only to the process instance that performed them.

5.6.1 Architectural Context

The calibration architecture distinguishes two orthogonal concerns: polling-frequency calibration, which bounds the minimum safe polling period for hardware-controlled metric sources, and delay calibration, which bounds the reaction latency between workload transitions and observable metric changes. Only polling-frequency calibration is integrated into Tycho's startup path. Delay calibration is treated as an external preparatory step and is consumed purely as static configuration.

Calibration parameters are consumed by the timing and analysis subsystems. They do not influence runtime attribution logic directly and do not observe live workloads.

5.6.2 Startup Strategy and Collector Gating

Polling-frequency calibration is executed during Tycho startup, prior to enabling the affected collectors. Collectors whose polling cadence depends on calibrated bounds are held inactive until calibration completes or is bypassed. As a consequence, no metrics from these collectors are emitted before a polling interval has been selected.

Calibration does not block system startup indefinitely. If insufficient observations are obtained or calibration fails for any reason, Tycho falls back to user-configured default polling intervals. This fallback is silent at the semantic level and does not alter runtime behavior, ensuring that metric availability is not contingent on successful calibration. Empirically derived bounds are preferred when available, but correctness does not depend on their presence.

When multiple devices contribute to a single collector on a node, calibration results are aggregated conservatively. The most restrictive bound across all observed devices is selected and applied uniformly, ensuring that no device-level publication is undersampled due to intra-node variability.

5.6.3 Polling-Frequency Calibration Mechanism

Polling-frequency calibration is realized as a short-lived hyperpolling phase. During this phase, Tycho queries the relevant hardware interface at a conservatively high rate and passively observes the arrival of distinct metric updates. From these observations, it derives a conservative bound on the minimum safe polling period that avoids undersampling under nominal conditions.

For GPU power metrics, calibration is performed independently for each device using NVML. Per-device observations are aggregated at node level, and the most restrictive bound is selected. The resulting polling period is then applied uniformly to all GPU collectors on that node, ensuring consistent temporal coverage across heterogeneous devices.

For Redfish power metrics, calibration operates at the level of the BMC. Observed updates across all exposed chassis contribute to the inferred cadence, allowing calibration to remain valid in multi-chassis configurations. When Redfish *heartbeat* is enabled, the calibrated polling period is additionally constrained by a hard cap derived from the heartbeat interval. Calibration therefore establishes a lower bound on safe polling, while heartbeat logic enforces upper limits on staleness during steady-state operation. The two mechanisms are strictly layered and do not overlap in responsibility.

No polling-frequency calibration is performed for RAPL or eBPF. RAPL counters update quasi-continuously relative to Tycho's temporal resolution, making undersampling architecturally irrelevant. eBPF metrics are event-driven and decoupled from device-side publication cadence, rendering polling-frequency discovery unnecessary.

5.6.4 Delay Calibration Integration

Delay calibration is not performed within Tycho. Estimating the latency between workload transitions and observable metric reactions requires controlled, high-intensity workload generation that is incompatible with Tycho's non-intrusive monitoring constraints.

Instead, delay calibration is carried out offline using external tooling that executes directly on the target system. These measurements derive conservative, device-specific delay bounds for GPU power metrics. The resulting bounds are supplied to Tycho exclusively via configuration. At runtime, Tycho treats these bounds as static parameters and applies them during analysis to prevent premature attribution and to align metric data with workload phases.

When multiple GPU devices are present, Tycho selects the smallest configured delay bound across devices and applies it uniformly. This choice favors temporal responsiveness while remaining consistent with the best-effort nature of delay estimation.

No delay calibration is applied to Redfish. Irregular publication intervals, variable network latency, and opaque BMC-internal behavior preclude stable delay estimation. Redfish metrics are therefore treated as coarse signals whose temporal coherence is enforced through freshness tracking and scheduling constraints rather than delay correction.

5.6.5 Implementation Consequences

Calibration improves attribution correctness by reducing avoidable temporal uncertainty in hardware-controlled metric sources. It provides best-effort bounds that constrain polling and alignment decisions without introducing runtime adaptation or control coupling. By resolving these uncertainties ahead of steady-state operation, Tycho preserves deterministic execution, bounded timing behavior, and strict separation between observation and analysis.

5.7 Analysis and Attribution Infrastructure

5.7.1 Analysis Engine Responsibilities and Cycle Lifecycle

This section describes how the orchestration model defined in § 4.8.1 is enforced at runtime. The analysis engine is a minimal orchestration authority whose sole responsibility is to execute window-scoped attribution deterministically and without hidden coupling. It constructs analysis cycles, selects attribution windows, enforces a fixed execution order, and establishes a materialization boundary for derived results. The engine does not participate in metric semantics, dependency inference, modeling decisions, result interpretation, or exporter interaction.

Each invocation of the engine corresponds to exactly one analysis cycle. Cycles are triggered externally; the engine does not self-schedule, maintain timers, or perform background work. Invocation cadence and jitter are therefore treated as external concerns and do not affect correctness, provided that invocations are serialized and the monotonic timebase is strictly increasing.

At cycle entry, the engine atomically constructs a fresh execution context that fully determines the behavior of the cycle. This context includes the selected attribution window, admissibility constraints for reading observations, read-only access to upstream buffers, access to node-local metadata, access to shared cross-window state, and a cycle-local materialization boundary. No additional execution context is injected after construction, and no global mutable analysis state is consulted during execution.

Once constructed, the cycle is executed exactly once. The engine invokes all metrics sequentially according to a fixed execution plan. There is no re-entry into a partially executed cycle, no mid-cycle rescheduling, and no orchestration-level retry or backtracking. After execution completes, all cycle-local structures are discarded, including the materialization store, and no derived quantities persist implicitly into subsequent cycles.

Failures are isolated to the cycle in which they occur. If an individual metric fails to produce a result, the failure is logged and execution continues for remaining metrics. Such failures affect only the completeness of results for the current window and do

not abort the cycle. Each subsequent invocation constructs a new cycle with a fresh execution context, independent of prior errors or partial results.

By enforcing atomic cycle construction, single-pass execution, and explicit teardown, the engine guarantees that each cycle yields at most one coherent set of window-scoped results. There is no opportunity for partial publication, retroactive correction, or cross-cycle interference. This execution discipline provides the structural foundation on which staging, materialization, and cross-window modeling are implemented while preserving determinism, auditability, and non-retrospective semantics.

5.7.2 Attribution Window Selection and Temporal Safety

This section describes how the attribution window defined in § 4.8.1.3 is selected and enforced at runtime. Window selection is performed exactly once at cycle entry and is derived exclusively from the global monotonic timebase, which serves as the sole temporal authority. Wall-clock time, collector timestamps, and exporter behavior are not consulted, ensuring a strictly ordered and unambiguous temporal reference.

The window end t_k is selected with a fixed intentional lag relative to real-time execution. This lag corresponds to the maximum admissible metric delay plus a safety margin obtained from configuration and optional calibration. By construction, each window is therefore placed in a region of the past where all participating metrics are guaranteed to have observed the samples required to interpret their contributions under their declared delay semantics. The lag is constant across cycles, yielding attribution windows with fixed duration and uniform semantics in steady state.

During startup, when insufficient observation history exists to populate the intended window fully, the window start may be clamped to the beginning of the monotonic timeline. This behavior is explicit, deterministic, and confined to the initial phase of execution. No other deviations from the steady-state window definition are permitted.

Window selection is deliberately decoupled from collector sampling behavior. Collectors may operate at different frequencies, with irregular timing or transient gaps, without influencing window boundaries. The engine does not impose an alignment grid or attempt to synchronize with sampling schedules. Instead, windows are defined purely in terms of monotonic ticks, and metrics interpret the contents of upstream buffers over the selected interval using interval semantics and metric-local delay correction.

Once selected, the attribution window is immutable for the duration of the cycle. All metrics observe the same base window, and any effective windows derived through delay correction are computed deterministically from this reference. The engine does not revise window boundaries mid-cycle and does not reopen or reinterpret windows after execution.

By combining a monotonic timebase, a fixed safety lag, and immutable window selection, the implementation enforces temporal admissibility by construction. Attribution correctness is insulated from collector jitter and delayed observations, speculative window closure is avoided, causality is preserved, and each cycle yields a single, final temporal interpretation of the available evidence.

5.7.3 Staged Pipeline Execution and Dependency Discipline

This section explains how the dependency discipline defined in § 4.8.1.4 is enforced at runtime. Dependency correctness is not inferred dynamically and is not validated during execution. Instead, it is achieved by construction through a fixed execution order that reflects the semantic structure of the analysis pipeline.

For each analysis cycle, the engine constructs a static execution plan consisting of an ordered list of metric invocations. This plan is invariant across cycles for a given build and configuration. Metrics are registered into the analysis registry in an order that encodes their semantic dependencies, and the engine preserves this order exactly during execution. As a result, metrics executed later in the plan may depend on outputs produced earlier in the same cycle, while reverse dependencies are structurally impossible.

Stages are not represented as explicit runtime entities. Instead, stage boundaries are implicit and correspond to contiguous segments of the execution plan. Each segment groups metrics that operate at the same semantic level, such as aggregation, decomposition, or attribution. Downstream segments assume that all metrics in earlier segments have either materialized their window-scoped outputs or abstained from doing so due to missing or inadmissible inputs.

The implementation deliberately avoids constructing dependency graphs, performing topological sorting, or validating dependency satisfaction at runtime. There are no per-metric dependency declarations and no control flow conditioned on the availability of upstream results. If a metric observes an undefined input, it degrades according to its semantics rather than triggering reordering, backtracking, or failure.

This design treats dependency correctness as an architectural obligation rather than an algorithmic problem. The runtime enforces execution order faithfully but does not attempt to infer semantic validity. By resolving dependencies explicitly at composition time, the implementation preserves determinism, avoids hidden coupling between metrics, and ensures that degradation under partial observability propagates monotonically through the pipeline without compromising internal consistency.

5.7.4 Metric Materialization and Intra-Cycle Visibility

This section describes how the materialization model is enforced at runtime. At the beginning of each analysis cycle, the engine establishes a cycle-local materialization boundary that serves as the sole authoritative representation of all derived results for the current attribution window. All metric emissions during the cycle are routed through this boundary, ensuring that materialization is strictly window-scoped and isolated from other cycles.

Derived results are recorded as immutable, window-scoped facts. Within a cycle, each metric is expected to materialize at most one final value per metric identity and label set. Multiple emissions for the same identity deterministically overwrite earlier ones, but such behavior is not relied upon for correctness. The effective semantic contract is therefore exactly-once materialization per window.

All materialized results are conceptually visible to metrics executed later in the same

cycle. There is no notion of stage-local visibility or scoped access control. Dependency correctness relies entirely on execution order rather than on restricting access to intermediate results. Metrics that consume undefined inputs must degrade according to their semantics rather than delaying execution or attempting recovery.

Materialized results never persist implicitly across cycles. When a cycle completes, the materialization boundary is discarded in its entirety, and all derived quantities cease to exist from the perspective of subsequent cycles. Any dependence on prior windows must be mediated through explicit cross-window state owned and managed by the consuming metric.

By enforcing a per-cycle materialization boundary with global intra-cycle visibility and strict teardown semantics, the implementation guarantees that each cycle yields a single, final, and internally consistent set of derived quantities for its attribution window. This prevents hidden cross-window coupling, eliminates incremental refinement of results, and allows later attribution stages to operate on materialized facts rather than raw observations while preserving determinism and auditability.

5.7.5 Cross-Window State and Explicit Memory

This section describes how limited cross-window memory is supported without violating the window-scoped and non-retrospective execution model defined in § 4.8. While derived results never persist across cycles, certain attribution models require controlled statefulness in order to converge or adapt over time. The implementation accommodates such models through an explicit and narrowly scoped state mechanism.

Cross-window state is provided through a shared state store that persists for the lifetime of the analysis process and is made available to each cycle at construction time. The state store is passive and provides no execution logic or semantic interpretation. The analysis engine does not read from, write to, or reason about its contents; its sole responsibility is to supply access to metrics during cycle execution.

All cross-window state is strictly metric-owned. Metrics that require memory across windows must explicitly retrieve, initialize, and update their own state entries. Metrics that do not access the state store remain purely window-scoped and stateless by construction. State entries are keyed by metric identity and labels, making ownership and scope explicit and preventing implicit sharing between unrelated metrics.

Use of cross-window memory is an explicit opt-in. Any temporal coupling introduced by stateful behavior is therefore visible at the point of use and auditable in isolation. State is updated only after a cycle completes and influences only subsequent cycles. Previously materialized results are never revised, and no stateful mechanism can retroactively alter the interpretation of earlier windows.

By confining cross-window memory to explicit, metric-owned state and maintaining strict cycle boundaries, the implementation supports stateful attribution models where required while preserving determinism, isolation, and the architectural guarantee that each cycle yields a single, final interpretation of its attribution window.

5.7.6 Output Commit and Sink Boundary

This section describes how analysis results are committed and published without allowing downstream mechanisms to influence attribution semantics. At cycle construction time, the engine establishes a collecting sink that serves as the sole emission boundary for all metrics executed during the cycle. All derived results emitted by metrics are routed through this boundary and are treated as belonging to the same attribution window.

Result commitment occurs at the moment of materialization. Once a derived quantity is recorded within the cycle-local materialization boundary, it is final for the current window. Publication to downstream sinks is strictly observational and occurs after materialization without providing feedback into the analysis process. The engine never reads from sinks, waits for acknowledgements, or conditions execution on publication success.

Sinks are therefore non-authoritative by design. Exporter behavior may delay, drop, aggregate, or reorder published results, but such behavior does not alter the meaning or validity of the computed window-scoped quantities. Attribution correctness is defined entirely within the analysis layer and is independent of downstream reliability or performance characteristics.

All results produced during a cycle are committed as a logical batch. There is no partial publication of intermediate results and no distinction between provisional and final outputs. Once cycle execution completes, the set of materialized results represents the maximal, internally consistent interpretation achievable for the attribution window.

By strictly separating analysis from publication, the implementation preserves reproducibility and robustness. Failures at the export layer degrade only the visibility of results, not their correctness, and cannot introduce hidden coupling or timing dependencies into the attribution process. This boundary ensures that attribution semantics remain stable, auditable, and invariant under changes to exporter implementation or behavior.

5.7.7 Implementation Consequences and Guarantees

The implementation described in this chapter enforces the architectural contract of the analysis layer directly through execution structure rather than dynamic control logic. Each analysis cycle yields a single, deterministic, window-scoped interpretation of the available evidence, constructed under fixed temporal assumptions and executed in a strictly ordered, non-retrospective manner. All derived results are materialized explicitly, remain immutable for the duration of the cycle, and are isolated from both prior and subsequent cycles.

Temporal correctness is ensured by construction. Attribution windows are selected once per cycle from a global monotonic timebase using a fixed safety lag, are immutable during execution, and are interpreted without reliance on collector sampling grids or exporter timing. As a result, causality is preserved and attribution semantics are insulated from collection jitter, delayed observations, and downstream publication behavior.

Dependency correctness is enforced structurally. Metric execution order is fixed and reproducible, stages are implicit in the execution plan, and no runtime dependency inference or reordering occurs. Under partial observability, results degrade monotonically through omission or explicitly defined fallback semantics, and previously materialized interpretations are never revised.

Stateful attribution models are supported exclusively through explicit, metric-owned cross-window state. No derived quantities persist implicitly across cycles, and any temporal coupling introduced by memory is localized, visible, and auditable. This preserves isolation between cycles while allowing convergence or adaptation where required.

Equally important are the properties the implementation does not guarantee. The analysis layer does not ensure completeness of results for every window, does not backfill or reinterpret prior windows, does not validate semantic correctness of pipeline composition at runtime, and does not provide reliability guarantees for result publication. These non-guarantees are deliberate and reflect the prioritization of correctness, determinism, and transparency over forced coverage or convenience.

Together, these consequences establish a stable execution contract for attribution. They enable later analysis stages to operate on materialized, window-scoped quantities with well-defined temporal and dependency semantics, while ensuring that increasing analytical sophistication does not compromise determinism, auditability, or adherence to the architectural model.

5.7.8 Stage 1: Component Metric Construction

5.7.8.1 Component-Level eBPF Utilization Metrics (Totals)

Architectural Context This subsubsection realizes the utilization metrics defined in § 4.8.2.1. It implements the window-aligned construction of node-level CPU time-share ratios and cumulative kernel and hardware counters from discrete eBPF observations, without redefining architectural semantics or introducing additional modeling assumptions.

Implementation Strategy Discrete eBPF observations are consumed as per-tick deltas. For each analysis window, deltas are integrated over an effective window interval to approximate the continuous quantities defined architecturally. CPU execution time is normalized against node capacity to obtain ratios, while all other eBPF-derived signals are aggregated across processes and accumulated into persistent node-level counters.

Core Mechanisms Per-tick deltas for CPU idle, hardware interrupt, and software interrupt execution are integrated independently over the window. Normalization uses the product of window duration and logical CPU count to obtain dimensionless time-share ratios. Active CPU utilization is derived as the complement of the integrated non-active components, enforcing exact conservation of schedulable CPU capacity. For event-based signals, per-process deltas are summed at each tick, integrated over the window, and added to cumulative counters that advance monotonically across analysis cycles.

Robustness and Edge Cases Window boundaries may intersect eBPF tick intervals. Integration therefore accounts for partial overlap between ticks and windows to preserve conservation and avoid bias at window edges. Internal accumulation admits fractional contributions to accommodate overlap, while exported counters are materialized as integer-valued quantities. If insufficient eBPF samples are available to conservatively integrate a window, no metrics are emitted for that window.

Implementation Consequences The implementation enforces the architectural guarantees of strict monotonicity for counters and exact partitioning of CPU capacity across utilization classes. All cumulative metrics are scoped to the lifetime of the Tycho process and may reset on restart. These semantics ensure stable interpretation under sampling variability and allow downstream stages to rely on consistent utilization signals.

Exported Metrics The metrics exported by this implementation are summarized in the table 5.17. Only fully materialized utilization metrics intended for external consumption are listed.

Metric	Type	Unit	Labels
CPU time-share ratios			
`bpf_cpu_idle_ratio`	Gauge	ratio	`source`
`bpf_cpu_irq_ratio`	Gauge	ratio	`source`
`bpf_cpu_softirq_ratio`	Gauge	ratio	`source`
`bpf_cpu_active_ratio`	Gauge	ratio	`source`
Aggregated cumulative counters			
`bpf_cpu_instructions`	Counter	count	`source`
`bpf_cpu_cycles`	Counter	count	`source`
`bpf_cache_misses`	Counter	count	`source`
`bpf_page_cache_hits`	Counter	count	`source`
`bpf_irq_net_tx`	Counter	count	`source`
`bpf_irq_net_rx`	Counter	count	`source`
`bpf_irq_block`	Counter	count	`source`

Label domain: `source` = `bpf`.

TABLE 5.9: Exported utilization metrics derived from eBPF observations.

5.7.8.2 RAPL Component Metrics (Totals)

Architectural Context This section realises the cumulative RAPL energy model defined in the corresponding architecture subsubsection, producing zero-based, monotonic energy counters per RAPL domain and an auxiliary, window-averaged power signal. Only total energy and total power are constructed here; no decomposition or attribution is performed at this stage.

Implementation Strategy The implementation consumes time-ordered RAPL counter samples within the effective analysis window and aggregates them across sockets for each domain. Energy counters are constructed directly from native cumulative readings, while power is derived secondarily from in-window energy differences. All logic is structured to ensure that exported energy counters remain monotonic, zero-based, and independent of window boundaries.

Core Mechanisms For each domain, the implementation identifies the first and last available cumulative RAPL counters within the effective window. The last counter represents the native cumulative energy at window end. To eliminate hardware-defined initial offsets, the first observed native value per domain is stored once and subtracted from all subsequent exports, yielding a zero-based cumulative energy counter.

Window-local energy increments are computed by differencing the first and last counters within the window. Because raw RAPL inputs are already corrected for wraparound upstream, no additional wraparound handling is required at this stage. Average power is then derived by dividing the in-window energy increment by the window duration. This power signal is emitted alongside the energy counter but is not used for any downstream computation.

Robustness and Edge Cases If fewer than two valid RAPL samples are available within a window, no metrics are emitted, avoiding partial or misleading updates. Non-positive or ill-defined window durations suppress emission entirely. All aggregation is performed per domain and summed across sockets conservatively, ensuring that missing socket data cannot inflate reported energy. Since cumulative energy is always derived from native counters and offset subtraction is monotonic, exported energy values never decrease.

Implementation Consequences The implementation guarantees that exported RAPL energy metrics are stable cumulative counters suitable as authoritative inputs for later stages. Auxiliary power metrics are provided solely for inspection and convenience and are explicitly excluded from attribution logic. Optional quality or diagnostic metadata may be emitted for debugging purposes, but it does not affect metric semantics.

Exported Metrics The metrics exported by this implementation are summarized in the table 5.10. Only cumulative energy counters intended as authoritative inputs and their auxiliary, user-facing power counterparts are listed.

Metric	Type	Unit	Labels
RAPL component totals (per domain)			
`rapl_energy_mj`	Counter	mJ	`domain, kind, source`
`rapl_power_mw`	Gauge	mW	`domain, kind, source`

Label domain: `domain` $\in$ {pkg, core, uncore, dram}, `kind` = total, `source` = `rapl`.

TABLE 5.10: Exported RAPL component energy and power metrics.

5.7.8.3 GPU Component Metrics (Totals)

Architectural Context This section realizes the architectural definition of GPU power and energy reconstruction as a history-aware, constraint-based process. Unlike collectors that derive window-local quantities directly from raw samples, the GPU metric maintains a corrected power signal over a retained corrected-time horizon and derives windowed quantities as projections of that maintained signal. Historical state is therefore treated as a correctness mechanism rather than an optimization, enabling reconciliation of delayed, averaged, and cumulative GPU observations into

a single authoritative timeline. All execution-time mechanisms described below exist to uphold this contract under discretization, partial observability, and bounded computation.

Implementation Strategy GPU reconstruction is implemented by maintaining a per-device corrected power series on a uniform corrected-time grid that persists across analysis cycles. Rather than recomputing power independently per window, the implementation incrementally extends and updates this series using newly available observations while preserving previously reconstructed history. To bound computation, reconstruction is confined to a moving tail region near the current analysis window, while constraints are derived from observations spanning a longer retained history. Windowed GPU energy and power are obtained by projecting the maintained series onto the analysis window, ensuring temporal coherence across windows and alignment with the accuracy-first architectural objective.

Constraint Realization Raw GPU telemetry is realized as weighted constraints on the corrected power series. Instantaneous power samples contribute point-wise soft constraints, while one-second averaged power samples are realized as boxcar-mean constraints over the preceding approximately one-second interval on the uniform grid. Cumulative energy counters, when present and validated, contribute dominant consistency constraints derived from positive, monotonic energy deltas mapped to the corresponding grid intervals. Constraint families use fixed internal relative weights reflecting expected reliability, with cumulative energy dominating when enabled. All constraints act jointly on the reconstructed series in corrected time, avoiding sequential correction or signal prioritization.

Reconstruction and Update Semantics Reconstruction is performed on a moving tail of the corrected power history covering the most recent portion of the retained horizon. Only this tail segment is re-solved each cycle, after which it overwrites the corresponding region of the maintained history on the uniform grid. This moving-horizon approach bounds computational cost while allowing historical observations to influence the present reconstruction. If reconstruction cannot be performed due to insufficient or inconsistent observations, the previously retained history is preserved unchanged, ensuring continuity of the corrected signal across cycles.

Windowed Energy and Power Derivation Windowed GPU energy is derived by projecting the corrected power history onto the current analysis window. When validated cumulative energy counters are available and a prior baseline exists, the window energy increment is obtained directly from the counter delta to preserve absolute energy consistency. Otherwise, window energy is computed by integrating the corrected power series over the window interval. Windowed GPU power is derived from the corresponding window energy and duration and represents the same underlying quantity as a gauge. Per-window energy values are treated as auxiliary quantities, while the maintained reconstructed history remains authoritative.

Robustness and Edge Cases The implementation explicitly tolerates missing, delayed, and partially invalid GPU telemetry. Cumulative energy constraints are enabled only when counters are present, non-zero, strictly increasing, and yield valid deltas; otherwise they are disabled automatically. Non-negativity is enforced via

post-solve projection to prevent physically implausible power estimates. If projection affects a substantial fraction of bins, a conservative second reconstruction pass is attempted with cumulative energy constraints disabled, and the better-conditioned solution is retained. Numerical conditioning is ensured through a minimal diagonal stabilization term applied purely for solver robustness and without modeling semantics. Transient reconstruction failures preserve the previously retained history, preventing discontinuities in downstream metrics.

Implementation Consequences By maintaining a corrected GPU power history across analysis cycles, the implementation achieves temporal coherence and energy consistency that window-local estimation cannot provide. Historical context enables delayed, averaged, and cumulative observations to jointly constrain the reconstructed signal, improving stability and effective temporal resolution under realistic telemetry conditions. When cumulative energy counters are available, absolute energy consistency is preserved across windows; otherwise the system degrades gracefully to history-informed integration without violating physical plausibility. While no claim is made to recover ground-truth GPU power, all exported GPU energy and power metrics are guaranteed to derive from a single, internally consistent reconstructed signal that maximally exploits available information.

Exported Metrics The exported metrics are summarized in Table 5.11.

Metric	Type	Unit	Labels
Total GPU metrics			
`gpu_energy_mj`	Counter	mJ	`gpu_uuid, kind, source`
`gpu_power_mw`	Gauge	mW	`gpu_uuid, kind, source`

Label domain: `kind` = total, `source` = `nvml_corrected`.

TABLE 5.11: Exported GPU metrics derived from the corrected reconstruction.

5.7.8.4 Redfish Component Metrics (Totals)

Architectural Context This section realises the Redfish-based system power construction defined in § 4.8.2.4. The architecture specifies two complementary system-level series: a raw integration of Redfish telemetry and a corrected reconstruction that treats Redfish as an anchoring signal for a higher-rate proxy-based model. The implementation must therefore support delay-aware observation handling, horizon-spanning state, adaptive alignment, and a controlled transition from raw to corrected emission without violating counter continuity.

Implementation Strategy The implementation is split into three cooperating responsibilities. First, a raw producer integrates sparse Redfish samples over the effective analysis window and maintains the canonical system counter during warmup. Second, a fusion substrate maintains a fixed-grid horizon cache populated from component proxy metrics and refreshes Redfish observations under a selected effective delay. Third, a corrected producer fits reconstruction parameters against the cached observations, reconstructs per-bin system power, and integrates the reconstruction over the current window. A readiness flag stored in analysis state governs

takeover: raw emission remains authoritative until corrected reconstruction is feasible for the selected chassis.

Core Mechanisms Raw system metrics are produced by selecting all Redfish samples overlapping the delay-shifted effective window, including at most one predecessor sample to enable zero-order-hold integration. Window energy is obtained by integrating held power values over the window extent, and the exported cumulative counter is advanced monotonically in persistent state.

Corrected reconstruction operates on a fixed fusion grid with configurable bin width and horizon length. A horizon cache stores per-bin proxy features derived from CPU package energy, DRAM energy, GPU energy, and CPU instruction counts. Only newly required bins are populated each cycle, while overlapping cache content is preserved by shifting the horizon forward.

Redfish observations are projected into the corrected time domain by subtracting a candidate delay. An adaptive delay is selected by searching a bounded candidate set and scoring each candidate by the extent to which proxy-derived parts power exceeds Redfish power over a recent horizon segment, subject to an explicit noise margin. Delay updates are rate-limited between cycles, with a higher allowable slew when a step change is detected in the proxy power series. The selected delay is persisted in state and reused as a fallback when the search fails.

Model fitting is performed over the horizon using weighted least squares in scaled space. The reconstruction combines proxy features into per-bin system power using non-negative coefficients for physically interpretable terms and an unconstrained instruction-rate coefficient. When non-negativity constraints become active, a constrained refit is performed to reduce bias from post-fit truncation. Reconstructed bin power is integrated over the overlap with the current analysis window to obtain window energy and average power.

To preserve counter continuity at takeover, the corrected cumulative counter is represented as the sum of a local corrected accumulator and a one-time offset. The offset is seeded from the last available raw exported counter when corrected emission becomes active, ensuring that the canonical counter remains continuous across the transition.

Robustness and Edge Cases Corrected emission is suppressed until a sufficient number of usable Redfish observations exist within the horizon. Observations whose corrected timestamps would underflow are discarded to prevent degenerate kernel projections and unbounded bin scans. If proxy features are unavailable or the delay-selection search fails, the implementation conservatively retains the previously selected delay or falls back to the configured default.

Delay adaptation is explicitly rate-limited to avoid oscillation under noise, while step detection enables faster convergence after large workload transitions. All fitted coefficients are checked for finiteness before use; if fitting fails, the implementation falls back to the previously valid parameter vector or a conservative default. Corrected emission is withheld entirely if these safeguards cannot be satisfied.

Implementation Consequences During warmup, the raw Redfish integration remains the sole canonical system series. Once corrected reconstruction becomes ready, the implementation deletes the raw canonical series from the sink and emits only corrected values thereafter, preventing ambiguous double-publication under identical metric identifiers. The corrected counter does not reset at takeover due to the offset mechanism, but it remains a best-effort cumulative quantity that may restart on process restart. Overall, the implementation prioritises temporal consistency and conservatism: when alignment or anchoring is unreliable, raw integration remains authoritative.

Exported Metrics The exported metrics are summarized in Table 5.12.

Metric name	Type	Unit	Labels
System metrics			
`system_power_mw`	Gauge	mW	`chassis, source, kind`
`system_energy_mj`	Counter	mJ	`chassis, source, kind`

Label domain: `kind` = total, `source` ∈ {`redfish_raw`, `redfish_corrected`}.

TABLE 5.12: Exported Redfish-derived system metrics.

5.7.9 Stage 2: System-Level Energy Model and Residual

Architectural Context This stage realizes the system-level energy balance defined in § 4.8.3. Its role is to operationalize residual energy as a conservative, node-local quantity derived from system and component observations, while tolerating asynchronous and delayed inputs. No workload attribution or semantic decomposition is performed at this stage.

Implementation Strategy For each analysis window, the implementation derives window energy from window-averaged power and window duration for both system-level and component-level signals. Residual energy is computed as a window-local difference and accumulated into a monotonic counter. Power-level residual metrics are treated as auxiliary observables, whereas cumulative energy counters are considered authoritative. An explicit window validity signal is emitted to indicate when residual interpretation is temporally reliable.

Core Mechanisms Residual energy accumulation follows the architectural definition of E_{res} from § 4.8.3. Window energy increments are clamped to non-negative values before accumulation to preserve monotonicity of the exported counter. This clamping is applied strictly at the accumulation boundary and does not alter the conceptual definition of residual energy. Residual power is derived from the same window-local quantities but is not used as a basis for accumulation.

Robustness and Edge Cases Temporal misalignment between system-level and component-level signals may lead to transient inconsistencies at the power level. These effects are contained by decoupling instantaneous power from cumulative energy accounting. Rather than masking such artifacts, the implementation exposes an explicit window usability signal, allowing downstream stages to reason about residual validity without compromising conservation. Warmup behavior is handled by

maintaining continuity between raw and corrected system sources while preserving counter monotonicity.

Implementation Consequences The implementation guarantees strict energy conservation at both window and cumulative levels. Residual energy counters remain monotonic and conservative under all operating conditions. Transient timing artifacts originating from system-level measurement latency may appear in auxiliary power metrics but do not affect energy correctness. Residual energy thus forms a stable and auditable constraint for downstream decomposition and attribution stages.

Exported Metrics The exported metrics are summarized in Table 5.13.

Metric name	Type	Unit	Labels
Residual energy and power			
`residual_energy_mj`	Counter	mJ	`chassis, source, kind`
`residual_power_mw`	Gauge	mW	`chassis, source, kind`
Residual window validity			
`residual_window_usable`	Gauge	bool	`chassis, source`

Label domain: `kind` = total.

TABLE 5.13: Exported residual metrics.

5.7.10 Stage 3: Idle and Dynamic Energy Semantics

5.7.10.1 RAPL Idle and Dynamic Decomposition

Architectural Context This section realises the architectural idle and dynamic split defined in § 4.8.4.1 for RAPL domains by estimating a conservative idle baseline from utilization-conditioned observations and materialising a per-window energy decomposition that preserves strict conservation.

Implementation Strategy The implementation derives idle power from the already exported total RAPL energy by differencing cumulative counters per window and estimating a baseline power β_d from low-utilization operating points. Utilization proxies are obtained directly from raw eBPF process ticks within the effective window to avoid dependencies on intermediate metric availability. Idle estimation and smoothing are maintained as explicit cross-window state, while the per-window split is computed deterministically from the current baseline and total energy increment.

Core Mechanisms For each domain, the cumulative total energy is converted to a window increment by differencing against the last observed value and clamping negative deltas to zero. A utilization proxy u_d is computed by normalizing the window rate of eBPF-derived activity against a rolling p95 amplitude, yielding a bounded proxy in $[0,1]$. Pairs (u_d, P_d^{tot}) are fed into a scalar idle model that performs bucketed regression over low-utilization samples and returns the intercept as the candidate idle baseline. Baseline updates are asymmetrically smoothed in time, permitting faster decreases than increases and suppressing upward adaptation until the p95 normalization is deemed stable. The resulting idle power is clamped

to the observed total power for the same window, converted to an idle energy increment, and subtracted from the total increment to obtain the dynamic remainder. Both increments are accumulated into monotonic per-domain counters and exposed together with window-average powers.

Robustness and Edge Cases If total energy is unavailable or observed for the first time, the cycle is skipped to avoid poisoning state. Idle power is constrained to be non-negative and never exceed total power, ensuring that the split cannot generate energy even under transient noise or model error. When utilization normalization is not yet stable, baseline increases are disabled to prevent premature upward bias, while decreases remain bounded to resist single-sample outliers. All state required for differencing, normalization, modeling, and smoothing is scoped per domain, preventing cross-domain interference.

Implementation Consequences The realised split guarantees per-window energy conservation and produces a conservative idle estimate that converges under sustained low activity while remaining safe on permanently loaded systems. Dynamic energy is defined purely as the residual, ensuring that subsequent attribution stages operate on a well-bounded remainder without requiring access to the idle model internals. The approach tolerates missing or delayed observations and degrades to zero-idle attribution rather than emitting inconsistent metrics.

Exported Metrics The exported metrics are summarized in Table 5.14.

Metric name	Type	Unit	Labels
Idle and dynamic RAPL metrics			
`rapl_energy_mj`	Counter	mJ	`domain, kind, source`
`rapl_power_mw`	Gauge	mW	`domain, kind, source`

Label domain: `domain` $\in$ {pkg, core, uncore, dram}, `kind` $\in$ {idle, dynamic}, `source` = `rapl`.

TABLE 5.14: Exported RAPL idle and dynamic metrics.

5.7.10.2 Residual Idle and Dynamic Decomposition

Architectural Context This subsubsection realises the residual idle and dynamic decomposition defined in the architecture, which introduces a persistent residual idle baseline and a conditional interpretation contract based on window usability. The implementation enforces exact conservation on the clamped residual budget while ensuring that learning and interpretation are explicitly gated under temporal misalignment.

Implementation Strategy Residual idle and dynamic power are constructed from a non-negative residual budget derived per analysis window. A persistent idle baseline is maintained as explicit cross-window state and is reused whenever learning is not permitted. Learning of this baseline is strictly conditional on corrected system input, window usability, and a minimum residual magnitude. Metric emission remains continuous and conservative in all windows, while baseline updates are selectively enabled.

Core Mechanisms For each window, residual total power is obtained by subtracting the sum of aligned component power from system power and clamping the result to a non-negative budget. Temporal misalignment is detected using conservative window-local indicators, including sustained lag of system power behind accounted components and sharp increases in component power coinciding with near-zero or clamped residuals. A short hold horizon is applied to transient classification to prevent flapping. Window usability is defined as the conjunction of non-transient classification and the absence of residual clamping. The residual idle baseline is seeded on the first window that satisfies all learning preconditions. Subsequent updates follow a candidate-then-commit mechanism that tracks sustained low residual observations and applies bounded downward adjustments only after confirmation. Idle and dynamic residual power are materialized conservatively by capping idle at the clamped residual budget and assigning the remainder to dynamic, ensuring exact per-window conservation. Energy counters are obtained by integrating window-local power and accumulated monotonically using the clamped budget, with explicit handling of the raw-to-corrected system metric transition.

Robustness and Edge Cases Unusable windows do not trigger idle baseline learning and cannot decrease the baseline, preventing collapse during temporal misalignment. Learning is forbidden during warmup to avoid contamination from raw system metrics. Residual budgets below a minimum magnitude are excluded from learning to prevent noise fitting. Downward baseline adaptation is hardened by requiring persistence across multiple consecutive learnable windows and by rate-limiting the maximum permanent drop per commit. The idle component is always capped by the current clamped residual budget, preventing negative dynamic residuals even when the baseline temporarily exceeds the budget. Once corrected system metrics become active, raw residual series are explicitly removed to avoid overlapping series with incompatible semantics.

Implementation Consequences Residual idle and dynamic metrics are conservative by construction and conserve the clamped residual budget exactly in every window. Persistent idle state remains stable under aggressive workload changes because temporally invalid windows are excluded from learning and the last committed baseline is held constant. The usability signal establishes a hard contract for downstream consumers: residual idle and dynamic values may be present in all windows, but are only interpretable and learnable when usability is true. The exported idle baseline is explicit model state and must not be interpreted as a physical idle quantity.

Exported Metrics The exported metrics are summarized in Table 5.15.

Metric name	Type	Unit	Labels
Residual idle and dynamic metrics			
`residual_power_mw`	Gauge	mW	`chassis, source, kind`
`residual_energy_mj`	Counter	mJ	`chassis, source, kind`
Residual idle model state			
`residual_idle_baseline_mw`	Gauge	mW	`chassis, source`
Residual window validity			
`residual_window_usable`	Gauge	bool	`chassis, source`

Label domain: `kind` $\in$ {idle, dynamic}, `source` $\in$ {`redfish_raw`, `redfish_corrected`}.

TABLE 5.15: Exported residual idle and dynamic metrics.

5.7.10.3 GPU Idle and Dynamic Decomposition

Architectural Context This section realizes the architectural GPU idle and dynamic decomposition defined in § 4.8.4.3, operating exclusively on the corrected per-device total power and window-consistent duration.

Implementation Strategy For each GPU device, the implementation maintains a per-device idle estimator whose input is the corrected total power together with a compact utilization signal. Idle estimation is updated opportunistically under stable conditions and otherwise held constant, ensuring that transient load changes do not perturb the baseline. Idle and dynamic components are derived per window from the same total power observation and duration, then accumulated into monotonic energy counters.

Core Mechanisms The implementation retrieves the corrected total power gauge and the corresponding window duration, and maps the most recent device utilization observation into the corrected window. An idle estimator is instantiated per device and observes tuples $(u_{\text{sm}}, u_{\text{mem}}, P_{\text{total}})$. A new idle estimate is accepted only when utilization remains approximately constant and within a low-utilization region, yielding a stable baseline β_{uuid}. For each window, idle power is obtained by clamping β_{uuid} to the current total power, dynamic power is computed as the non-negative residual, and both are converted to window energy increments using the same duration as the total. All three cumulative energies (total, idle, dynamic) are updated atomically in per-device state.

Robustness and Edge Cases If total power is unavailable for a device in a window, no idle or dynamic update is performed to avoid inconsistent state. Idle estimates are bounded to the interval $[0, P_{\text{total}}]$ to prevent negative or superlinear components. Stability gating prevents sudden utilization changes from contaminating the idle baseline, causing such transients to be attributed entirely to dynamic power. All intermediate values are checked for non-finite results and clipped to preserve monotonicity of cumulative energy counters.

Implementation Consequences The implementation enforces a conservative decomposition in which idle power evolves slowly and only under stationary conditions, while dynamic power absorbs short-term fluctuations. Energy conservation

holds per window by construction, and cumulative counters remain monotonic over the lifetime of the system. The per-device state isolation allows heterogeneous GPUs to be handled independently without cross-coupling effects.

Exported Metrics The exported metrics are summarized in Table 5.16.

Metric name	Type	Unit	Labels
GPU idle and dynamic decomposition metrics			
`gpu_power_mw`	Gauge	mW	`gpu_uuid, kind, source`
`gpu_energy_mj`	Counter	mJ	`gpu_uuid, kind, source`

Label domain: `kind` $\in$ {idle, dynamic}, `source` = `nvml_corrected`.

TABLE 5.16: Exported GPU idle and dynamic decomposition metrics.

5.7.11 Stage 4: Workload Attribution and Aggregation

5.7.11.1 Workload Attribution of eBPF Utilization Counters

Architectural Context This section realizes the workload-level aggregation model, mapping per-process eBPF utilization deltas to workload-attributed monotonic counters while enforcing strict conservation and residual `__system__` semantics.

Implementation Strategy Attribution is implemented as a window-local aggregation over the effective eBPF observation window. All raw per-process deltas observed in the window are treated as authoritative inputs. Resolution to workload identity is attempted per process using the standard Stage 4 resolver, but aggregation into non-system workloads is conditional. Unresolved activity is not dropped or heuristically reassigned and is instead captured explicitly via residual construction.

Core Mechanisms For each effective window, per-process deltas are integrated over the window interval using fractional overlap factors to account for partial boundary intersections. Two accumulations are performed in parallel. First, signal-wise totals are computed by summing all observed per-process deltas, independent of resolution. Second, resolved per-process deltas are aggregated into per-workload buckets. After aggregation, the `__system__` workload is materialized as the residual between the total activity and the sum of all non-system workloads, with negative residuals clamped to zero to preserve non-negativity. All workload aggregates are accumulated into state-backed monotonic counters, preserving counter semantics across windows.

Robustness and Edge Cases Partial observability affects only resolution, not conservation. If process identity or workload metadata is unavailable, unstable, or inconsistent, the corresponding deltas contribute solely to the total and therefore increase the `__system__` residual. Window boundary truncation is handled via fractional scaling, with accumulators maintained in floating-point state to avoid systematic loss under repeated truncation. Emitted counter values are monotonically non-decreasing by construction, and defensive checks prevent regression under any execution order. Workload series are garbage-collected after a bounded inactivity period, while the `__system__` series is explicitly exempt from deletion.

Implementation Consequences The implementation guarantees strict conservation between system-level eBPF counters and the sum of workload-attributed counters over any analysis horizon. Resolution failure degrades monotonically into `__system__` without redistributing activity among resolved workloads. The resulting counters are suitable as first-class workload attribution outputs and as explanatory inputs for subsequent energy attribution and validation stages.

Exported Metrics The exported metrics are summarized in Table 5.17.

Metric name	Type	Unit	Labels
CPU execution activity			
`workload_bpf_cpu_instructions_total`	Counter	count	*common (see below)*
`workload_bpf_cpu_cycles_total`	Counter	count	*common (see below)*
`workload_bpf_cache_misses_total`	Counter	count	*common (see below)*
`workload_bpf_page_cache_hits_total`	Counter	count	*common (see below)*
Interrupt activity			
`workload_bpf_irq_net_tx_total`	Counter	count	*common (see below)*
`workload_bpf_irq_net_rx_total`	Counter	count	*common (see below)*
`workload_bpf_irq_block_total`	Counter	count	*common (see below)*
Process runtime			
`workload_bpf_process_run_us_total`	Counter	μs	*common (see below)*

Label domain: `source` = `bpf`; labels `namespace`, `pod`, and `container` identify the workload.

TABLE 5.17: Exported workload-attributed eBPF utilization counters.

5.7.11.2 Workload Resolution and Identity Enforcement

Architectural Context This section realizes the workload resolution abstraction introduced in the Stage 4 architecture. The resolver provides a conditional mapping from execution-level observations to Kubernetes workload identities and enforces the semantics of the distinguished `__system__` class. It is an auxiliary component of the attribution pipeline: attribution logic consumes its outputs but does not embed or compensate for resolution failures. All guarantees are enforced here under discretization, metadata delay, and partial observability.

Implementation Strategy Workload resolution is implemented as a best-effort, cycle-scoped join between execution identities and the metadata store associated with the current analysis cycle. Resolution is intentionally asymmetric: positive identification requires multiple consistency checks, while failure at any point causes immediate fallback to an unresolved state. The resolver never invents workload identities, never extrapolates beyond available metadata, and never retries resolution retroactively across cycles. This strategy ensures conservative behavior and monotone degradation toward `__system__` under uncertainty.

Core Mechanisms Resolution proceeds in three ordered stages. First, a process-based path attempts to resolve a stable process identity using a guarded `(PID, StartJiffies)` pair to harden against PID reuse. Second, when process identity is unavailable or unsafe, a cgroup-based fallback is attempted using only explicitly

attributable cgroup identifiers. Third, a resolved container identifier is mapped to Kubernetes namespace, pod, and container labels via the metadata store. Only when all required identity components are present is a workload key materialized; otherwise resolution fails. The resolver itself returns either a fully specified workload key or an unresolved outcome, with no intermediate states.

Robustness and Edge Cases All resolution steps are guarded against known failure modes. PID reuse is explicitly checked and causes conservative rejection rather than reassignment. Sentinel or root cgroup identifiers are excluded to prevent poisoning of the mapping chain. Missing, stale, or incomplete metadata entries immediately invalidate resolution. Importantly, resolution failure does not propagate partial identity information: unresolved observations are not weakly labeled but are handled uniformly by the attribution layer as `__system__`. This guarantees that loss of metadata cannot redistribute energy between resolved workloads.

Implementation Consequences The resolver enforces a strict correctness boundary for Stage 4 attribution. When identity information is reliable, workload attribution is precise and reproducible within the limits of the chosen fairness basis. When identity information degrades, attribution degrades conservatively and explicitly without violating conservation or introducing hidden assumptions. This behavior ensures that workload-resolved metrics remain interpretable across runs with varying metadata quality and system churn.

Exported Metrics The workload resolver does not export metrics directly. Its effects are observable only through the workload-labeled metrics produced by subsequent attribution stages, including the explicit appearance of the `__system__` workload class when resolution is not possible.

5.7.11.3 CPU Dynamic Energy Attribution

Architectural Context This section realizes the bin-level CPU dynamic attribution model defined in the corresponding architecture section. For each RAPL CPU domain, a per-window dynamic energy budget is distributed across workloads using execution-derived activity proxies, while enforcing conservation, non-negativity, completeness, and monotone degradation toward `__system__` under partial observability.

Implementation Strategy The implementation treats each RAPL domain uniformly and executes attribution independently per domain. The authoritative input is the per-window delta of the cumulative dynamic energy counter for the domain. Workload attribution is computed at native eBPF tick resolution and only aggregated to window scope after all bin-level decisions have been made. All attribution state is explicit and window-scoped, with no cross-window reinterpretation.

Core Mechanisms Per-bin activity weights are constructed from eBPF process counters by differencing against state-managed baselines. Baselines are keyed by a stable process identity when available and fall back conservatively when not. For each bin, total activity mass and per-workload activity mass are accumulated according to the domain-specific proxy. The window-level dynamic energy budget is then allocated across bins proportionally to their activity mass, and each bin's energy share

is further allocated across workloads proportionally to their per-bin activity. Exact conservation in integer millijoules is enforced using a largest-remainder finalization step, with any rounding remainder routed explicitly to `__system__`.

Robustness and Edge Cases Missing or zero activity mass is handled conservatively. If no activity is observed for a domain across the entire window, the full dynamic energy budget is assigned to `__system__`. If activity is absent in an individual bin, that bin's energy share is assigned to `__system__`. For the `dram` domain, a window-scoped fallback replaces cache-miss activity with CPU cycle activity when cache-miss mass is zero but cycle mass is non-zero. Counter resets, PID reuse, and partial process visibility are handled by baseline rebasing and by skipping unsafe deltas, which can only increase the `__system__` share and never redistribute energy among resolved workloads.

Implementation Consequences The implementation guarantees conservative, monotonic, and temporally causal workload attribution of CPU dynamic energy. Integer rounding is resolved locally at both allocation stages using a largest-remainder scheme, ensuring exact conservation without cross-bin interference. Under reduced observability, attribution degrades only by increasing the `__system__` share, without redistributing energy among resolved workloads. The explicit bin-level realization preserves the architectural contract and enables later extensions such as idle allocation and residual energy handling without modifying the dynamic attribution core.

Exported Metrics The exported metrics are summarized in Table 5.18.

Metric name	Type	Unit	Labels
CPU dynamic workload energy			
`workload_rapl_energy_mj`	Counter	mJ	*common (see below)*

Label domain: `domain` $\in$ {pkg, core, uncore, dram}, `kind` = dynamic, `source` = `rapl`; labels `namespace`, `pod`, and `container` identify the attributed workload.

TABLE 5.18: Exported CPU dynamic workload energy metrics.

5.7.11.4 CPU Idle Energy Attribution

Architectural Context This section realizes the CPU idle attribution model defined in the corresponding architecture subsubsection, enforcing a two-pool fairness policy under discretized, window-based execution. The implementation adheres to the Stage 4 invariants and mirrors the workload identity and lifecycle semantics used for CPU dynamic attribution.

Implementation Strategy Per-window idle energy budgets are derived by differencing cumulative RAPL idle energy counters for each supported domain. Attribution is performed independently per domain, using domain-specific reservation signals while reusing the window-sticky activity weights produced by CPU dynamic attribution. All allocation decisions are local to the current window and do not depend on future information.

Core Mechanisms For each domain, the idle budget is split into a reserved and an opportunistic pool using the domain-specific reservation fraction β. Reservation weights are obtained from container-level CPU requests for `pkg`, `core`, and `uncore`, and from container-level memory requests for `dram`. Activity weights are taken from the window-aggregated dynamic allocation maps.

The eligible workload set is defined as the union of workloads observed in dynamic attribution, currently running containers, and the mandatory `__system__` workload. The reserved pool is allocated proportionally among workloads with strictly positive requests. The opportunistic pool is allocated proportionally among workloads without requests and the `__system__` workload, using activity weights. Per-workload allocations from both pools are combined and accumulated into monotonic workload-level idle energy counters.

Robustness and Edge Cases Missing or negative idle deltas result in zero budget for the affected window. If no valid requests exist, the reserved pool collapses to zero without redistributing energy. If no activity weights are available, the opportunistic pool collapses and the full idle budget is attributed to `__system__`. All rounding discrepancies are resolved deterministically, with any remainder routed to `__system__`, ensuring exact per-window conservation. Short-lived or metadata-late workloads may receive idle energy only via the opportunistic pool. Inactive workload series are garbage-collected using the same TTL-based mechanism as dynamic CPU attribution, without retroactive reinterpretation.

Implementation Consequences The implementation guarantees strict conservation, non-negativity, and completeness for CPU idle energy attribution across all supported RAPL domains. Idle attribution degrades conservatively under partial observability and remains interpretable as a fairness policy rather than a causal signal. The resulting workload-level idle energy counters are directly comparable to dynamic CPU energy outputs and suitable for downstream aggregation and analysis.

Exported Metrics The exported metrics are summarized in Table 5.19.

Metric name	Type	Unit	Labels
Workload-attributed CPU idle energy			
`workload_rapl_energy_mj`	Counter	mJ	*common (see below)*

Label domain: `domain` $\in$ {pkg, core, uncore, dram}, `kind` = idle, `source` = `rapl`; labels `namespace`, `pod`, and `container` identify the attributed workload.

TABLE 5.19: Exported CPU idle workload energy metrics.

5.7.11.5 GPU Dynamic Energy Attribution

Architectural Context This subsection realises the Stage 4 GPU dynamic attribution rule by allocating corrected-series energy over process-sample intervals and aggregating by resolved workload identity, while routing unsupported fractions to `__system__`.

Implementation Strategy For each GPU UUID, the implementation combines (i) a corrected energy series that can be integrated over arbitrary sub-intervals, (ii) a dynamic window budget, and (iii) a timestamped stream of per-process `ComputeUtil` snapshots. Attribution is performed by iterating sub-intervals induced by the snapshot times and applying a hold-last policy for utilization between snapshots.

Core Mechanisms The corrected energy series is integrated over sub-intervals using zero-order hold on the fixed grid to obtain $\Delta E_{\text{gpu}}(I, \text{uuid})$. A per-window scale factor $f(W, \text{uuid})$ is computed from the ratio of the dynamic window budget to total corrected window energy and is clipped to $[0, 1]$. For each sub-interval, utilization mass is computed from the held PID map. If mass is zero, the entire sub-interval dynamic energy is accumulated to `__system__`. Otherwise, PID shares are computed proportionally and resolved to workloads using the existing resolver chain; unresolved shares are accumulated to `__system__`. Any floating-point remainder between interval budget and assigned shares is routed to `__system__` to preserve per-interval conservation.

Robustness and Edge Cases Snapshot ingestion clamps `ComputeUtil` into $[0, 100]$ and treats invalid values as zero. If corrected-series integration fails for a sub-interval, no energy is allocated for that sub-interval, which preserves non-negativity and avoids inventing energy. If the corrected window energy is non-positive, or the corrected series is unavailable, the dynamic budget is conservatively routed to `__system__`. Resolver failure for a PID share does not affect other shares and degrades monotonically by redirecting only the unresolved share to `__system__`.

Implementation Consequences Dynamic attribution preserves conservation against the constructed dynamic budget per GPU UUID and window, up to numerical round-off which is absorbed by `__system__`. Temporal allocation follows the observed snapshot cadence, preventing the coarse artifacts of reducing utilization to a single window statistic, while keeping the exported outputs window-scoped.

Exported Metrics The exported metrics are summarized in Table 5.20.

Metric name	Type	Unit	Labels
Workload-attributed GPU dynamic energy			
`workload_gpu_energy_mj`	Counter	mJ	*common (see below)*

Label domain: `kind` = dynamic; labels `gpu_uuid`, `namespace`, `pod`, and `container` identify the attributed workload.

TABLE 5.20: Exported metrics for GPU dynamic workload attribution.

5.7.11.6 GPU Idle Energy Attribution

Architectural Context This subsection realises the Stage 4 rule that GPU idle energy is not distributed to workloads and is instead emitted exclusively as `__system__`.

Implementation Strategy The implementation mirrors the corrected idle GPU energy counter into the workload GPU energy metric for the `__system__` workload key, per GPU UUID.

Core Mechanisms For each GPU UUID, the absolute corrected idle energy counter value is loaded and written into the corresponding `workload_gpu_energy_mj` series with `kind="idle"` and workload labels set to `__system__`. The write is monotonic-guarded to prevent counter regression if upstream inputs transiently decrease.

Robustness and Edge Cases Invalid or negative idle counter values are clamped to zero. If the idle counter is missing for a device, no idle workload point is emitted for that device in the current cycle. Monotonic guarding ensures that transient upstream regressions do not violate the counter contract at the exporter boundary.

Implementation Consequences Idle workload energy is complete by construction and exactly consistent with corrected idle energy, while avoiding speculative distribution. Together with dynamic attribution, the workload GPU energy metric admits a complete accounting view in which idle energy is explicitly represented as `__system__`.

Exported Metrics The exported metrics are summarized in Table 5.21.

Metric name	Type	Unit	Labels
Workload-attributed GPU idle energy			
`workload_gpu_energy_mj`	Counter	mJ	*common (see below)*

Label domain: `kind` = idle; labels `gpu_uuid`, `namespace`, `pod`, and `container` identify the attributed workload.

TABLE 5.21: Exported metrics for GPU idle workload attribution.

5.7.12 Prometheus Exporter Implementation

Architectural Context This implementation realizes the passive exposition model defined above by translating committed analysis points into a Prometheus-compatible pull interface.

Implementation Strategy Analysis points are pushed into the exporter as immutable values and retained only as the most recent sample per metric series. Metric families are created lazily on first observation, with a fixed label schema determined at discovery time.

Core Mechanisms Each analysis metric identifier is mapped to a sanitized Prometheus metric name with a mandatory "`tycho_`" prefix. Label keys are fixed on first sight and reused for all subsequent emissions. At scrape time, the exporter exposes the latest committed value for each active series without additional buffering or recomputation.

Robustness and Edge Cases Schema instability is handled conservatively by ignoring newly appearing labels after first observation. Exporter startup is decoupled from analysis initialization, ensuring availability even while upstream components perform long-running calibration or setup. Multiple sinks may coexist, allowing Prometheus export and auxiliary sinks such as logging to operate concurrently.

Implementation Consequences The exporter preserves analysis correctness by construction, as it neither modifies nor reinterprets metric values. All temporal guarantees are inherited directly from the analysis engine, while exposition remains strictly observational and replaceable.

5.8 Correctness, Robustness, and Degradation Behavior

5.8.1 Architectural Invariant Enforcement

5.8.1.1 Conservation Enforcement Strategy

5.8.1.2 Idle+Dynamic Consistency Enforcement

5.8.2 Partial Observability and Missing Data

5.8.2.1 Missing Source Samples

5.8.2.2 Missing Metadata Joins

5.8.3 Transient Pathologies

5.8.3.1 Temporary Drops in Idle Signals

5.8.3.2 Residual Negativity and Recovery

5.8.4 Graceful Degradation Paths

5.9 Implementation Trade-Offs and Design Decisions

5.9.1 Accuracy vs Complexity

5.9.2 Timing Precision vs System Overhead

5.9.3 Alternatives Considered

5.10 Summary

Bibliography

[1] Caspar Wackerle. *PowerStack: Automated Kubernetes Deployment for Energy Efficiency Analysis*. GitHub repository. 2025. URL: https://github.com/casparwackerle/PowerStack.

[2] Weiwei Lin et al. "A Taxonomy and Survey of Power Models and Power Modeling for Cloud Servers". In: *ACM Comput. Surv.* 53.5 (Sept. 2020), 100:1–100:41. ISSN: 0360-0300. DOI: 10.1145/3406208. (Visited on 04/20/2025).

[3] Saiqin Long et al. "A Review of Energy Efficiency Evaluation Technologies in Cloud Data Centers". In: *Energy and Buildings* 260 (Apr. 2022), p. 111848. ISSN: 0378-7788. DOI: 10.1016/j.enbuild.2022.111848. (Visited on 04/20/2025).

[4] Yewan Wang et al. "An Empirical Study of Power Characterization Approaches for Servers". In: *ENERGY 2019 - The Ninth International Conference on Smart Grids, Green Communications and IT Energy-aware Technologies*. June 2019, p. 1. (Visited on 04/23/2025).

[5] Charles Reiss et al. "Heterogeneity and Dynamicity of Clouds at Scale: Google Trace Analysis". In: *Proceedings of the Third ACM Symposium on Cloud Computing*. SoCC '12. New York, NY, USA: Association for Computing Machinery, Oct. 2012, pp. 1–13. ISBN: 978-1-4503-1761-0. DOI: 10.1145/2391229.2391236. (Visited on 11/26/2025).

[6] Muhammad Waseem et al. *Containerization in Multi-Cloud Environment: Roles, Strategies, Challenges, and Solutions for Effective Implementation*. July 2025. DOI: 10.48550/arXiv.2403.12980. arXiv: 2403.12980 [cs]. (Visited on 11/26/2025).

[7] Emiliano Casalicchio and Stefano Iannucci. "The State-of-the-Art in Container Technologies: Application, Orchestration and Security". In: *Concurrency and Computation: Practice and Experience* 32.17 (2020), e5668. ISSN: 1532-0634. DOI: 10.1002/cpe.5668. (Visited on 11/26/2025).

[8] Spencer Desrochers, Chad Paradis, and Vincent M. Weaver. "A Validation of DRAM RAPL Power Measurements". In: *Proceedings of the Second International Symposium on Memory Systems*. MEMSYS '16. New York, NY, USA: Association for Computing Machinery, Oct. 2016, pp. 455–470. DOI: 10.1145/2989081.2989088. (Visited on 05/21/2025).

[9] Steven van der Vlugt et al. *PowerSensor3: A Fast and Accurate Open Source Power Measurement Tool*. Apr. 2025. DOI: 10.48550/arXiv.2504.17883. arXiv: 2504.17883 [cs]. (Visited on 05/09/2025).

[10] UEFI Forum. *Advanced Configuration and Power Interface Specification Version 6.6*. Accessed April 2025. Sept. 2021. URL: https://uefi.org/sites/default/files/resources/ACPI_Spec_6.6.pdf.

[11] Richard Kavanagh, Django Armstrong, and Karim Djemame. "Accuracy of Energy Model Calibration with IPMI". In: *2016 IEEE 9th International Conference on Cloud Computing (CLOUD)*. June 2016, pp. 648–655. DOI: 10.1109/CLOUD.2016.0091. (Visited on 04/23/2025).

[12] Richard Kavanagh and Karim Djemame. "Rapid and Accurate Energy Models through Calibration with IPMI and RAPL". In: *Concurrency and Computation: Practice and Experience* 31.13 (2019), e5124. ISSN: 1532-0634. DOI: 10.1002/cpe.5124. (Visited on 04/23/2025).

[13] Magnus Herrlin. "Accessing Onboard Server Sensors for Energy Efficiency in Data Centers". In: (Sept. 2021). (Visited on 11/27/2025).

[14] Ghazanfar Ali et al. "Redfish-Nagios: A Scalable Out-of-Band Data Center Monitoring Framework Based on Redfish Telemetry Model". In: *Fifth International Workshop on Systems and Network Telemetry and Analytics*. Minneapolis MN USA: ACM, June 2022, pp. 3–11. ISBN: 978-1-4503-9315-7. DOI: 10.1145/3526064.3534108. (Visited on 11/27/2025).

[15] Intel Corporation. *Intel® 64 and IA-32 Architectures Software Developer's Manual*. Volume 3B, Chapter 16.10: Plaform Specific Power Management Support. Available online: https://www.intel.com/content/www/us/en/developer/articles/technical/intel-sdm.html. 2024.

[16] Guillaume Raffin and Denis Trystram. "Dissecting the Software-Based Measurement of CPU Energy Consumption: A Comparative Analysis". In: *IEEE Transactions on Parallel and Distributed Systems* 36.1 (Jan. 2025), pp. 96–107. ISSN: 1558-2183. DOI: 10.1109/TPDS.2024.3492336. (Visited on 04/02/2025).

[17] Daniel Hackenberg et al. "An Energy Efficiency Feature Survey of the Intel Haswell Processor". In: *2015 IEEE International Parallel and Distributed Processing Symposium Workshop*. May 2015, pp. 896–904. DOI: 10.1109/IPDPSW.2015.70. (Visited on 04/28/2025).

[18] Daniel Hackenberg et al. "Power Measurement Techniques on Standard Compute Nodes: A Quantitative Comparison". In: *2013 IEEE International Symposium on Performance Analysis of Systems and Software (ISPASS)*. Apr. 2013, pp. 194–204. DOI: 10.1109/ISPASS.2013.6557170. (Visited on 04/28/2025).

[19] Lukas Alt et al. "An Experimental Setup to Evaluate RAPL Energy Counters for Heterogeneous Memory". In: *Proceedings of the 15th ACM/SPEC International Conference on Performance Engineering*. ICPE '24. New York, NY, USA: Association for Computing Machinery, May 2024, pp. 71–82. ISBN: 979-8-4007-0444-4. DOI: 10.1145/3629526.3645052. (Visited on 04/02/2025).

[20] Tom Kennes. *Measuring IT Carbon Footprint: What Is the Current Status Actually?* June 2023. DOI: 10.48550/arXiv.2306.10049. arXiv: 2306.10049 [cs]. (Visited on 04/23/2025).

[21] Robert Schöne et al. "Energy Efficiency Features of the Intel Alder Lake Architecture". In: *Proceedings of the 15th ACM/SPEC International Conference on Performance Engineering*. London United Kingdom: ACM, May 2024, pp. 95–106. ISBN: 979-8-4007-0444-4. DOI: 10.1145/3629526.3645040. (Visited on 04/07/2025).

[22] Robert Schöne et al. "Energy Efficiency Aspects of the AMD Zen 2 Architecture". In: *2021 IEEE International Conference on Cluster Computing (CLUSTER)*. Sept. 2021, pp. 562–571. DOI: 10.1109/Cluster48925.2021.00087. (Visited on 04/28/2025).

[23] Kashif Nizam Khan et al. "RAPL in Action: Experiences in Using RAPL for Power Measurements". In: *ACM Trans. Model. Perform. Eval. Comput. Syst.* 3.2 (Mar. 2018), 9:1–9:26. ISSN: 2376-3639. DOI: 10.1145/3177754. (Visited on 04/07/2025).

[24] Mathilde Jay et al. "An Experimental Comparison of Software-Based Power Meters: Focus on CPU and GPU". In: *2023 IEEE/ACM 23rd International Symposium on Cluster, Cloud and Internet Computing (CCGrid)*. May 2023, pp. 106–118. DOI: 10.1109/CCGrid57682.2023.00020. (Visited on 04/21/2025).

[25] Moritz Lipp et al. "PLATYPUS: Software-based Power Side-Channel Attacks on X86". In: *2021 IEEE Symposium on Security and Privacy (SP)*. May 2021, pp. 355–371. DOI: 10.1109/SP40001.2021.00063. (Visited on 05/21/2025).

[26] Intel Corporation. *Intel® 64 and IA-32 Architectures Software Developer's Manual Volume 4: Model-Specific Registers*. Tech. rep. 335592-081US. Accessed 2025-04-28. Intel Corporation, Sept. 2023. URL: https://cdrdv2.intel.com/v1/dl/getContent/671098.

[27] Zeyu Yang, Karel Adamek, and Wesley Armour. "Accurate and Convenient Energy Measurements for GPUs: A Detailed Study of NVIDIA GPU's Built-In Power Sensor". In: *SC24: International Conference for High Performance Computing, Networking, Storage and Analysis*. Nov. 2024, pp. 1–17. DOI: 10.1109/SC41406.2024.00028. (Visited on 05/09/2025).

[28] Oscar Hernandez et al. "Preliminary Study on Fine-Grained Power and Energy Measurements on Grace Hopper GH200 with Open-Source Performance Tools". In: *Proceedings of the 2025 International Conference on High Performance Computing in Asia-Pacific Region Workshops*. Hsinchu Taiwan: ACM, Feb. 2025, pp. 11–22. ISBN: 979-8-4007-1342-2. DOI: 10.1145/3703001.3724383. (Visited on 11/27/2025).

[29] Le Mai Weakley et al. "Monitoring and Characterizing GPU Usage". In: *Concurrency and Computation: Practice and Experience* 37.3 (2025), e8341. ISSN: 1532-0634. DOI: 10.1002/cpe.8341. (Visited on 11/27/2025).

[30] The Linux Kernel Community. *The proc Filesystem*. https://www.kernel.org/doc/html/latest/filesystems/proc.html. Accessed: 2025-06-17. 2025.

[31] The Linux Kernel Community. *Control Group v1 — Linux Kernel Documentation*. https://www.kernel.org/doc/html/latest/admin-guide/cgroup-v1/index.html. Accessed: 2025-06-17. 2025.

[32] The Linux Kernel Community. *Control Group v2 — Linux Kernel Documentation*. https://www.kernel.org/doc/html/latest/admin-guide/cgroup-v2.html. Accessed: 2025-06-17. 2025.

[33] Cilium Authors. *eBPF and XDP Reference Guide*. https://docs.cilium.io/en/latest/reference-guides/bpf/index.html. Accessed: 2025-06-17. 2025.

[34] Cyril Cassagnes et al. "The Rise of eBPF for Non-Intrusive Performance Monitoring". In: *NOMS 2020 - 2020 IEEE/IFIP Network Operations and Management Symposium*. Apr. 2020, pp. 1–7. DOI: 10.1109/NOMS47738.2020.9110434. (Visited on 06/14/2025).

[35] Brendan Gregg. *CPU Utilization is Wrong*. Blog post. Accessed 29 June 2025. May 2017. URL: https://www.brendangregg.com/blog/2017-05-09/cpu-utilization-is-wrong.html.

[36] smartmontools developers. *smartmontools: Control and monitor storage systems using S.M.A.R.T.* https://github.com/smartmontools/smartmontools/. Accessed May 2025. 2025.

[37] Linux NVMe Maintainers. *nvme-cli: NVMe management command line interface*. https://github.com/linux-nvme/nvme-cli. Accessed May 2025. 2025.

[38] Seokhei Cho et al. "Design Tradeoffs of SSDs: From Energy Consumption's Perspective". In: *ACM Trans. Storage* 11.2 (Mar. 2015), 8:1–8:24. ISSN: 1553-3077. DOI: 10.1145/2644818. (Visited on 05/18/2025).

[39] Yan Li and Darrell D.E. Long. "Which Storage Device Is the Greenest? Modeling the Energy Cost of I/O Workloads". In: *2014 IEEE 22nd International Symposium on Modelling, Analysis & Simulation of Computer and Telecommunication Systems*. Sept. 2014, pp. 100–105. DOI: 10.1109/MASCOTS.2014.20. (Visited on 05/19/2025).

[40] Eric Borba, Eduardo Tavares, and Paulo Maciel. "A Modeling Approach for Estimating Performance and Energy Consumption of Storage Systems". In: *Journal of Computer and System Sciences* 128 (Sept. 2022), pp. 86–106. ISSN: 0022-0000. DOI: 10.1016/j.jcss.2022.04.001. (Visited on 05/18/2025).

[41] Ripduman Sohan et al. "Characterizing 10 Gbps Network Interface Energy Consumption". In: *IEEE Local Computer Network Conference*. Oct. 2010, pp. 268–271. DOI: 10.1109/LCN.2010.5735719. (Visited on 05/30/2025).

[42] Robert Basmadjian et al. "Cloud Computing and Its Interest in Saving Energy: The Use Case of a Private Cloud". In: *Journal of Cloud Computing: Advances, Systems and Applications* 1.1 (June 2012), p. 5. ISSN: 2192-113X. DOI: 10.1186/2192-113X-1-5. (Visited on 06/01/2025).

[43] Saeedeh Baneshi et al. "Analyzing Per-Application Energy Consumption in a Multi-Application Computing Continuum". In: *2024 9th International Conference on Fog and Mobile Edge Computing (FMEC)*. Sept. 2024, pp. 30–37. DOI: 10.1109/FMEC62297.2024.10710253. (Visited on 05/30/2025).

[44] TechNotes. *Deciphering the PCI Power States*. Accessed June 2025. Feb. 2024. URL: https://technotes.blog/2024/02/04/deciphering-the-pci-power-states/.

[45] Xiaobo Fan, Wolf-Dietrich Weber, and Luiz Andre Barroso. "Power Provisioning for a Warehouse-Sized Computer". In: *SIGARCH Comput. Archit. News* 35.2 (June 2007), pp. 13–23. ISSN: 0163-5964. DOI: 10.1145/1273440.1250665. (Visited on 05/21/2025).

[46] Chung-Hsing Hsu and Stephen W. Poole. "Power Signature Analysis of the SPECpower_ssj2008 Benchmark". In: *(IEEE ISPASS) IEEE International Symposium on Performance Analysis of Systems and Software*. Apr. 2011, pp. 227–236. DOI: 10.1109/ISPASS.2011.5762739. (Visited on 05/21/2025).

[47] Shuaiwen Leon Song, Kevin Barker, and Darren Kerbyson. "Unified Performance and Power Modeling of Scientific Workloads". In: *Proceedings of the 1st International Workshop on Energy Efficient Supercomputing*. E2SC '13. New York, NY, USA: Association for Computing Machinery, Nov. 2013, pp. 1–8. ISBN: 978-1-4503-2504-2. DOI: 10.1145/2536430.2536435. (Visited on 05/21/2025).

[48] Jordi Arjona Aroca et al. "A Measurement-Based Analysis of the Energy Consumption of Data Center Servers". In: *Proceedings of the 5th International Conference on Future Energy Systems*. E-Energy '14. New York, NY, USA: Association for Computing Machinery, June 2014, pp. 63–74. ISBN: 978-1-4503-2819-7. DOI: 10.1145/2602044.2602061. (Visited on 06/01/2025).

[49] Inc. Meta Platforms. *Kepler v0.9.0 (pre-rewrite): Kubernetes-based power and energy estimation framework*. Accessed: 2025-04-28. 2023. URL: https://https://github.com/sustainable-computing-io/kepler/releases/tag/v0.9.0.

[50] Bjorn Pijnacker. "Estimating Container-level Power Usage in Kubernetes". MA thesis. University of Groningen, Nov. 2024. (Visited on 03/17/2025).

[51] Linux Foundation Energy and Performance Working Group. *Kepler: Kubernetes-based Power and Energy Estimation Framework*. Accessed: 2025-11-14. 2025. URL: https://github.com/sustainable-computing-io/kepler.

[52] Bjorn Pijnacker, Brian Setz, and Vasilios Andrikopoulos. *Container-Level Energy Observability in Kubernetes Clusters*. Apr. 2025. DOI: 10.48550/arXiv.2504.10702. arXiv: 2504.10702 [cs]. (Visited on 07/02/2025).

[53] Hubblo-org. *Scaphandre Documentation*. Accessed: 2025-04-28. 2024. URL: https://github.com/hubblo-org/scaphandre-documentation.

[54] Guillaume Fieni, Romain Rouvoy, and Lionel Seinturier. "SmartWatts: Self-Calibrating Software-Defined Power Meter for Containers". In: *2020 20th IEEE/ACM International Symposium on Cluster, Cloud and Internet Computing (CCGRID)*. May 2020, pp. 479–488. DOI: 10.1109/CCGrid49817.2020.00-45. (Visited on 05/21/2025).

[55] MLCO2. *CodeCarbon: Track emissions from your computing*. Accessed: 2025-04-28. 2023. URL: https://github.com/mlco2/codecarbon.